Statistical Mechanics of Rotaxane Switches

Hao He

A thesis submitted for the degree of Doctor of Philosophy of
The Australian National University

August 2018

Declaration

This thesis is an account of research undertaken between March 2014 and August 2018 at Research School of Chemistry, College of Science, The Australian National University, Canberra, Australia. Except where acknowledged in the customary manner, the material presented in this thesis is, to the best of my knowledge, original and has not been submitted in whole or part for a degree in any university.

Hao He

August 2018

Acknowledgements

I would like to express my sincere gratitude to my PhD supervisor Prof. Edith M. Sevick. She is a passionate researcher and has an acute awareness of finding what can be done. To me, she is an important mentor. We are never in a "supervisor said, student do" situation. I enjoyed high degree of freedom (entropically-dominated) in research and we debate for best scientific outcome. She is a great mother. She showed me that quality research outcome really should not come at the expense of family time.

I would like to acknowledge my co-supervisor Prof. David R.M. Williams for his insightful guidance through the theoretical details. He helped me built up a basic understanding of many tools in statistical mechanics so I can truly do-it-myself.

I thank the Research School of Chemistry for the amazing people and facility, also for the support of my first international science conference.

I would also like express my thanks to former Honors student Mr Darren Sharpe Tsweigh. For help and advice of making important life decisions during my candidature.

I would like to acknowledge the tremendous support from my wife Mrs Yuexi Tan for over ten years. And I acknowledge our 11-day-old daughter Raven for being an angel while daddy works this thesis out.

Abstract

A solution of rotaxane switches, which can switch their length by external stimuli, is described using statistical thermodynamics. We show that this solution can exhibit different behaviors.

This solution can rapidly switch between isotropic and nematic liquid crystalline phases without altering temperature and concentration. There is a minimum of 13% length extension for which transition from pure isotropic to pure nematic phase is possible in idealistic system. We provided a framework to help synthetic chemists understand the requirements of switching efficiency, length change and concentration in rotaxane chemical design to create a macroscopic liquid crystalline phase change.

When external rotaxane switches are depletants in the solution, length switching of rotaxane can significantly change the range and magnitude of colloid depletion interaction. This indicates a possible application of rotaxane switch in controlling colloid stability.

We also investigate liquid crystalline behavior in solution of a rotaxane switches which change length to "adapt" to surrounding environment. We find the effect of adaptive length change on liquid crystalline behaviors is most dramatic at relatively low length extension.

List of Abbreviation and Symbols

F	Free energy
T	Temperature
S	Order parameter
ΔE	Energy difference between states
Z	Partition function
N	Number of particles
f	Depletion force
W	Depletion interaction
k_B	Boltzmann constant
Z_0	The entropic part of partition function
Z_1	The interaction part of partition function
F_0	Entropic part of free energy
F_1	Inter-molecule interaction energy
V	Volume
β	Excluded volume
D	Diameter of rods
L	Length of rods
q	Length ratio between states of rotaxane switch
c	Concentration
Ψ	Orientation distribution
$\mathbf{u}$	Director vector of rods
x	Fraction of long rods
γ	Angle between two rods
α_{2n}, d_{2n}	Coefficients of even-order Legendre polynomial
P_{2n}	Even-order Legendre polynomial

AFM	Atomic Force Microscopy
$BYPM^{2+}$	N,N-dialkylated-4,4-bipyridinium
$CBPQT^{4+}$	Tetracationic cyclophane, cyclobis(paraquat-p-phenylene)
CTAB	Cetyltrimethylammonium bromide
CUAAC	Copper-catalyzed Azide-Alkyne Cycloaddtion
DMSO	Dimethylsulfoxide
dpp ligand	2,9-diphenyl-1,10-phenanthroline
DSM	Dynamic scattering mode
LCD	Liquid-crystal display
MIM	Mechanically-interlocked molecule
SANS	Small-angle neutron scattering
TIRM	Total internal reflection microscopy
UV light	Ultra-violet light
SCF	Self-consistent field

Contents

List of Figures

Chapter 1

Introduction

While molecules have fixed connectedness or bonds between constituent atoms, these bonds themselves can rotate and create different shapes or molecular conformations. The chemical drawing diagrams are only the best "snapshots" of these dynamic molecules. For example, the staggered and eclipsed conformations of ethane are only two extreme conformations, between which ethane molecules rotate constantly. This endless rotational motion within a molecule has inspired many researchers to try to harvest useful work from bond rotation. However, direction of motion is hardly controllable due to the symmetry of energy barrier between conformers, let alone the storm of thermal energy.

There are molecules synthesized specifically to achieve controlled motion and this is achieved with two strategies: First, the conformational energy barrier must be high enough to withstand thermal energy, so that only external excitation can drive the movement. Second, the energy barrier must be asymmetric with respect to direction to achieve unidirectional ratchet-like motion. Feringa et al.[1] reported such a molecular rotor driven by light, as shown in figure 1.1. The rotor is a molecule with two chiral structures connected by a carbon-carbon double bond. The light radiation triggers the cis-trans isomerization of the double bond and turns the bulky group to an unstable position. The molecule then thermally relaxes to a stable state, resulting in an overall unidirectional rotation under constant exposure of light. With proper arrangement, Feringa et al.[2] proceeded further to build the world's smallest 4-wheel drive of 4 by 2 nanometers, powered by four of such light-driven motors tethered to an frame axle.

While such a fully covalently-bonded molecules can serve as a molecular propeller, the nature of covalent bonding limits them for more sophisticated mechanical motion, such as

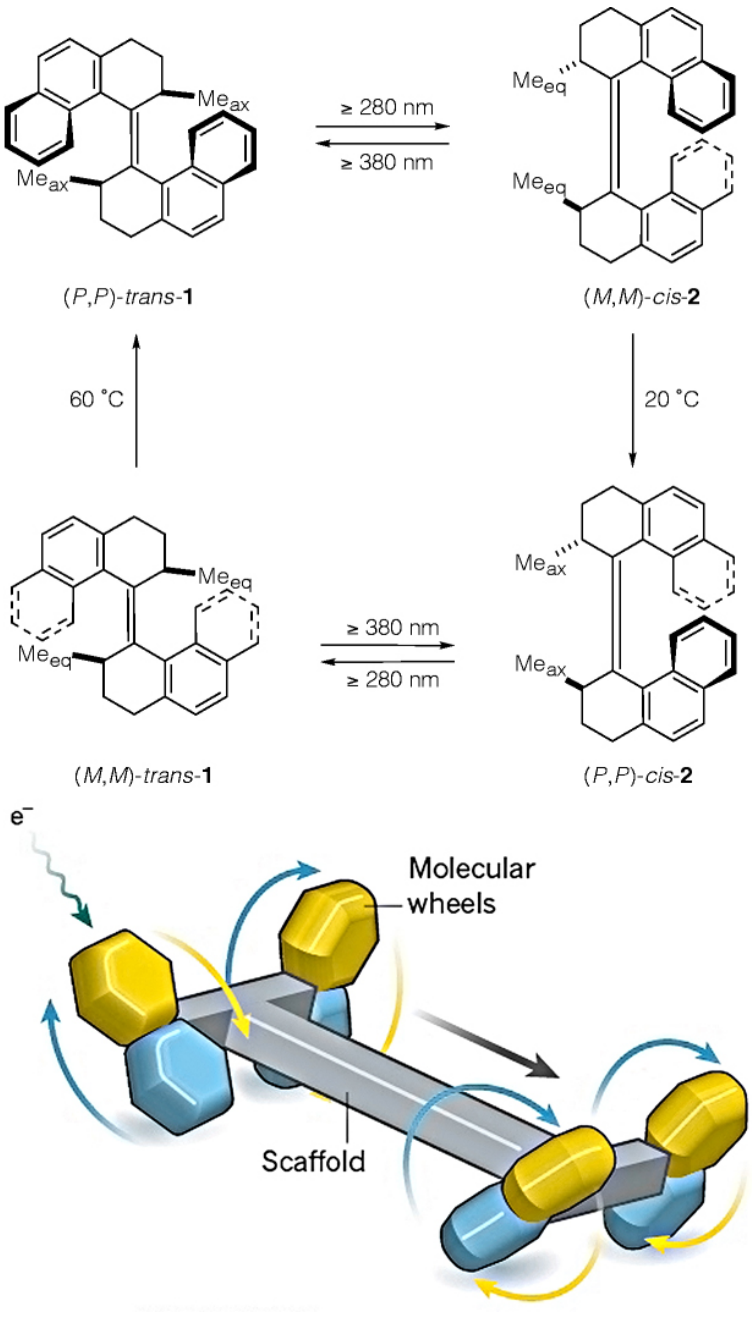

Figure 1.1: Top: The work cycle of the light driven unidirectional molecular motor.[1] The light radiation triggers the cis-trans isomerization of the double bond and turns the bulky group to an unstable position. The molecule then thermally relaxes to a stable state, resulting in an overall unidirectional rotation. Bottom: The molecular 4-wheel-drive powered by 4 molecular motors made by Feringa et al.[2]

linear actuation. To achieve motion over elongated length scales, researchers turn their attention to mechanically interlocked molecules (MIMs). Each of these molecules features two or more covalent structures interlocked or connected by topology. Each topological linkage provides at least one additional degrees of conformational freedom. For example,

a catenane (shown in figure 1.2 left), with two rings interlocked together, allows one of the rings to rotate as well as slide around the perimeter of the other. A rotaxane is another MIM with rings threaded on an axle stoppered by bulky ends (shown in figure 1.2 right), allowing freedom of ring position along the axle. These mechanical degrees of freedom can be far more versatile compare to the degrees of freedom that arise from bond rotation, as they provide more available motion and greater flexibility in chemical design. For example, a rotaxane made with non-interacting rings that freely translate along the contour of an axle possess extra conformational entropy due to the mechanical degrees of freedom. Such a rotaxane is ideal as a molecular shock absorber,[3] which absorbs compression energy by reducing translational entropy of rings (shown in figure 1.3).

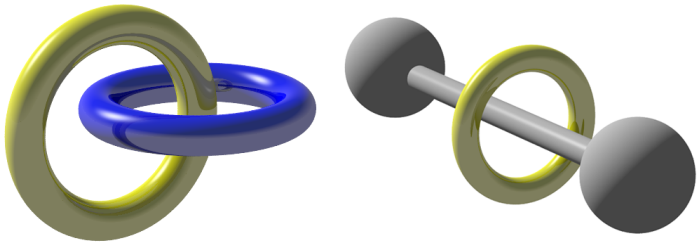

Figure 1.2: Graphic illustration of a catanane (left) and a rotaxane (right). A catenane, a word derived from Latin word "catena" of chain, has two or more rings mechanically interlocked to each other. A rotaxane, from "rota" in Latin meaning wheel, has one or more rings threaded on a dumbbell-shaped axle.

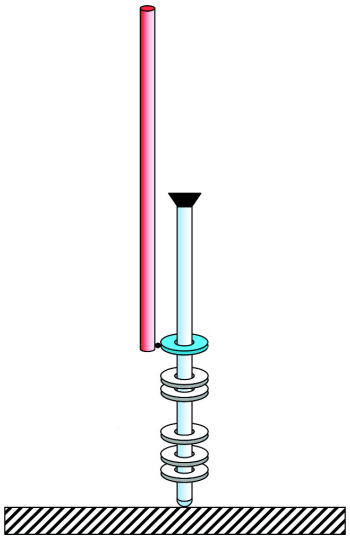

Figure 1.3: Graphic illustration of a rotaxane with free-sliding rings utilized as molecular shock absorber.[3] When compressed, the external force confines the rings to part of the axle. Upon removal of external force, rings redistribute to the complete axle to maximize translational entropy.

1.1 Development of mechanically interlocked molecules (MIMs)

After the important breakthrough in synthesis of macrocyclic rings,[27–29] the idea of mechanical interlocking was a reasonable goal but proved to be a far greater challenge. Catenanes were first isolated using a statistical method by Wassermann in 1960,[30] as extremely unfavored by-products of macrocyclic ring closure reaction. The statistical method relies on rings interlocked by lottery-winning chance at great loss of translation entropy of the components. As a result, the yield was exceptionally low. The statistical synthesis of a rotaxane in 1967 was achieved with 6% yield by repeating threading reactions repeated seventy times.[31]

Due to the limitation of the statistical method, chemists immediately searched for more effective and controllable alternatives. More specifically, some interactions are needed to scaffold intermediates before interlocking. Schill introduced directed synthesis method in 1964[8] using covalent bonds as scaffolds. Macrocyclic interlocking rings were build on to an aromatic backbone. The interlocking rings remain covalently bonded (see figure 1.4) until the final step which cleaves the connection to afford a [2]catenane. For the following 20 years, directed synthesis remained the most effective method to synthesize MIMs such as [3]catenanes[4] and [2]rotaxanes.[5]

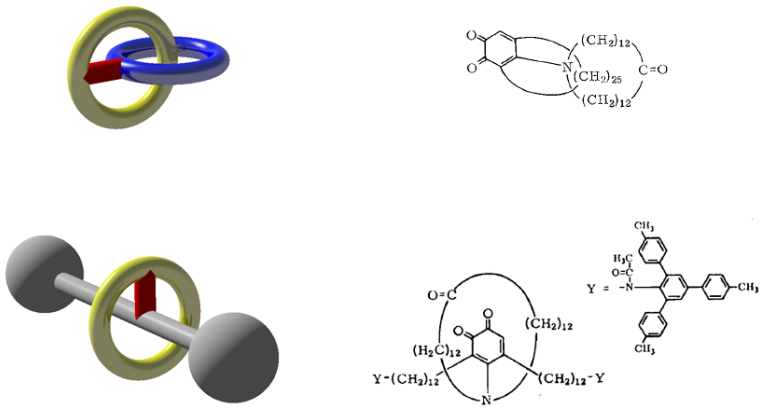

Figure 1.4: Graphic illustration of catanane (top) and rotaxane (bottom) intermediates of Schill's directed synthesis.[4,5] Both intermediates have covalent bond linkage to position the components of mechanically-interlocked molecules. The connection (red) is subsequently cleaved to afford either a catenane or a rotaxane.

While directed synthesis was a controlled method, the process remained lengthy. As a result, catenanes and rotaxanes were not much further explored apart from being synthetic wonders. The game changer was the discovery of the metal template synthesis, in which transition metal coordination replaces the covalent bond as the scaffold. Discovered by Sauvage,[6,32] a 2,9-diphenyl-1,10-phenanthroline (dpp) ligand was threaded through a related macrocycle perpendicularly held by tetrahedral coordination of a copper-I cation. The dpp ligands were subsequently "clipped" as new macrocycles by a Williamson ether reaction. The copper(I) cation was subsequently removed to afford a catenane. With this method, the Synthesis was greatly shorten to only three steps (see figure 1.5), with the ring clipping reaction being the only non-quantitative step (42% yield). Based upon metal templating, MIMs become readily synthesizable and the field of mechanically-interlocked molecules started to grow rapidly. Various different coordinate geometry, such as octahedral[33] and square planar[34] can be used and the transition metal can serve as catalyst at the same time. CUAAC (Copper-catalyzed Azide-Alkyne Cycloaddtion) is often used in current synthesis of catenane and rotaxane,[7] with copper(I) cations serving as metal template as well as catalyst of the ring clicking process, making the synthesis a one-pot reaction. Many other interactions, including but not limited to π-π stacking interaction,[35] hydrogen bonds[36,37] and radical-radical interaction,[38] have been employed as alternatives to pre-scaffold MIMs.

1.2 Switching motif of MIM switches

For years, synthetic chemists designed strategies to effectively manipulate motion in mechanical linkages of MIMs. Attraction sites or "stations" were incorporated into the backbones of covalent structures to lock the MIMs in two or more preferable configurations, turning them into molecular switches. Stoddart introduced a symmetric "molecular shuttle" driven by Brownian motion (see figure 1.6) in 1991.[9] By simply removing the symmetry in molecular architecture, many physical and chemical external inputs can then temporarily perturb the equilibrium between states and create well-defined, controllable ring motion.

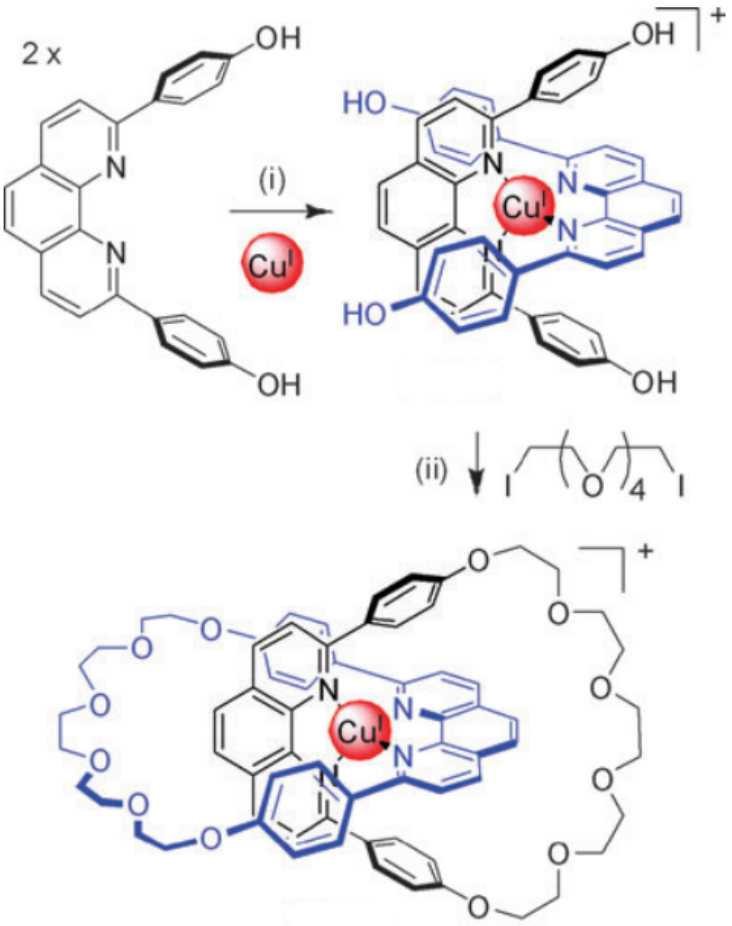

Figure 1.5: Illustration of catenane Sauvage's synthesis using metal template.[6,7] The metal template method uses far fewer steps compare to directed synthesis,[8] with step (ii) being the only non-quantitative step at 42% yield.

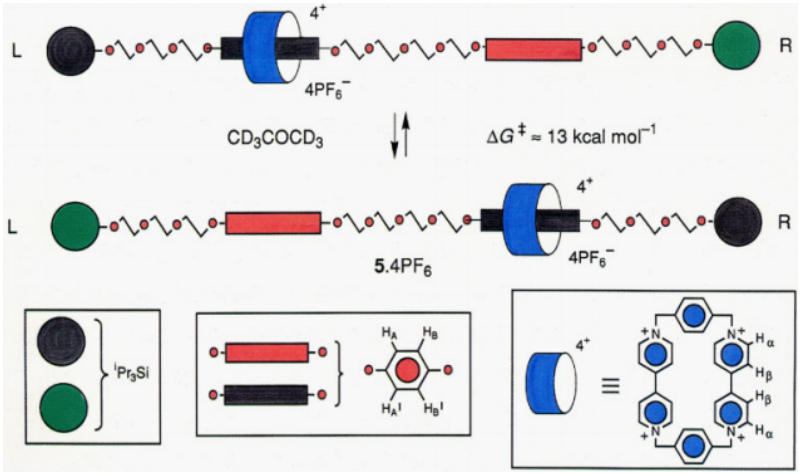

Figure 1.6: The first molecular switch by Stoddart's group,[9] a symmetric [2]rotaxane with 2 identical sites for ring. The ring shifts between sites by Brownian motion.

1.2.1 Molecular switch by physical input

Several groups[10,39,40] reported reversible photoisomerization of stilbene units on an axle of rotaxane to utilize light-driven switching. These molecular switches are Janus [2]rotaxanes, in which two identical units of covalently bonded ring-rod structure interlocked together (see figure 1.7).

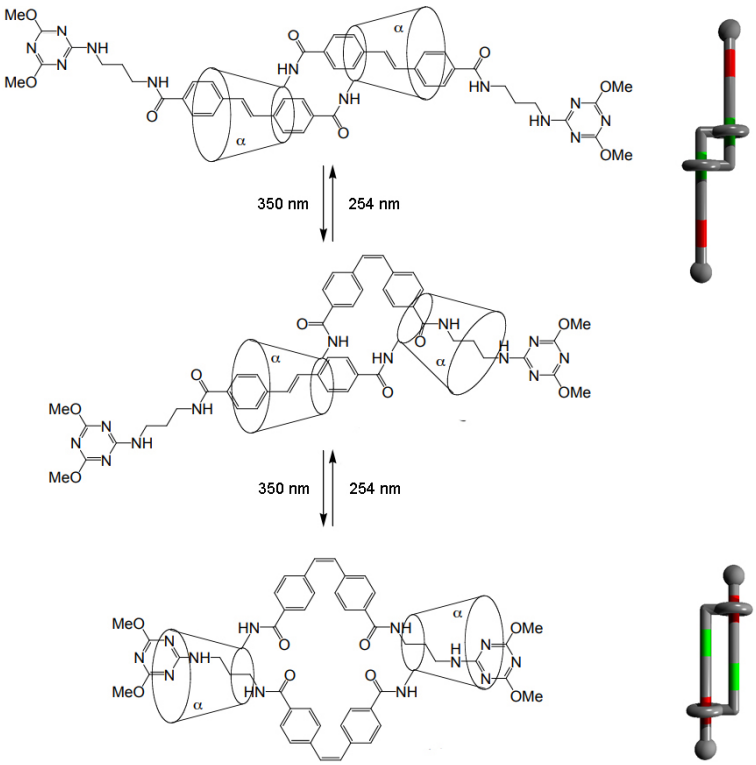

Figure 1.7: Contraction and elongation of a light-driven molecular switch with stilbene and α-cyclodextrin rings by Easton et al.,[10] accompanied by simplified models on the right.

Solvent polarity is a common control factor of isomerization. Leigh et al.[18] reported a [2]rotaxane with an axle consisting of a C_{11} alkyl chain and a glycylglycine hydrogen-bonding binding site for a ring containing nitrophenyl and pyridinium moieties. This rotaxane switch operates by disruption of hydrogen bonding between ring and axle upon addition of solvent polarity such as DMSO (see figure 1.13).

Temperature-controlled switching is inherently driven by entropy. Starting from its enthalpically favorable state, thermally driven rotaxane switches rearrange to the entropically favored state as increasing temperature scales up the entropic part of free energy.

Bottari et al.[11] reported a rotaxane of benzylic amide ring, which forms hydrogen-bonds to two sites on the bended axle at room temperature. Gentle heating stretches out the molecular axle in high efficiency and harbors the ring in amide ester site (See figure 1.8).

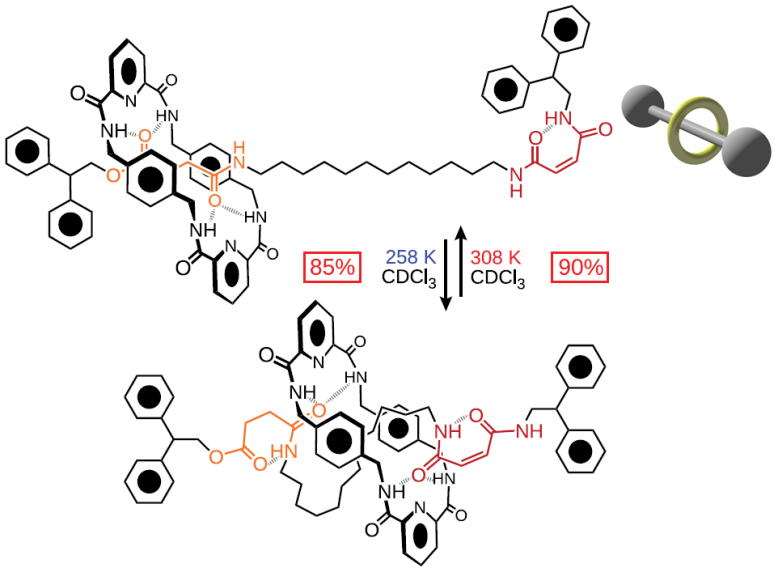

Figure 1.8: Thermally driven rotaxane switch.[11] At room temperature benzylic amide ring forms hydrogen-bonds to two sites of the bended axle. Gentle heating will result in ring harboring in amide ester site and stretching out of molecular axle. Figure from Carson and Stoddart[12] , accompanied by simplified model on the right.

1.2.2 Molecular switch by chemical input

Redox-driven switching is the first switching mechanism to be developed making use of oxidation-reduction to change the ring's site preference. Shortly following the first report of "molecular shuttle", Stoddart's group reported a refined version of molecular shuttle which is controlled electrochemically[13] (see figure 1.9). A [2]rotaxane with tetracationic cyclophane, cyclobis(paraquat-p-phenylene) ($CBPQT^{4+}$) ring is threaded onto an axle with biphenol and benzidine sites as π-electron donor. Following the oxidation in which benzidine site loses an electron,the biphenol site becomes a stronger π-electron donor and grabs the ring. This process can be reversed by reduction.

Sauvage's group succeeded in imitating muscle sarcomere expansion and contraction in molecular length by exchanging transition metal ion templates in a Janus [2]rotaxane.[41] In one of their work on ionic-driven molecular switch[14] (see figure 1.10), copper-I ions

pair with phenanthroline ligands on both the rings and axles in a tetrahedral geometry, resulting in a rotaxane in elongated state. Replacement of copper-I ions with zinc-II ions will see zinc ions pairing up with tridentate terpyridine ligands instead to afford the contracted state of rotaxane.

Pairing of dialkylammonium salts and crown ethers provides a suitable mechanism to design molecular switches driven by pH. Stoddart's group have carried out extensive work on this type of switch.[15,42] The ring sits at the dialkylammonium site under acidic conditions and the molecule is in a contracted state. Addition of base deprotonates the dialkylammonium site and sabotages the hydrogen-bonds. The ring then resides on the $BYPM^{2+}$ site instead and the molecule is stretched out to an elongated state. This rotaxane switch can be polymerized to create macroscopic motion accumulated by switching on all rotaxane monomers (see figure 1.11).

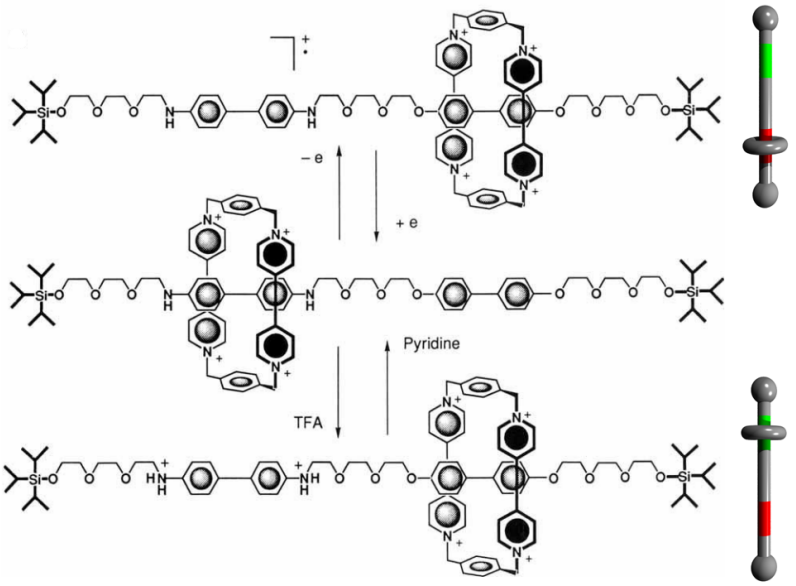

Figure 1.9: The first redox driven molecular switch by Stoddart's group,[13] accompanied by simplified models on the right. In this rotaxane switch the $CBPQT^{4+}$ ring prefer to harbor at benzidine site on the left. Either by oxidation or protonation on benzidine site, the ring shifts to the biphenyl site preferentially.

1.3 Harvesting motion of MIMs

Externally-driven motion, particularly single molecule actuation, has been demonstrated in a growing list of examples. Juluri et al.[17] reported a redox-driven palindromic [3]rotax-

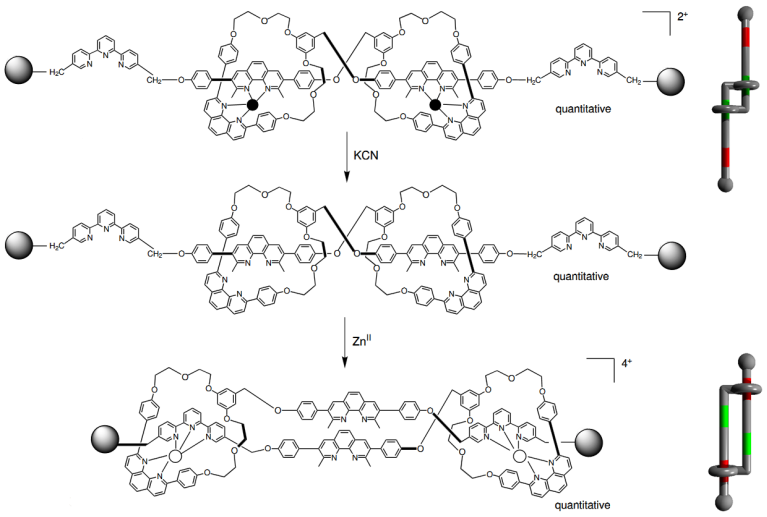

Figure 1.10: Rotaxane switching by replacement of copper-I ion with zinc-II ion,[14] accompanied by simplified models on the right.

ane switch with the two rings tethered to a mica-surface (see figure 1.12 right). The redox reaction drives the two rings to stations closer to each other, resulting in an optically-detectable bend of mica surface. Rotaxane switches also see application as valves in recently developed controlled-release mechanism,[43–45] in which rotaxane switches are end-grafted on mesoporous silica drug carriers. At specific external signals such as light[16,46,47] or redox reaction,[48] rings switch between stations to plug or unplug the drug carriers (see figure 1.12 left).

Apart from utilizing a rotaxane switch as a single-molecule mechanical component, the ring location on a rotaxane switch can impact on physical properties of the molecules in solutions. One currently reported example is the solvent-driven rotaxane switch by Leigh et al.[18] In non-polar solvent, no fluorescence can be detected under UV-light because the macrocycle ring resides near an anthracene stopper and effectively quenches the anthracene fluorescence. Addition of a polar solvent like dimethylsulfoxide (DMSO) results in relocation of the ring and recovery of the fluorescence. By masking part of solution containing their solvent-driven switch away from DMSO vapor (shown in figure 1.13), fluorescence patterns of the unmasked area can be observed.

Other than the notion of these length-extending switches to produce mechanical work, these molecules in solution also provide interesting properties. Such rotaxane switches

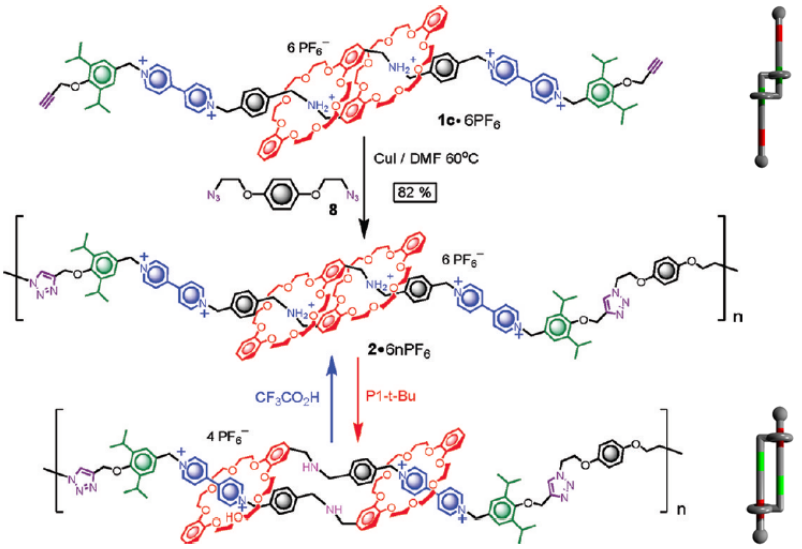

Figure 1.11: A polymerized Janus[2]rotaxane switch driven by addition of acid or base,[15] accompanied by simplified models on the right. Length change of monomers are accumulated to create macroscopic motion.

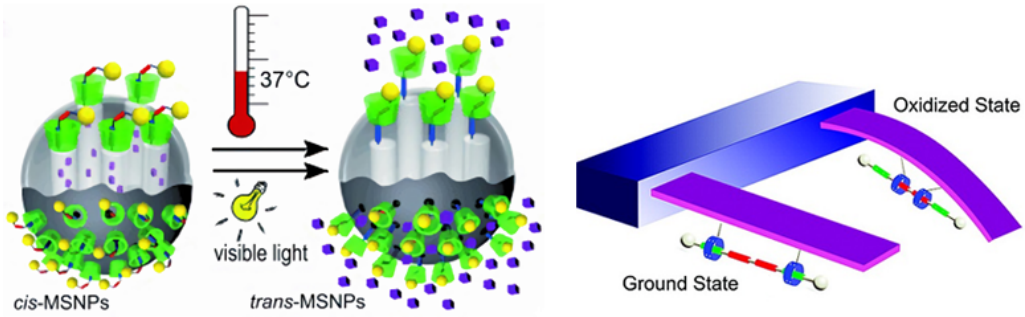

Figure 1.12: Left: A controlled delivery molecular device with rotaxane switch valves which can open under heat or light by switching the ring to sites further from drug carrier.[16] Right: A Palindromic [3]rotaxane switch with two rings tethered to a mica surface. Switching by redox reacting is strong enough to produce an optically-detectable bend on surface.[17]

change not only length but also excluded volume, i.e. the volume that a molecule excludes other molecules from. In this thesis, we describe two physical features associated with the change in excluded volume with switching of a 2-state rotaxane molecules: isotropic-nematic liquid crystalline phase transition and colloidal depletion interaction.

1.3.1 Isotropic-nematic liquid crystalline phase transition

Liquid crystalline phases are phases where particles align like crystals and simultaneously flow like liquid. The discovery of liquid crystals dates back to the mid-late 19th century. Chemists and biologists back then observed anisotropic optical behavior in liquefied sub-

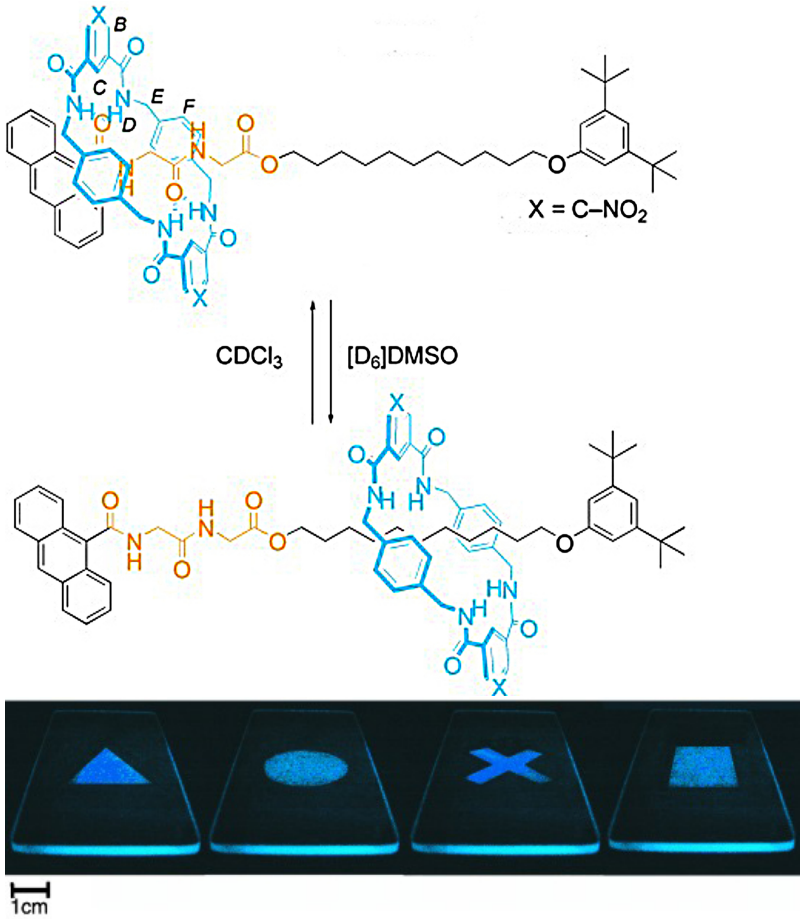

Figure 1.13: Top: Rotaxane switches by Leigh et al.[18] driven by solvent polarity. Bottom: One of the Leigh's solvent-driven switches[18] shows fluorescence controlled by switching. Different fluorescence patterns are shown by masking the solution film containing the solvent-driven switch and exposing the unmasked area with DMSO vapor.

stances near their melting points. In 1888, Austrian botanist Friedrich Reinitzer observed two "melting points" of cholesteryl benzonate, between which an iridescent color was observed.[49] He later discussed his findings with German physicist Otto Lehmann, who later confirmed and investigated the discovery using polarized optical microscope with a hot stage.[50] This marked the discovery of the liquid crystalline phase. Early work on liquid crystals were primarily focused on observation and classification level. In 1922, George Friedel introduced a classification scheme and identified 3 main liquid crystalline phases (shown in figure 1.14) based on the alignment pattern of liquid crystal.[19]

Liquid Crystal Displays (LCD) are currently the most recognizable application of liquid crystals. In 1962 Richard Williams[51] discovered that an electric field can direct the orien-

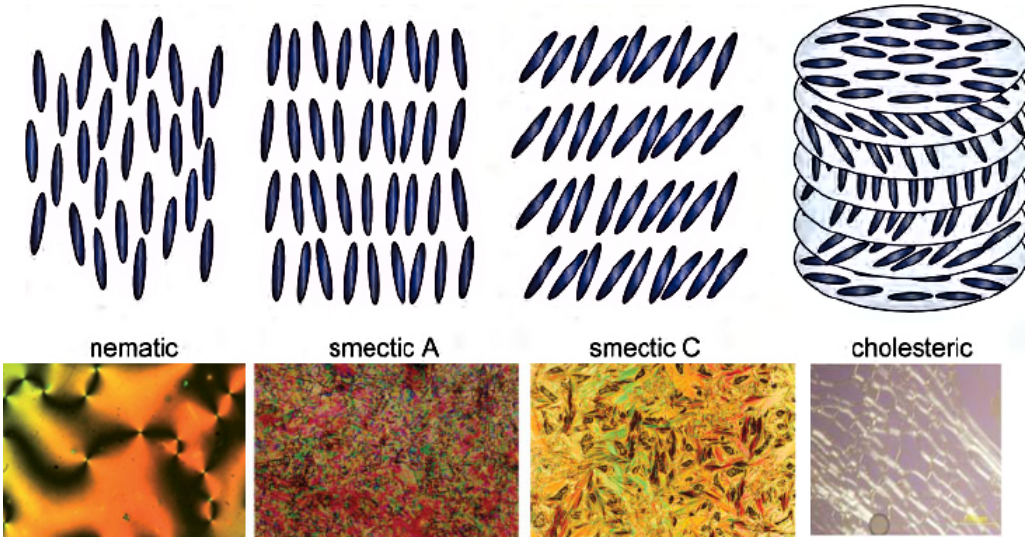

Figure 1.14: Top: Graphic illustration of liquid crystalline phases characterized by George Friedel.[19] Figure from Matsui.[20] Bottom: The texture of nematic phase,[21] smectic A & C phases[22] and cholesteric phase[23] under microscope. In nematic phase, molecule has long-range orientation order but no translational order; In smetic phase, paticles are ordered along one direction as well as forming well-defined layers; For chiral particles only, cholesteric phase is a phase consists of layers of nematic phase with different directors.

tation of a nematic liquid crystal, forming what he referred to as "domain". Commercial application of this discovery remain elusive though as Williams' liquid crystal must be heated over 100 °C to operate. Based on Williams' work, George Heilmeier[25] discovered what he named the "dynamic scattering mode" (DSM) by applying a stronger electric field on the liquid crystal in Williams' "domain" (see figure 1.15). Combined with the synthesis of room temperature p-aminophenyl acetate liquid crystals by his group, DSM became the first commercially feasible liquid crystal display (LCD). Compared to the display instrument of that date, like the Nixie tubes which operated at over 100V, the LCD proved far superior and took over as the major display component since its major commercialization in 1970s.[24]

Traditionally, Liquid crystals is also classified by the control factor of formation. Temperature controlled liquid crystals are thermotropic and those controlled by concentration are lyotropic. From a solid-fluid transition point of view,thermotropic and lyotropic liquid crystallinity are actually related. One can consider a system of asymmetric particles as McMillan - Mayer solution and construct phase diagram of dimensionless pressure versus dimensionless density. Ordering phase occurs as pressure increase. Pressure is propor-

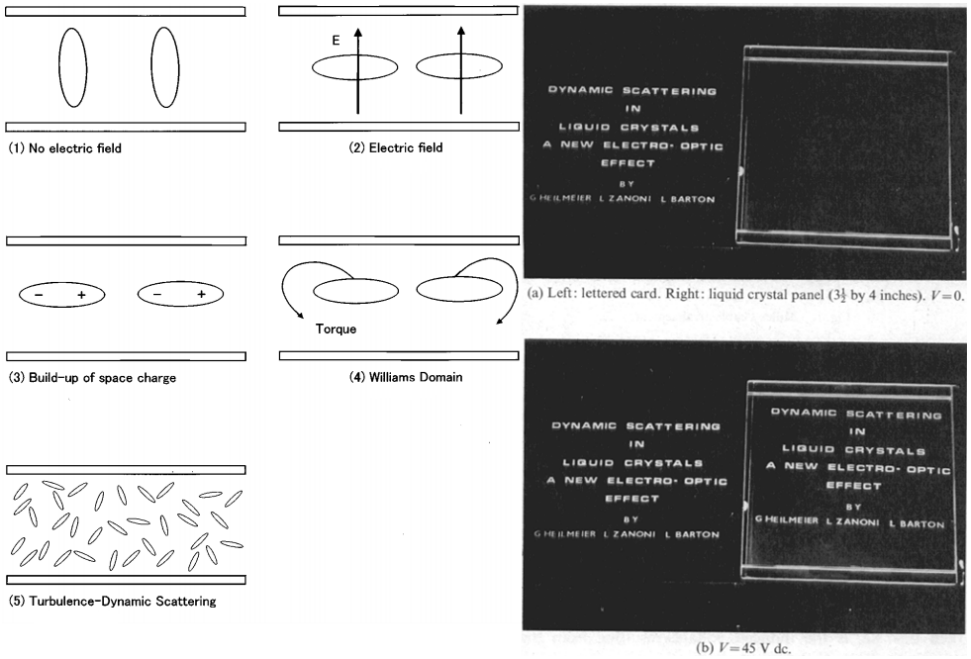

Figure 1.15: Left: Graphic illustration of DSM by T.Wada.[24] As the applied electric field on liquid crystal increase, the liquid crystal lines up parallel to the electrode plates (2), and build up charge (3). A shear torque then occur as a result of induced field and external field, causing spinning of molecules, corresponding to the Williams domain (4). Further increase of electric field then drives the molecules into mechanically unstable turbulence, in which molecules randomly scatter light and turn the solution from transparent to milky white (5). Right: Laboratory Demonstration of DSM working, figure by Heilmeier et al.[25]

tional to the inverse temperature. Thus the ordering phase can be considered as brought by either pressure increase or concentration decrease. Similar arguments were made on hard-sphere solid liquid transition by Monson and Kofke.[52]

Onsager[53] first predicted an isotropic-nematic transition of lyotropic liquid crystals, by treating the system as a non-ideal gas of rod-like molecules, which excluded each other by their own volume. Onsager's work considers the lyotropic liquid crystal formation as a purely entropic process: At low concentration, particles have full orientational and translational freedom to maximize entropy. As the concentration increases, particles with large aspect ratio and unrestricted directors attract a high energy penalty due to mutual exclusion. The nematic phase is formed by lining up directors of particles so that more particles can be accommodated with the same level of translational freedom. Onsager predicted two critical concentrations in the isotropic-nematic phase transition: the maximum concentration of pure isotropic phase and minimum concentration of a pure nematic

phase. At constant temperature, the only way to obtain a nematic phase from an isotropic solution is to added more molecules. In this PhD thesis, I describe how the switching of 2-state rotaxane molecules can lead to an isotropic to nematic lyotropic phase transition without changing the overall concentration. A more surprising result is that at certain concentrations, direct isotropic-nematic phase transition bypassing coexistent phase can be achieved and that not all molecules need to be switched to affect a transition.

Other important theoretical work on liquid crystal not presented in this thesis includes theory of isotropic-nematic transition of thermotropic liquid crystal using a mean-field approach averaging inter-molecular potential between adjacent particles, by Maier and Saupe[54–56] in 1958 . This theory was later extended to model transition to smetic phase by McMillan.[57] We do not consider thermotropic systems in this thesis.

1.3.2 Depletion interaction

Well before the 1950s, the depletion interaction had been observed in dense solutions and was applied practically in industry. In the early 20th century, the booming rubber industry required a way to effectively concentrate rubber latex for the sake of transportation. Traube[58] showed that adding polysaccharides extracted from seaweed results in separation of a rubber-rich layer from latex. Baker[59] then systematically investigate this process and found out that the rubber rich phase can return to suspension upon dilution. In 1953, Asakura and Oosawa[60,61] rationalised this behavior as an entropic effect arising from excluded-volume interactions. They presented a theory of a pair of parallel plate immersed in an ideal solution of non-adsorbing particles (The AO model). When the parallel plates are spaced close together, a separation smaller than depletant size, an attractive interaction between the plates develops, because of an osmotic pressure difference between pure solvent in the gap and solution outside the gap. This attractive interaction due to these smaller additive molecules was coined the "depletion interaction". Asakura and Oosawa's theory was subsequently proved by Sieglaff 's experiment,[62] in which a depletion-induced aggregation occurred by adding polystyrene in a microgel-toluene solution. The short range of the depletion attractions and the presence of long-ranged interaction, such as electrostatic interactions, makes measurement of the depletion interaction a challeng-

ing task. Pashley et al[63] and Richetti et al[64] successfully measured the depletion force between two mica plates coated with cetyltrimethylammonium bromide (CTAB) using surface force apparatus. Later measurement methods employ small-angle neutron scattering (SANS),[65] optical tweezer,[66] Total internal reflection microscopy (TIRM)[67–70] and colloidal probe AFM.[71] Also worth mentioning is a direct depletion force measurement by Ohshima et al[72] using a gradually increase in laser radiation pressure.

As an extension of the AO model, Vrij[73] worked on the theory of depletion due to non-adsorbing polymers treated as small penetrable spheres (illustrated in figure 1.16). Theoretical methods of polymers such as mean-field treatment[74,75] and numerical self-consistent field (SCF) method[76] were used to describe the depletion interaction.

Asakura and Oosawa[61] have recognized rod-like particles to be highly effective depletant (illustrated in figure 1.17). This was confirmed by Koenderink et al.[77] by experiment which found depletion driven crystallization occur at $\approx 0.5\%$ of rod-like depletants. Mao, Cates and Lekkerkerker[78–80] presented detailed theory of the depletion interaction due to rod-like particles. In this thesis, their numerical methods are generalised to find the depletion interaction due to any mixture of rod-like depletants. As the depletion interaction depends strongly on the dimension of depletant, we suggest using length-extending rotaxane switches as depletant molecules. These novel depletants allow one to "switch" the attractive depletion interaction, possibly allowing one to change colloidal stability not by dilution, but by external factors (light, pH) that switch individual molecules.

1.4 Thesis Outline

The main goal of this thesis is to investigate the effect rotaxane switching on liquid crystalline behavior and on the depletion interaction, using statistical mechanical methods.

In Chapter 2, A liquid crystal solution of rotaxane switch that change length under external stimuli is described using the statistical mechanical theory of lyotropic liquid crystals. In our first publication,[81] we assume the rotaxane switch isomerizes quantitatively between two different lengths. We predicted possible isotropic-nematic phase transition by length

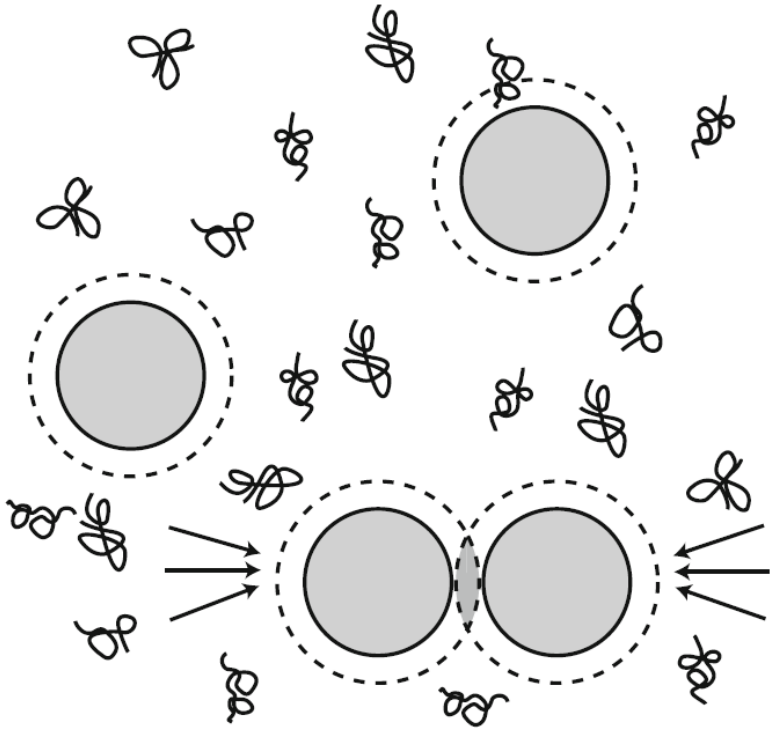

Figure 1.16: Graphic illustration of depletion interaction of colloidal spheres due to non-adsorbing depletants. The dashed area around the sphere indicates the depletion layer, in which depletion force takes effect. When the spheres are in close proximity, the polymers lost translational freedom in the space of overlapping depletion layers, resulting in an unbalanced force pushing colloidal spheres together. Figure from Lekkerkerker and Tuinier.[26]

switching of the rotaxanes at constant concentration. A direct isotropic to nematic phase transition bypassing the coexistence phase can be achieved. The second publication of this chapter is a further development of the theory taking into account switching inefficiency,[82] that is, where external driving force does not quantitatively switch the rotaxane in solution. We introduce a framework that will inform synthetic chemists of requirements in chemical design, such as switching efficiencies, length changes, and concentrations, in order to create rotaxane switches capable of driving isotropic-nematic phase transition by external switching.

In Chapter 3, our publication[83] on the statistical mechanical description of a liquid crystalline solution of adaptive rotaxane switch is presented. "Adaptive" means the free energy difference between states of a rotaxane switch are small and can therefore respond to its surrounding environment-molecular switching does not need to be driven by an external factor. We present the critical concentration of adaptive rotaxane liquid crystal of various

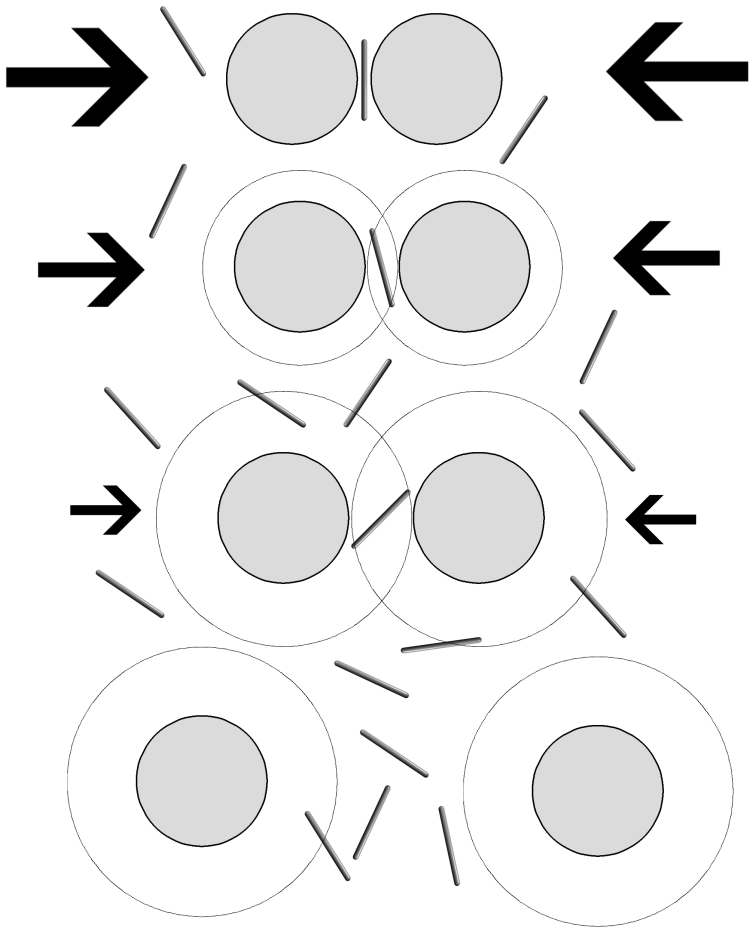

Figure 1.17: Graphic illustration of depletion interaction of colloidal spheres due to rod-like depletants. The dashed area around the sphere indicates the depletion layer, in which depletion force takes effect. Compare to spherical depletants at same volume fraction, rod-like depletants are more effective depletants. Elongated shape and rotational freedom of rods increase the range of depletion interaction.

length ratio, and the composition of rotaxane switch states in both isotropic and nematic phase.

In Chapter 4, our manuscript on the theory of depletion due to a rod-like molecular switch that changes length under external stimuli (not adaptive) is presented. We provided a statistical mechanical description of depletion due to bidisperse rod-like molecules. And based on this description, we predict that a solution of rotaxane switches as depletants can dramatically change the range and magnitude of the depletion force via externally-driven switching, providing a new strategy to manipulate colloid stability.

1.5 References

[1] Nagatoshi Koumura, Robert W. J. Zijlstra, Richard A. van Delden, Nobuyuki Harada, and Ben L. Feringa. Light-Driven Monodirectional Molecular Rotor. *Nature*, 401:152–155, 1999.

[2] Tibor Kudernac, Nopporn Ruangsupapichat, Manfred Parschau, Beatriz Maciá, Nathalie Katsonis, Syuzanna R. Harutyunyan, Karl-Heinz Ernst, and Ben L. Feringa. Electrically Driven Directional Motion of a Four-Wheeled Molecule on a Metal Surface. *Nature*, 479:208–211, 2011.

[3] E. M. Sevick and D. R. M. Williams. Piston-Rotaxanes as Molecular Shock Absorbers. *Langmuir*, 26(8):5864–5868, 2010.

[4] G. Schill and C. Zürcher. [3]-Catenanes. *Angew. Chem. Int. Ed.*, 8(12):988–988, 1969.

[5] Gottfried Schill and Hubertus Zollenkopf. Rotaxan-Verbindungen, I1). *Justus Liebigs Ann. Chem.*, 721(1):53–74, 1969.

[6] Christaine O. Dietrich-Buchecker, Jean Pierre Sauvage, and Jean Marc Kern. Templated Synthesis of Interlocked Macrocyclic Ligands: The Catenands. *J. Am. Chem. Soc*, 106(10):3043–3045, 1984.

[7] James D. Crowley, Stephen M. Goldup, Ai-Lan Lee, David A. Leigh, and Roy T. McBurney. Active Metal Template Synthesis of Rotaxanes, Catenanes and Molecular Shuttles. *Chem. Soc. Rev.*, 38:1530–1541, 2009.

[8] G. Schill and A. Lüttringhaus. The Preparation of Catena Compounds by Directed Synthesis. *Angew. Chem. Int. Ed.*, 3(8):546–547, 1964.

[9] Pier Lucio Anelli, Neil Spencer, and J. Fraser Stoddart. A molecular shuttle. *J. Am. Chem. Soc.*, 113(13):5131–5133, 1991.

[10] Ryan E. Dawson, Stephen F. Lincoln, and Christopher J. Easton. The Foundation of a Light Driven Molecular Muscle Based on Stilbene and Alpha-Cyclodextrin. *Chem. Commun.*, (34):3980–3982, 2008.

[11] Giovanni Bottari, Francois Dehez, David A. Leigh, Phillip J. Nash, Emilio M. Pérez, Jenny K. Y. Wong, and Francesco Zerbetto. Entropy-Driven Translational Isomerism: A Tristable Molecular Shuttle. *Angew. Chem. Int. Ed.*, 42(47):5886–5889, 2003.

[12] Carson J. Bruns and J. Fraser Stoddart. *The Nature of the Mechanical Bond: From Molecules to Machines*. John Wiley & Sons, Inc., Hoboken, New Jersey, 2017.

[13] Richard A Bissell, Emilio Córdova, Angel E. Kaifer, and J. Fraser Stoddart. A Chemically and Electrochemically Switchable Molecular Shuttle. *Nature*, 369:133–137, 1994.

[14] M. Consuelo Jiménez, Christiane Dietrich-Buchecker, and Jean-Pierre Sauvage. Towards Synthetic Molecular Muscles: Contraction and Stretching of a Linear Rotaxane Dimer. *Angew. Chem. Int. Ed.*, 112(18):3422–3425, 2000.

[15] Lei Fang, Mohamad Hmadeh, Jishan Wu, Mark A. Olson, Jason M. Spruell, Ali Trabolsi, Ying-Wei Yang, Mourad Elhabiri, Anne-Marie Albrecht-Gary, and J. Fraser Stoddart. Acid-Base Actuation of [c2]Daisy Chains. *J. Am. Chem. Soc.*, 131(20):7126–7134, 2009.

[16] Hong Yan, Cathleen Teh, Sivaramapanicker Sreejith, Liangliang Zhu, Anna Kwok, Weiqin Fang, Xing Ma, Kim Truc Nguyen, Vladimir Korzh, and Yanli Zhao. Functional Mesoporous Silica Nanoparticles for Photothermal-Controlled Drug Delivery in-Vivo. *Angew. Chem. Int. Ed.*, 51(33):8373–8377, 2012.

[17] Bala Krishna Juluri, Ajeet S. Kumar, Yi Liu, Tao Ye, Ying-Wei Yang, Amar H. Flood, Lei Fang, J. Fraser Stoddart, Paul S. Weiss, and Tony Jun Huang. A Mechanical Actuator Driven Electrochemically by Artificial Molecular Muscles. *ACS Nano*, 3(2):291–300, 2009.

[18] David A. Leigh, M. Ángeles F. Morales, Emilio M. Pérez, Jenny K. Y. Wong, Carlos G. Saiz, Alexandra M. Z. Slawin, Adrian J. Carmichael, David M. Haddleton, A. Manfred Brouwer, Wybren Jan Buma, George W. H. Wurpel, Salvador León, and Francesco Zerbetto. Patterning through Controlled Submolecular Motion: Rotaxane-Based Switches and Logic Gates that Function in Solution and Polymer Films. *Angew. Chem. Int. Ed.*, 44(20):3062–3067, 2005.

[19] G. Friedel. Les États Mésomorphes de la Matière. *Ann. Phys.*, 9(18):273–474, 1922.

[20] Tatsunosuke Matsui. Numerical Simulation of Lasing Dynamics in Choresteric Liquid Crystal Based on ADE-FDTD Method. In *Numerical Simulations of Physical and Engineering Processes*, chapter 9. InTech, Rijeka, 2011.

[21] Sharmistha Ghosh, Nazma Begum, Srikanth Turlapati, Subir Kr. Roy, Abhijit. Kr. Das, and Nandiraju V. S. Rao. Ferroelectric-Like Switching in the Nematic Phase of Four-Ring Bent-Core Liquid Crystals. *J. Mater. Chem. C*, 2:425–431, 2014.

[22] Fabiano V. Pereira, Redouane Borsali, Olga M.S. Ritter, Paulo F. Gonçalves, Aloir A. Merlo, and Nadya P. da Silveira. Structure-Property Relationships of Smectic Liquid Crystalline Polyacrylates as Revealed by SAXS. *J. Braz. Chem. Soc*, 17:333 – 341, 04 2006.

[23] Maher A. Qaddoura, Kevin D. Belfield, and Paul A. Heiney. Liquid Crystal-Directed Assembly and Phase Morphology of a Squaraine Dye. *Supramol. Chem.*, 24(5):299–311, 2012.

[24] H. Kawamoto. The History of Liquid-Crystal Displays. *Proc. IEEE*, 90(4):460–500, 2002.

[25] G. H. Heilmeier, L. A. Zanoni, and L. A. Barton. Dynamic Scattering: A New Electrooptic Effect in Certain Classes of Nematic Liquid Crystals. *Proc. IEEE*, 56(7):1162–1171, July 1968.

[26] Henk N.W. Lekkerkerker and Remco Tuinier. *Colloids and the Depletion Interaction*. Springer Netherlands, 2011.

[27] L. Ruzicka, M. Stoll, and H. Schinz. Zur Kenntnis des Kohlenstoffringes II. Synthese der carbocyclischen Ketone vom Zehner- bis zum Achtzehnerring. *Helv. Chim. Acta*, 9(1):249–264, 1926.

[28] K. Ziegler, L. Jakob, H. Wollthan, and A. Wenz. XIII. Die ersten Einwirkungsprodukte von Alkalimetallen auf Butadiene. *Justus Liebigs Ann. Chem.*, 511(1):64–88, 1934.

[29] V. Prelog, L. Frenkiel, Magrit Kobelt, and P. Barman. Zur Kenntnis des Kohlenstoffringes. Ein Herstellungsverfahren für vielgliedrige Cyclanone. *Helv. Chim. Acta*, 30(6):1741–1749, 1947.

[30] Edel Wasserman. The Preparation of Interlocking Rings: a Catenane[1]. *J. Am. Chem. Soc*, 82(16):4433–4434, 1960.

[31] Ian Thomas Harrison and Shuyen Harrison. Synthesis of a Stable Complex of a Macrocycle and a Threaded Chain. *J. Am. Chem. Soc.*, 89(22):5723–5724, 1967.

[32] C.O Dietrich-Buchecker, J.P Sauvage, and J.P Kintzinger. Une Nouvelle Famille de Molecules : Les Metallo-Catenanes. *Tetrahedron Lett.*, 24(46):5095 – 5098, 1983.

[33] Pierre Mobian, Jean-Marc Kern, and Jean-Pierre Sauvage. A [2]Catenane Constructed around a Ru(Diimine)$_3^{2+}$ Complex Used as a Template. *J. Am. Chem. Soc.*, 125(8):2016–2017, 2003.

[34] Anne-Marie L. Fuller, David A. Leigh, Paul J. Lusby, Alexandra M. Z. Slawin, and D. Barney Walker. Selecting Topology and Connectivity through Metal-Directed Macrocyclization Reactions: A Square Planar Palladium [2]Catenate and Two Noninterlocked Isomers. *J. Am. Chem. Soc.*, 127(36):12612–12619, 2005.

[35] Peter R. Ashton, Timothy T. Goodnow, Angel E. Kaifer, Mark V. Reddington, Alexandra M. Z. Slawin, Neil Spencer, J. Fraser Stoddart, Cristina Vicent, and David J. Williams. A [2] Catenane Made to Order. *Angew. Chem. Int. Ed.*, 28(10):1396–1399, 1989.

[36] Christopher A. Hunter. Synthesis and Structure Elucidation of a New [2]-Catenane. *J. Am. Chem. Soc.*, 114(13):5303–5311, 1992.

[37] Harry Adams, Fiona J. Carver, and Christopher A. Hunter. [2]Catenane or not [2]Catenane? *J. Chem. Soc. , Chem. Commun.*, pages 809–810, 1995.

[38] Jonathan C. Barnes, Albert C. Fahrenbach, Dennis Cao, Scott M. Dyar, Marco Frasconi, Marc A. Giesener, Diego Benítez, Ekaterina Tkatchouk, Oleksandr Chernyashevskyy, Weon Ho Shin, Hao Li, Srinivasan Sampath, Charlotte L. Stern, Amy A. Sarjeant, Karel J. Hartlieb, Zhichang Liu, Raanan Carmieli, Youssry Y. Botros, Jang Wook Choi, Alexandra M. Z. Slawin, John B. Ketterson, Michael R. Wasielewski, William A. Goddard, and J. Fraser Stoddart. A Radically Configurable Six-State Compound. *Science*, 339(6118):429–433, 2013.

[39] Susumu Tsuda, Yoshio Aso, and Takahiro Kaneda. Linear Oligomers Composed of a Photochromically Contractible and Extendable Janus [2] Rotaxane. *Chem. Commun.*, (29):3072–3074, 2006.

[40] Shujing Li, Daisuke Taura, Akihito Hashidzume, and Akira Harada. Light-Switchable Janus [2]Rotaxanes Based on alpha-Cyclodextrin Derivatives Bearing Two Recognition Sites Linked with Oligo(ethylene glycol). *Chem. Asian. J.*, 5(10):2281–2289, 2010.

[41] Benoit Champin, Pierre Mobian, and Jean-Pierre Sauvage. Transition Metal Complexes as Molecular Machine Prototypes. *Chem. Soc. Rev.*, 36:358–366, 2007.

[42] Jishan Wu, Ken Cham-Fai Leung, Diego Benitez, Ja-Young Han, Stuart J. Cantrill, Lei Fang, and J. Fraser Stoddart. An Acid-Base-Controllable [c2]Daisy Chain. *Angew. Chem. Int. Ed.*, 47(39):7470–7474, 2008.

[43] I.I. Slowing, B.G. Trewyn, S. Giri, and V.S.-Y. Lin. Mesoporous Silica Nanoparticles for Drug Delivery and Biosensing Applications. *Adv. Funct. Mater*, 17(8):1225–1236, 2006.

[44] Monty Liong, Sarah Angelos, Eunshil Choi, Kaushik Patel, J. Fraser Stoddart, and Jeffrey I. Zink. Mesostructured Multifunctional Nanoparticles for Imaging and Drug Delivery. *J. Mater. Chem.*, 19:6251–6257, 2009.

[45] Fangqiong Tang, Linlin Li, and Dong Chen. Mesoporous Silica Nanoparticles: Synthesis, Biocompatibility and Drug Delivery. *Adv. Mater.*, 24(12):1504–1534, 2011.

[46] Derrick Tarn, Daniel P. Ferris, Jonathan C. Barnes, Michael W. Ambrogio, J. Fraser Stoddart, and Jeffrey I. Zink. A Reversible Light-Operated Nanovalve on Mesoporous Silica Nanoparticles. *Nanoscale*, 6:3335–3343, 2014.

[47] Menghuan Li, Hong Yan, Cathleen Teh, Vladimir Korzh, and Yanli Zhao. NIR-Triggered Drug Release from Switchable Rotaxane-Functionalized Silica-Covered Au Nanorods. *Chem. Commun.*, 50:9745–9748, 2014.

[48] Thoi D. Nguyen, Hsian-Rong Tseng, Paul C. Celestre, Amar H. Flood, Yi Liu, J. Fraser Stoddart, and Jeffrey I. Zink. A Reversible Molecular Valve. *Proc. Natl. Acad. Sci. U.S.A*, 102(29):10029–10034, 2005.

[49] Friedrich Reinitzer. Beiträge zur Kenntniss des Cholesterins. *Monatsh. Chem. Verw. Teile. Anderer. Wiss*, 9(1):421–441, 1888.

[50] Otto Lehmann. Über Fliessende Krystalle. *Z. Phys. Chem*, 4:462–472, 1889.

[51] Richard Williams. Domains in Liquid Crystals. *J. Chem. Phys*, 39(2):384–388, 1963.

[52] P. A. Monson and D. A. Kofke. *Solid-Fluid Equilibrium: Insights from Simple Molecular Models*, pages 113–179. John Wiley & Sons, Ltd, 2000.

[53] L Onsager. The Effects of Shape on the Interaction of Colloidal Particles. *Ann. N. Y. Acad. Sci.*, 51(4):627–659, 1949.

[54] W. Maier and A. Saupe. Eine Einfache Molekulare Theorie des Nematischen Kristallinflüssigen Zustandes. *Z. Naturforsch. A*, 13(7):564–566, 1958.

[55] W. Maier and A. Saupe. Eine Einfache Molekular-Statistische Theorie der Nematischen Kristallinflüssigen Phase. Teil l. *Z. Naturforsch. A*, 14(10):882–889, 1959.

[56] W. Maier and A. Saupe. Eine Einfache Molekular-Statistische Theorie der Nematischen Kristallinflüssigen Phase. Teil II. *Z. Naturforsch. A*, 15(4):287–292, 1960.

[57] W. L. McMillan. Simple Molecular Model for the Smectic *A* Phase of Liquid Crystals. *Phys. Rev. A*, 4:1238–1246, 1971.

[58] J. Traube. *Gummi Zeitung.*, 39:434, 1929.

[59] H. C. Baker. The Concentration of Latex by Creaming. *Trans. Inst. Rubb. Ind.*, 13(1):70–82, 1937.

[60] Sho Asakura and Fumio Oosawa. Interaction between Particles Suspended in Solutions of Macromolecules. *J. Polym. Sci. A*, 33(126):183–192, 1958.

[61] Sho Asakura and Fumio Oosawa. On Interaction between Two Bodies Immersed in a Solution of Macromolecules. *J. Chem. Phys*, 22(7):1255–1256, 1954.

[62] Charles L. Sieglaff. Phase Separation in Mixed Polymer Solutions. *J. Polym. Sci. A*, 41(138):319–326, 1959.

[63] R. M. Pashley and B. W. Ninham. Double-Layer Forces in Ionic Micellar Solutions. *J. Phys. Chem*, 91(11):2902–2904, 1987.

[64] P. Richetti and P. Kékicheff. Direct Measurement of Depletion and Structural Forces in a Micellar System. *Phys. Rev. Lett.*, 68:1951–1954, 1992.

[65] X. Ye, T. Narayanan, P. Tong, J. S. Huang, M. Y. Lin, B. L. Carvalho, and L. J. Fetters. Depletion Interactions in Colloid-Polymer Mixtures. *Phys. Rev. E*, 54:6500–6510, 1996.

[66] Ritu Verma, J. C. Crocker, T. C. Lubensky, and A. G. Yodh. Attractions between Hard Colloidal Spheres in Semiflexible Polymer Solutions. *Macromolecules*, 33(1):177–186, 2000.

[67] Amber Sharma and John Y. Walz. Direct Measurement of the Depletion Interaction in a Charged Colloidal Dispersion. *J. Chem. Soc., Faraday Trans.*, 92:4997–5004, 1996.

[68] K. D. Hörner, M. Töpper, and M. Ballauff. Assessment of the Depletion Forces in Mixtures of a Polystyrene Latex and Hydroxyethyl Cellulose by Turbidimetry. *Langmuir*, 13(3):551–558, 1997.

[69] D. Rudhardt, C. Bechinger, and P. Leiderer. Direct Measurement of Depletion Potentials in Mixtures of Colloids and Nonionic Polymers. *Phys. Rev. Lett.*, 81:1330–1333, 1998.

[70] Dzina Kleshchanok, Remco Tuinier, and Peter R. Lang. Depletion Interaction Mediated by a Polydisperse Polymer Studied with Total Internal Reflection Microscopy. *Langmuir*, 22(22):9121–9128, 2006.

[71] W. Knoben, N. A. M. Besseling, and M. A. Cohen Stuart. Direct Measurement of Depletion and Hydrodynamic Forces in Solutions of a Reversible Supramolecular Polymer. *Langmuir*, 23(11):6095–6105, 2007.

[72] Y. N. Ohshima, H. Sakagami, K. Okumoto, A. Tokoyoda, T. Igarashi, K. B. Shintaku, S. Toride, H. Sekino, K. Kabuto, and I. Nishio. Direct Measurement of Infinitesimal Depletion Force in a Colloid-Polymer Mixture by Laser Radiation Pressure. *Phys. Rev. Lett.*, 78:3963–3966, 1997.

[73] A.Vrij. Polymers at Interfaces and the Interactions in Colloidal Dispersions. *Pure Appl. Chem*, 48(1):471 – 483, 1976.

[74] J. F. Joanny, L. Leibler, and P. G. De Gennes. Effects of Polymer Solutions on Colloid Stability. *Journal of Polymer Science: Polymer Physics Edition*, 17(6):1073–1084, 1979.

[75] Robert I Feigin and Donald H Napper. Depletion Stabilization and Depletion Flocculation. *J. Colloid Interface Sci*, 75(2):525 – 541, 1980.

[76] J.M.H.M. Scheutjens and G.J. Fleer. Effect of Polymer Adsorption and Depletion on the Interaction between Two Parallel Surfaces. *Adv. Colloid Interface Sci*, 16(1):361 – 380, 1982.

[77] G. H. Koenderink, G. A. Vliegenthart, S. G. J. M. Kluijtmans, A. van Blaaderen, A. P. Philipse, and H. N. W. Lekkerkerker. Depletion-induced crystallization in colloidal rodsphere mixtures. *Langmuir*, 15(14):4693–4696, 1999.

[78] Y. Mao, M. E. Cates, and H. N. W. Lekkerkerker. Depletion Stabilization by Semidilute Rods. *Phys. Rev. Lett.*, 75:4548–4551, 1995.

[79] Y. Mao, M. E. Cates, and H. N. W. Lekkerkerker. Theory of the Depletion Force due to Rodlike Polymers. *J. Chem. Phys*, 106(9):3721–3729, 1997.

[80] Y. Mao, P. Bladon, H. N. W. Lekkerkerker, and M. E. Cates. Density Profiles and Thermodynamics of Rod-Like Particles between Parallel Walls. *Mol. Phys*, 92(1):151–159, 1997.

[81] Hao He, Edith M. Sevick, and David R. M. Williams. Fast Switching from Isotropic Liquids to Nematic Liquid Crystals: Rotaxanes as Smart Fluids. *Chem. Commun.*, 51:16541–16544, 2015.

[82] Hao He, Edith M. Sevick, and David R. M. Williams. Rotaxane Liquid Crystals with Variable Length: The Effect of Switching Efficiency on the Isotropic-Nematic Transition. *J. Chem. Phys*, 148(13):134905, 2018.

[83] Hao He, Edith M. Sevick, and David R. M. Williams. Isotropic and Nematic Liquid Crystalline Phases of Adaptive Rotaxanes. *J. Chem. Phys*, 144(12):124901, 2016.

Chapter 2

Fast Switching from Isotropic to Nematic Liquid Crystal with Rotaxane Switch

Work on this topic consists of 2 major publications. The first paper published in Chemical Communications is a qualitative study showing that rotaxane switches is capable of triggering isotropic-nematic phase transition by change in molecule dimension during switching. The second publication published in The Journal of chemical Physics is a detailed follow-up study taking switching inefficiency into account.

The research presented in this publication was solely completed by the author of this thesis. The author was the main contributor to the statistical mechanical model and numerical calculations in these two publication.

2.1 Isotropic-Nematic Phase Switching upon Complete Isomerization of Rotaxane Switch

ChemComm

COMMUNICATION

View Article Online
View Journal | View Issue

Cite this: *Chem. Commun.*, 2015, **51**, 16541

Received 21st August 2015,
Accepted 23rd September 2015

DOI: 10.1039/c5cc07048a

www.rsc.org/chemcomm

Fast switching from isotropic liquids to nematic liquid crystals: rotaxanes as smart fluids

Hao He,[a] Edith M. Sevick[a] and David R. M. Williams[b]

We examine a solution of rod-like piston-rotaxanes, which can switch their length by external excitation (for example optically) from a short state of length *L* to a long state of length *qL*. We show that this solution can exhibit a number of different behaviours. In particular it can rapidly switch from an isotropic to a nematic liquid crystalline state. There is a minimum ratio *q = 1.13 for which transitions from a pure isotropic state to a pure nematic state are possible. We present a phase-switching diagram, which gives the six possible behaviours for this system. It turns out that a large fraction of the phase switching diagram is occupied by the transition from a pure isotropic to a pure nematic state.**

A rotaxane is a "wheel and axle" molecule,[1–3] where a ring is threaded onto an axle that is capped with stoppers at both ends to prevent the ring from falling off. Such mechanically or topologically interlocked molecules have been synthesized for many years and represent a very active area of chemical synthesis. Chemists have designed these rotaxanes to act as a 2-state switch: they build 2 different "stations" or attractive sites into the axle and entice the ring to reside at one or the other station, depending upon external influences. The external influence, can be due to pH[4] and ion interaction, redox reaction,[5] solvent quality, or light.[5,6] Many examples are given in the review by Bruns and Stoddart.[5] A rigid rod attached to the moveable ring provides one way to monitor or control this internal switch: using AFM, Brough *et al.*[7] measured the work required to mechanically push a ring off of an attractive station and Sevick and Williams[8] predicted how such a rotaxane, loaded with inert rings that freely translate on the axle, acts as a molecular-scale shock absorber. As the rod is of the same length as the axle (or larger) switching also brings about a considerable change in the dimension of the molecule (Fig. 1)

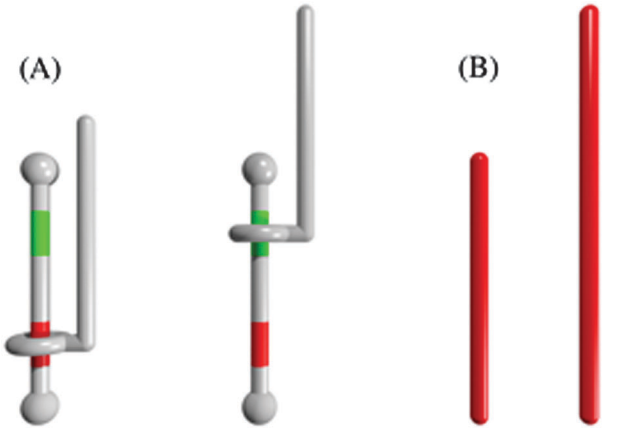

Fig. 1 (A) An illustration of a [2]-rotaxane with attractive stations (denoted by red & green) built into the axle and a rod attached to the interlocked ring in (left) the short state, and (right) the long state. The reversible switching between short and long states provides an added mechanism to switch between an isotropic and a nematic liquid crystalline phases, which exhibit strikingly different optical properties. (B) The simplified model of this structure where a cylinder extends from a length *L* to a length *qL*, at fixed diameter *d*.

and this switchable molecular size can create interesting new smart fluids. In this communication, we describe quantitatively how a solution of 2-state rotaxane switches, appended with a rigid rods, provides externally switchable liquid crystalline phase transitions. There has been some previous work on liquid crystalline rotaxane systems,[9–11] but our study is very different.

Liquid crystals are solutions of anisotropic molecules which flow like a liquid, but can have phases which possess different degrees of molecular orientation.[12] They come in many different forms. Here we examine a lyotropic system where a solution of rods undergoes the transition. In dilute solutions, the fixed-sized, anisotropic molecules have no long-range translational or orientational order – the solution of molecules is isotropic. However, with increased concentration a nematic phase appears where the molecules have no long-range translational order, but self-align to have directional order along their long axis.[12]

[a] *Research School of Chemistry, The Australian National University, Canberra, ACT, 0200, Australia*
[b] *Department of Applied Mathematics, Research School of Physical Sciences & Engineering, The Australian National University, Canberra, ACT, 0200, Australia. E-mail: D.Williams@anu.edu.au*

The important point for applications is that the aligned nematic phase is birefringent, and can be easily detected optically using cross polarised filters. This fact, and their alignment by electric fields is the basis of liquid crystalline displays.

The usual transition from isotropic to nematic is based either on increasing the concentration (lyotropics) or decreasing the temperature (thermotropics). In this paper we show that, for a lyotropic system, by keeping the concentration fixed, but switching the rod length, we can easily transition from an optically inactive isotropic phase to a birefringent nematic phase. This gives us a system whose bulk optical properties can be externally switched.

Our quantitative calculation is based upon Onsager's classical treatment,[13] applied to a simple model of a 2-state rotaxane switch. Onsager's theory assumes a solution of volume-excluding rods where the solvent fills the space surrounding the rods. Alignment of the rods leads to a decrease in rotational entropy but may also increase the volume available for placement of the rod's center of mass, or in other words, may increase the translational entropy. Onsager's theory captures this competition between rotational and translational entropy over a concentration range of rods of fixed length. In our extension of this model, we consider a molecular switch that has two possible states, long and short, depending upon the residential station of the ring With the rod and axle of the same length, and with the stations placed near the ends of the axle, the extent of the molecule can switch from length L to length qL. In our description, we limit the ratio of long to short states to $1 \leq q \leq 2$ although q can be increased beyond 2 by linearly concatemerizing several such switches into a daisy-chain of extendable molecules. We assume that the switching action is 100% efficient: that is, the switches are all in either the short state or long state and there is no mixture of switch states. Analysis of a more complicated "polydisperse" systems is possible,[14] but for simplicity is avoided here in this first study.

The physics is essentially as follows. Consider the molecules as hard rods of length L, and diameter d. We assume only hard body interactions between the molecules. The model does have a solvent, but this is implicit, just as in the Flory theory for polymers – the effect of all the solvent and rod interactions is assumed to produce a hard-body interaction between the rods. The model does not rely on the chemical details of the solvent or the rods, and encompasses any system with effective hard-body interactions. At low concentrations c (number of molecules per unit volume), the molecules do not touch each other and do not interact. They thus minimise their free energy by maximising their entropy. Each rod has both translational entropy (associated with where in space its centre of mass is located), and rotational entropy (associated with the direction in which it points in space). At low c the cylinders thus are found distributed randomly throughout their container and point in random directions. This is the isotropic state. At higher concentrations the cylinders begin to interact. However, we have hard-body interactions and no overlaps are allowed. We now imagine two rods which are close to each other. The hard-body interactions imply that the only terms in the free energy are entropic. When two cylinders approach each other they suffer an excluded-volume interaction, which decreases their translational entropy. This penalty is lower if the angle between the cylinder axes, γ, is small, *i.e.* if they are closely aligned. The cylinders can thus increase their translational entropy by aligning. However, aligning, by definition decreases their rotational entropy, and they are now restricted in the directions they can point. In order to maximize the total entropy the cylinders adopt a compromise, and some alignment is the result. Because all the cylinders can interact in this way this produces a system where all the cylinders align roughly along one direction, producing a nematic phase. The degree of alignment is never perfect, but it increases as the concentration increases.

Experiments, computer simulation, and theory show that the transition from isotropic to nematic is 1st order, so there is a sudden jump in alignment from 0 to some finite value at critical concentration c_1. Moreover there is always a coexistence regime, where isotropic and nematic states coexist in a single sample. Furthermore the concentration of molecules in the nematic state, c_2, is always greater than c_1. By gradually increasing c the following behaviour is observed. At small c the whole sample is isotropic. As c is increased the whole sample remains isotropic until c is slightly greater than c_1. At this point a small volume becomes nematic. Further small increases in c does not change the concentration in either phase, it remains at c_1 and c_2. All that occurs is that the volume of the nematic phase gradually grows at the expense of the isotropic phase. Eventually when $c = c_2$ the entire sample is nematic. Beyond this point any further increase in concentration leads to nematic phase with the concentration c.

This system is analogous to that of a hard sphere fluid with attractive interactions between the spheres. For a closed container, at low densities a gas phase is formed. As more material is added the gas density increases, until at a critical density a small section of the liquid phase forms in coexistence with the gas phase. As still more material is added the liquid phase increases in size but the gas and liquid phases each have constant density. Eventually all the container is liquid, and further addition of material merely increases the density of the liquid. The gas phase corresponds here to the isotropic phase, and the liquid phase to the higher density nematic phase.

We will not reproduce the calculation for the concentrations c_1 and c_2 here.[13–15] We note in passing that the excluded volume between two rods at an angle γ is $2L^2d|\sin\gamma|$. This is very different from the volume of a rod $\frac{\pi}{4}d^2L$, by a factor of $\sim L/d$, so that in the isotropic state a rod affects a volume much larger than its actual volume. We would thus expect that the critical concentrations c_1 and c_2 would be roughly $\sim 1/(L^2d)$. We shall use the results of the exact numerical solution:[14]

$$c_1 = 3.290(L^2d)^{-1} \quad c_2 = 4.191(L^2d)^{-1} \qquad (1)$$

It is helpful to define dimensionless critical concentrations as $c_1^* = c_1L^2d = 3.290$ and $c_2^* = c_2L^2d = 4.191$ This classical Onsager treatment tells us that for monodisperse molecular cylinders, there is a purely isotropic phase for the concentration

range $0 < c < c_1$, an isotropic–nematic phase coexistence region for $c_1 < c < c_2$, and a purely nematic phase for $c > c_2$. Thus, to affect a transition between phases one uses the rather slow process of increasing the concentration of molecules of fixed length (Fig. 2A). A solution of rotaxane-based switches potentially allows an entirely different and much more rapid way of transforming between phases. Rather than changing the concentration of molecules, we simply switch each molecule to its more extended or long state, or back again to its short state, to transform reversibly between the phases, (Fig. 2B).

To illustrate this, we use a very simple model of a rotaxane-based switch (Fig. 1B). We let each rotaxane be represented by a cylinder whose length is either L or qL, *i.e.* it increases by a factor q. The cylinder diameter is fixed at d. The only other parameter is the dimensionless number concentration of cylinders $c^* \equiv cL^2d$.

The initial system, before switching is a monodisperse collection of cylinders of length L, diameter d and concentration c^*. This system could be in three different regimes, depending on the concentration c_L^* as given by eqn (1). For low concentrations $c_L^* < 3.290$ we have a pure isotropic phase, labelled (i). For intermediate concentrations $3.290 < c_L^* < 4.191$ we have coexisting nematic and isotropic phases, (ni), while for high concentrations, $c_L^* > 4.191$ there is a pure nematic phase (n), or

$$\text{Short state} = \begin{cases} \text{i} & c_L^* < 3.290 \\ \text{ni} & 3.290 < c_L^* < 4.191 \\ \text{n} & c_L^* > 4.191 \end{cases} \quad (2)$$

We now switch the rotaxane to the long state, so that each cylinder now has a length qL, but the same diameter d. The concentration of cylinders is still the same, c, but crucially, the scaled concentration is now $c_{qL}^* = q^2 c_L^*$, *i.e.* the scaled concentration (which determine the particular regime the system is in), is now a factor of q^2 higher. Again, in the switched state we have the same possible 3 regimes (i, ni, n) depending on c_L^*:

$$\text{Long state} = \begin{cases} \text{i} & c_L^* < 3.290/q^2 \\ \text{ni} & 3.290/q^2 < c_L^* < 4.191/q^2 \\ \text{n} & c_L^* > 4.191/q^2 \end{cases} \quad (3)$$

At constant concentration and upon complete switching of all molecules from short to long states, there are 6 possible reversible transitions: i → i, i → ni, i → n, ni → ni, ni → n, and n → n. Each of these transitions is reversible by switching the molecules back to their short states. We can represent these transitions on what we call a "phase-switching diagram" which given the two parameters q and c_L^* allows us to determine what the initial and final states will be. To draw such a diagram all we need are the two eqn (2) and (3). We draw the four curves: $c_L^* = 3.290,\ 4.191,\ 3.290/q^2,\ 4.191/q^2$. These delineate the 6 regions Fig. 3.

As can be seen from the switching diagram, all the theoretical processes are in fact possible, *i.e.* there are 6 regions in the diagram. The most important region is the large region associated with i ↔ n switching: as this transition is between 100% isotropic and 100% nematic phases, it provides the greatest optical contrast. The bordering i ↔ ni region is also of interest as the transition is between an 100% isotropic phase and some nematic phase which would also provide optical contrast. The diagram also shows that the minimum length of the long state

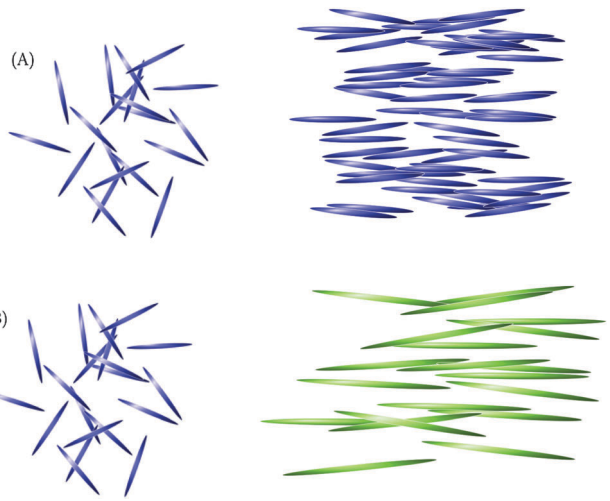

Fig. 2 The initial isotropic phase (left) and final nematic phase (right) associated with (A) increasing molecular concentration at fixed molecular length, and (B) increasing molecular length at fixed molecular concentration. At left is the isotropic phase, where the rods point in all directions. At right is the nematic phase where the rods preferentially point in one direction. This transition is usually accomplished by increasing the concentration, as in (A). Here we show that it is possible to switch between isotropic and nematic by increasing the rod length (B), *via* the use of a rotaxane.

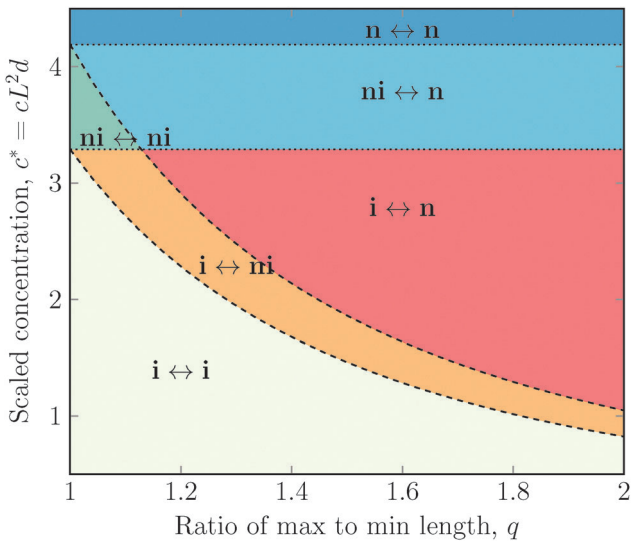

Fig. 3 The phase-switching diagram for this system. We have plotted the scaled concentration *versus* the ratio of the two lengths. There are three possible initial states (isotropic (i), coexisting isotropic and nematic (ni), and pure nematic (n)) and the same final states, leading to six possible regions in the switching diagram. Although most of the regions will show a change in optical contrast using crossed polars, the region of most interest is shaded in red, where a transition from pure isotropic to pure nematic is predicted.

that is required for the easily observable i → n transition corresponds to $q_{\min}$ = 1.13, which can be found by solving $c_L^* = 3.290 = 4.191/q^2$. For a q ratio lower than this, it is not possible to undergo the transition from a pure isotropic to a pure nematic state, although a transition from a pure isotropic to a coexisting nematic–isotropic state is certainly possible. We also see that the i ↔ n transition occurs at lower concentrations as q, the ratio of extension in the long to short state, increases. Optical contrast is still expected in switching regions ni ↔ ni, i ↔ ni, and ni ↔ n, because each of these regions leads to a change in the fraction of the sample which is in the nematic phase. The transition n → n might seem like it is rather uninteresting. However, in fact this transition involves an increase in order. The typical angle from which a cylinder deviates from the mean is[13] $\theta \approx 2\pi^{-1/2}(L^2dc)^{-1}$. Thus by increasing the length by factor q the angular variation decreases by a factor of q^{-2}. As a general rule, as long as we are not in the region where i ↔ i, we will always see some increase in optical contrast. In other words, to see an increase in contrast we need to have $c_L^* > 3.290/q^2$.

It is important to ask if our model systems have significant overlap with experimentally accessible systems. In particular, we require a ratio of long to short states, q at least of 1.13, in order to see the most startling transition of i ↔ n, *i.e.* going from no nematic to all nematic. Bruns and Stoddart[5] have done a survey of molecular switching systems which undergo extension. They list 22 systems (their table 2) with q values ranging from 1.19 to 3. The length cited for ordinary liquid crystals[12] is 300 Angstroms, which is of the same order as many of these listed switching systems. This is good indication that the liquid crystalline switching transitions that we predict are feasible. None of the molecules mentioned by Bruns and Stoddard are perfectly rigid; conformational fluctuations provide flexibility and fluctuations in the length of the axle. However, the theory used here is still valid, provided the molecule does not become very flexible. *i.e.* the length fluctuations are small in comparison to the change in length caused by the switching of the molecule. The issue of extreme flexibility has been examined by Khokhlov and Semenov[16] and Odijk[15] who have shown that even in the case of polymeric systems with rigid elements connected by flexible spacers, a nematic transition is possible. Moreover, for thermotropic systems there are many examples of main-chain liquid crystalline polymers.

From the experimental point of view it would be useful to have the concentrations in molarity. The typical critical concentration (in units of number of rods per volume) is $c_T = L^{-2}d^{-1}$. If we say that a typical molecule is λ angstroms long and δ angstroms in diameter, then converting from cubic metres to litres gives us the number of molecules per litre as $n_T = 10^{-3}/(\lambda^2\delta 10^{-30})$. The number of moles per litre is then $n_T = 1667/(\lambda^2\delta)$. With λ = 100 and δ = 2 we find a molarity of n_T = 0.08, as the typical scale. With rods 10 times as long, the typical molarity is reduced by a factor of 100.

The model used here still suffers from some well-known limitations. The first is that the rod and axle are parallel to each other. In the case where they are at an angle, or where the angle could fluctuate, the theory would need to be modified. The second, and more involved assumption is that all interactions are those of hard-bodies. Although this is the traditional assumption in lyotropic liquid crystalline systems, in reality there will be dispersion forces between the rods which often promote the formation of liquid crystalline phases. Despite these limitations our calculations suggest that a system of rod-like rotaxanes can form the basis of a solution capable of rapid optical switching.

In conclusion we have shown using a simple model that it should be possible to switch between isotropic and nematic solutions using a rotaxane system, without changing the concentration. This could be done rapidly, for example using an optical trigger for the switch. In practice this is most likely to be seen with a long molecule which is relatively stiff, which undergoes an extension by at least a factor of 1.2 and cross-polarised filters must be used to see the effect.

References

1 G. Barin, R. S. Forgan and J. F. Stoddart, *Proc. R. Soc. A*, 2012, **468**, 2849–2880.
2 R. S. Forgan, J.-P. Sauvage and J. F. Stoddart, *Chem. Rev.*, 2011, **111**, 5434–5464.
3 L. Fang, M. A. Olson, D. Benitez, E. Tkatchouk, W. A. Goddard, III and J. F. Stoddart, *Chem. Soc. Rev.*, 2010, **39**, 17–29.
4 J. Wu, K. C.-F. Leung, D. Benitez, J.-Y. Han, S. J. Cantrill, L. Fang and J. F. Stoddart, *Angew. Chem., Int. Ed.*, 2008, **47**, 7470–7474.
5 C. J. Bruns and J. F. Stoddart, *Acc. Chem. Res.*, 2014, **47**, 2186–2199.
6 S. Tsuda, Y. Aso and T. Kaneda, *Chem. Commun.*, 2006, 3072–3074.
7 B. Brough, B. Northrop, J. Schmidt, H. Tseng, K. Houk, J. Stoddart and C. Ho, *Proc. Natl. Acad. Sci. U. S. A.*, 2006, **103**, 8583–8588.
8 E. M. Sevick and D. R. M. Williams, *Langmuir*, 2010, **26**, 5864–5868.
9 N. D. Suhan, S. J. Loeb and S. H. Eichhorn, *J. Am. Chem. Soc.*, 2013, **135**, 400–408.
10 I. Aprahamian, O. S. Miljanic, W. R. Dichtel, K. Isoda, T. Yasuda, T. Kato and J. F. Stoddart, *Bull. Chem. Soc. Jpn.*, 2007, **80**, 1856–1869.
11 T. Kato, Y. Shoji, M. Yoshio, S. Yamane and T. Yasuda, *J. Synth. Org. Chem., Jpn.*, 2010, **68**, 1169–1174.
12 P. de Gennes and J. Prost, *The Physics of Liquid Crystals*, Oxford University Press, Oxford, UK, 1993.
13 L. Onsager, *Ann. N. Y. Acad. Sci.*, 1949, **51**, 627–659.
14 G. Vroege and H. Lekkerkerker, *Rep. Prog. Phys.*, 1992, **55**, 1241–1309.
15 T. Odijk, *Macromolecules*, 1986, **19**, 2313–2329.
16 A. Khokhlov and A. Semenov, *Physica A*, 1981, **108**, 546–556.

2.2 Isotropic-Nematic Phase Switching upon Incomplete Isomerization of Rotaxane Switch

Rotaxane liquid crystals with variable length: The effect of switching efficiency on the isotropic-nematic transition

Hao He, Edith M. Sevick, and David R. M. Williams

Citation: The Journal of Chemical Physics **148**, 134905 (2018); doi: 10.1063/1.5022134
View online: https://doi.org/10.1063/1.5022134
View Table of Contents: http://aip.scitation.org/toc/jcp/148/13
Published by the American Institute of Physics

THE JOURNAL OF CHEMICAL PHYSICS **148**, 134905 (2018)

Rotaxane liquid crystals with variable length: The effect of switching efficiency on the isotropic-nematic transition

Hao He,[1,a)] Edith M. Sevick,[1,b)] and David R. M. Williams[2,c)]
[1]*Research School of Chemistry, The Australian National University, Canberra, ACT 2601, Australia*
[2]*Department of Applied Mathematics, Research School of Physical Sciences and Engineering, The Australian National University, Canberra, ACT 2601, Australia*

(Received 11 January 2018; accepted 14 March 2018; published online 3 April 2018)

We examine a solution of non-adaptive two-state rotaxane molecules which can switch from a short state of length L to a long state of length qL, using statistical thermodynamics. This molecular switching is externally driven and can result in an isotropic-nematic phase transition without altering temperature and concentration. Here we concentrate on the limitation imposed by switching inefficiency, i.e., on the case where molecular switching is not quantitative, leading to a solution of rotaxanes in different states. We present switching diagrams that can guide in the design of rotaxanes which affect a macroscopic phase change. *Published by AIP Publishing.* https://doi.org/10.1063/1.5022134

I. INTRODUCTION

Liquid crystals are comprised of anisotropic or rod-like molecules that can be partially aligned or ordered like a crystal, while simultaneously able to flow like a liquid. Onsager[1] described how a solution of rods, interacting only via hard-body repulsion, can transit from a low concentration isotropic phase to an ordered nematic phase at higher concentrations. This transition is understood in terms of a competition between the translational and orientational entropy of the rods. In the isotropic state, the orientational entropy is maximised, so the rods point freely in every direction. As the concentration of rods increases, this orientational freedom limits the translational freedom of the rods. At a critical concentration, a trade-off occurs: rods begin to align with one another (with a reduction in orientational entropy) so as to increase the translational freedom of the rods. This emerging alignment provides an optical signal; similar to crystals, the aligned nematic phase interacts with polarised light. This lyotropic isotropic-nematic transition, first recognised in cholesterol, also occurs for colloidal particles, such as the tobacco mosaic virus, as well as polymers which are not strictly rod-like but have internal flexibility.[2]

However, a very different kind of molecule with internal degrees of freedom imparted by mechanical bonding[3] can also exhibit liquid crystallinity, but without the required change in concentration. Such mechanical bonds, which consist of a topological linkage of at least two covalent structures, have existed for about half a century.[4] The original example is a catenane, where two macrocycles or rings are mechanically linked or interlocked together. These molecules were first made statistically in low yield by Wasserman,[5] but Sauvage *et al.*[6,7] revolutionised the synthesis of catenanes and other interlocked molecules with a metal templating method. Another example of an interlocked molecule, which is the focus here, is a rotaxane, or a "wheel" and "axle" molecule, where a ring is threaded onto a molecular axle that is stoppered by a bulky group to prevent de-threading. A rotaxane-switch corresponds to a molecular axle into which attractive stations are built; the ring switches between stations depending upon external factors, including chemical reactions,[8–10] solvent polarity,[11] pH,[12–16] and light.[17–19] Bruns and Stoddart[20] have recently reviewed a class of length-extending two-state rotaxane switches which can be switched from a short to a long state, where the ratio of lengths in these cited examples can be as high as 3.

In two recent publications, He *et al.*[21,22] introduced the idea of using a solution of two-state rotaxane switches to affect a switchable liquid crystalline phase. A generic two-state rotaxane, predicted to exhibit lyotropic liquid crystalline phase behavior, is illustrated in Fig. 1. In the case of 100% switching efficiency, or where the two-state rotaxane switches quantitatively between two different lengths, He *et al.*[21,22] predicted a crystalline phase change that occurs without a change in concentration. However, these molecules usually do not switch quantitatively; i.e., a fraction of the molecules do not switch.[12,13] Instead, solutions of these two-state rotaxane switches consist of a mixture of long and short rods, and switching changes the relative composition of short to long states.

In this paper, we predict the macroscopic change in liquid crystalline phases that result from the molecular switching of two-state rotaxanes, controlled externally, but where switching is not quantitative. The liquid crystalline phases of binary mixtures of rods of fixed length (and small diameter) were previously predicted by Lekkerkerker *et al.*[23] and Birshtein *et al.*[24] who constructed phase diagrams for a mixture of rods of length L and qL ($q > 1$), with different fractions of long rods, x. Here we use those predictions to construct a liquid crystalline phase

[a)]Electronic mail: u4785782@anu.edu.au
[b)]Electronic mail: Edie.Sevick@anu.edu.au
[c)]Electronic mail: D.Williams@anu.edu.au

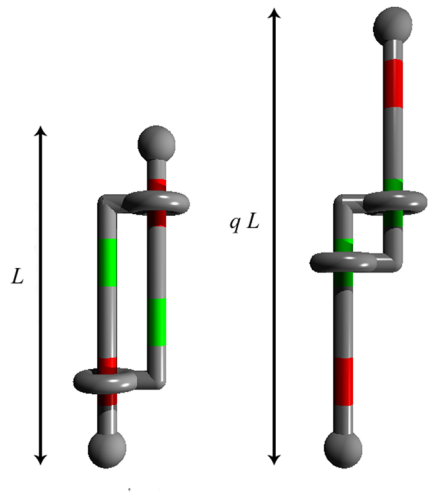

FIG. 1. A two-state rotaxane consisting of two axles or rods interlocked to each other. When the rings are engaged at the red stations, the molecule is in a short state of length L. When the rings are engaged to the green station, the molecule is in a long state of length qL. Switching between long and short states is by external influences such as light or a change in pH which alters the state of minimal energy. We assume that the energy difference in the long and short states is always much greater than k_BT, irrespective of which state is minimal. This means that the switch is unaffected by the local alignment or density of molecules. That is, we consider only non-adaptive switches. If the state is affected by the local alignment or density, then the rotaxane switch is adaptive.[22] This length switching process provides a possible mechanism to accomplish a direct macroscopic transition from an isotropic to nematic phase, which is not possible in conventional lyotropic liquid crystals without a change in concentration.

switching diagram, predicting the concentration range and q which provides maximal optical signal or when the solution macroscopically switches from isotropic to nematic phases. The remainder of the paper is organised in the following way: First, we briefly review the case of isotropic to nematic phase change with 100% molecular switching efficiency. This provides the framework upon which the incomplete or inefficient switching predictions are constructed. Next, we briefly outline the free energy minimisation or entropy maximisation for binary mixtures of rods. Then we construct switching diagrams for four different switching scenarios to demonstrate the range of concentration and length ratio where observable, macroscopic optical changes can occur by molecular switching.

II. MONODISPERSE RODS

Here we review the thermodynamics of isotropic/nematic phase transition for a solution of monodisperse rods of length L which have no interactions other than hard-body or volume-excluding interactions. This means that the free energy comprises the translational entropy of the rods in solution, the orientational entropy of the rods, and a term that describes the reduction in translational entropy due to the pairwise hard-body interactions. If we let $\mathbf{u}$ be the unit vector specifying the rod direction and $\Psi(\mathbf{u})$ be the orientational distribution so that $\Psi(\mathbf{u})d\mathbf{u}$ is the probability that a molecule has an orientation vector between $\mathbf{u}$ and $\mathbf{u} + d\mathbf{u}$, then the free energy per molecule of a homogeneous solution of N molecules of length L and diameter d in a volume V is

$$\frac{F[N,V,\Psi]}{Nk_BT} = \ln\frac{N}{V} - 1 + \int d\mathbf{u}\,\Psi(\mathbf{u})\ln[\Psi(\mathbf{u})] + \frac{1}{2}\frac{N}{V}\int\int d\mathbf{u}d\mathbf{u}'\,\Psi(\mathbf{u})\Psi(\mathbf{u}')2L^2d\mid \mathbf{u}\times\mathbf{u}'\mid . \tag{1}$$

Here the term involving $\ln[\Psi(\mathbf{u})]$ is the orientational entropy of the solution, while the final term is the reduction in translational entropy due to pairwise, volume excluding interactions between two rods of orientations $\mathbf{u}$ and $\mathbf{u}'$. At low concentrations, this free energy is minimised when $\Psi(\mathbf{u}) = (4\pi)^{-1}$ or when all orientations are equally likely and the solution of molecules is isotropic. However, at intermediate concentrations $c_i < N/V < c_a$, two different orientation distributions minimise the energy, indicating that two coexisting phases exist. These two phases are an isotropic phase with $\Psi_i(\mathbf{u}) = (4\pi)^{-1}$ of concentration $c_i = N_i/V_i$ and a nematic phase with preferential orientation, $\Psi_a(\mathbf{u})$, and concentration $c_a = N_a/V_a$. The free energy in the isotropic phase is $F_i = F[N_i, V_i, (4\pi)^{-1}]$; the free energy in the nematic phase is $F_a = F[N_a, V_a, \Psi_a(\mathbf{u})]$. The volume of each phase varies within the concentration range $c_i < c < c_a$, where $c = (N_i + N_a)/(V_i + V_a)$, and is determined by minimising the free energy of the solution, $F = F_i + F_a$, with respect to N_i, V_i, subject to the constraints of $V = V_i + V_a$ and $N = N_i + N_a$. Equivalently, we can determine phase concentrations and volumes by equating the chemical potential of molecules in each coexisting phase (or $\frac{\partial F_i}{\partial N_i} = \frac{\partial F_a}{\partial N_a}$) and equating the osmotic pressure in each phase (or $\frac{\partial F_i}{\partial V_i} = \frac{\partial F_a}{\partial V_a}$).

For a solution of homogenous fixed rods of length L and diameter d, solutions for the critical concentrations, c_i and c_a, have been obtained by numerical minimisation or, as first achieved by Onsager, by parameterisation of the orientational distribution function, $\Psi(\mathbf{u})$. These critical concentrations are reported in units of the inverse average excluded volume of the cylindrical rods or $v_o = \frac{\pi}{4}L^2d$, when $L \gg d$. Herein we report dimensionless concentration as $c^* = cv_0$. The values of c_i^* and c_a^* vary slightly with different numerical solutions. Lekkerkerker's solution is $c_i^* = 3.290$ and $c_a^* = 4.191$, that is, the minimum density at which a nematic phase is present is 3.290 molecules per average excluded volume, and the maximum density at which the isotropic phase persists is 4.191 molecules per average excluded volume. For two-state rotaxane switches with external and quantitative (100%) conversion from short to long state, we can compare the isotropic and nematic concentration boundaries (always given relative to the short state, that is, $c^* = cv_0$, where $v_0 = \frac{\pi}{4}L^2d$) to relate the switching of individual molecules to the switching of liquid crystalline phases. That is, we can compare the isotropic nematic concentration boundaries for solution of homogeneous molecules of short length L,

$$\text{short state} = \begin{cases} \text{isotropic}, & c^* \le c^*_{i,\text{short}} = 3.290, \\ \text{nematic-isotropic}, & c^*_{i,\text{short}} \le c^* \le c^*_{a,\text{short}}, \\ \text{nematic}, & c^* \ge c^*_{a,\text{short}} = 4.191 \end{cases}$$

to that of a solution of homogeneous molecules of long length, qL,

$$\text{long state} = \begin{cases} \text{isotropic} & c^* \le c^*_{i,\text{long}} = 3.290q^{-2} \\ \text{nematic-isotropic} & c^*_{i,\text{long}} \le c^* \le c^*_{a,\text{long}} \\ \text{nematic} & c^* \ge c^*_{a,\text{long}} = 4.191q^{-2} \end{cases}.$$

The isotropic to nematic transition provides the dominant optical contrast, so our aim is to identify a concentration, c^*, and a length ratio q, where molecular switching changes the solution from an isotropic to a nematic solution. Initially, the phase of short rods is isotropic, $c^* \le c^*_{i,\text{short}}$, but after quantitative switching to long rods, the solution is in a nematic phase, or $c^* \ge c^*_{a,\text{long}}$. This corresponds to a solution of two-state rotaxanes of $c^* \le 3.290$ with a strategic extension ratio of $q > \sqrt{4.49/3.34}$, which provides a first principles approach which can guide synthetic chemists constructing two-state switches with the capacity to phase switch. However most synthesised two-state molecular switches are not quantitative, as a solution of rotaxanes may be in a 80/20 ratio of short to long state; after molecular switching, the ratio may change to a 10/90 ratio of short to long state. How sensitive is the switching of the liquid crystalline phase to the inefficiency of molecular switching? To address this question, we make use of predictions of the isotropic/nematic transition of a solution of rods of fixed but bidisperse length.

III. A SOLUTION OF RODS OF BIDISPERSE LENGTH

Lekkerkerker *et al.*[23] extended Onsager's treatment to model a solution of rod-like molecules of two different fixed lengths, with a length ratio of long to short rods q, again in the limit of $L \gg d$. Knowing the liquid crystalline phases of a binary mixture of rods of two different fixed lengths allows us to construct a switching diagram of two-state rotaxanes with inefficient molecular switching. The free energy derivation is similar to that for the monodisperse rods,[1] with the exception that we allow the short and long rods to orient differently, or in other words, we have two orientational distribution functions, one for short rods, Ψ_s, and another for long rods, Ψ_ℓ. Additionally, there is a mixing entropy contribution to the free energy, $S_{mix}/(Nk_B) = x\ln x + (1-x)\ln(1-x)$, where x is the fraction of molecules that are in the long state, of length qL. The corresponding free energy for this solution of rods of bidisperse length is

$$\begin{aligned}\frac{F[N,V,x,\Psi_s,\Psi_\ell]}{Nk_BT} &= \ln\frac{N}{V} - 1 + x\ln x + (1-x)\ln(1-x) + (1-x)\int d\mathbf{u}\,\Psi_s(\mathbf{u})\ln[\Psi_s(\mathbf{u})] + x\int d\mathbf{u}\,\Psi_\ell(\mathbf{u})\ln[\Psi_\ell(\mathbf{u})] \\ &+ \frac{1}{2}\frac{N}{V}\Big[(1-x)^2\int\int d\mathbf{u}d\mathbf{u}'\,\Psi_s(\mathbf{u})\Psi_s(\mathbf{u}')2L^2d\mid\mathbf{u}\times\mathbf{u}'\mid + 2x(1-x)\int\int d\mathbf{u}d\mathbf{u}'\,\Psi_s(\mathbf{u})\Psi_\ell(\mathbf{u}')2qL^2d\mid\mathbf{u}\times\mathbf{u}'\mid \\ &+ x^2\int\int d\mathbf{u}d\mathbf{u}'\,\Psi_\ell(\mathbf{u})\Psi_\ell(\mathbf{u}')2q^2L^2d\mid\mathbf{u}\times\mathbf{u}'\mid\Big]. \end{aligned} \tag{2}$$

As in the homogeneous, fixed length problem, the critical concentrations are found by determining the orientation distributions that minimise the free energy, and where coexisting phases exist, equating chemical potentials and osmotic pressures of the phases. However, the critical concentrations now depend upon the fraction of long rods, x in the solution. We do not consider the de-mixing of short/long rods, as van Roij and Mulder[25] demonstrated that de-mixing within isotropic or nematic phases occurs when the diameter ratio between different rods is more than 5:1. Here, our rods are of fixed diameter irrespective of the short or long state.

The major difficulty in solving Eq. (2) is in approximating the orientational distribution functions for the two kinds of rods, $\Psi_i(\mathbf{u})$, where $i = \{s, \ell\}$. Here we express the orientational vector $\mathbf{u}$ in terms of a shorthand Ω for the spherical polar angles (θ, ϕ) so that the usual normalisation conditions can be written as

$$1 = \int d\mathbf{u}\Psi_i(\mathbf{u}) = \int_0^{2\pi} d\phi\int_0^{\pi} d\theta\sin\theta\,\Psi_i(\theta,\phi) = \int d\Omega\,\Psi_i(\Omega), \quad i = \{s,\ell\}, \tag{3}$$

and the orientational entropy term in Eq. (2) is written as

$$\int d\mathbf{u}\,\Psi_i(\mathbf{u})\ln[\Psi_i(\mathbf{u})] \to \int d\Omega\,\Psi_i(\Omega)\ln[4\pi\Psi_i(\Omega)].$$

The contribution to the free energy due to pairwise volume-excluding interactions involves integrals which we identify as ρ_{ij},

$$\int\int d\mathbf{u}d\mathbf{u}'\,\Psi_i(\mathbf{u})\Psi_j(\mathbf{u}')2L^2d\mid\mathbf{u}\times\mathbf{u}'\mid \to \frac{4}{\pi} \times\int\int d\Omega d\Omega'\,\sin[\gamma(\Omega,\Omega')]\Psi_i(\Omega)\Psi_j(\Omega') = \rho_{ij}.$$

Here $\gamma(\Omega,\Omega')$ is the angle made by two rods with orientations Ω and Ω', where this integral can be written for 3 possible pairings, ρ_{ss}, $\rho_{s\ell}$, and $\rho_{\ell\ell}$, for short-short, short-long, and long-long pairs. Minimising the free energy [Eq. (2)] results in a set of coupled equations

$$\begin{aligned}\ln[4\pi\Psi_s(\Omega)] &= C_s - 2DL^2c\int d\Omega'\,\sin[\gamma(\Omega,\Omega')] \times[(1-x)\Psi_s(\Omega') + qx\Psi_\ell(\Omega')], \\ \ln[4\pi\Psi_\ell(\Omega)] &= C_\ell - 2DL^2qc\int d\Omega'\,\sin[\gamma(\Omega,\Omega')] \times[(1-x)\Psi_s(\Omega') + qx\Psi_\ell(\Omega')],\end{aligned} \tag{4}$$

where the constants C_s and C_ℓ are determined by the normalisation of orientation distribution function, Eq. (3). Equation (4) provides the orientational distribution function of short and long rods, Ψ_s and Ψ_ℓ, for a given concentration, $c = N/V$ and

fraction of long rods, x. Like the monodisperse case, at low concentrations, all orientations are equally likely with $\Psi_s = \Psi_\ell = (4\pi)^{-1}$. But at an intermediate range of concentrations, $c_i \le c \le c_a$, there are two pairs of orientation functions that satisify Eq. (4) indicating coexistence of an isotropic phase, identified with a subscript 1, and a nematic phase, identified with subscript 2. Let c_1 and c_2 denote the concentrations of rods in the isotropic and nematic phases and x_1 and x_2 be the fraction of long rods in the isotropic and nematic phases. The coexisting phases at overall concentration c and a fraction of long rods, x, are described by the 6 variables $\{\Psi_{s,2}\Psi_{\ell,2}, c_1, c_2, x_1, x_2\}$ which are determined by Eq. (4) and cast for a nematic phase [as $\Psi_{s,1}\Psi_{\ell,1} = (4\pi)^{-1}$], an equation matching the osmotic pressure in each phase,

$$\Pi_1 = \Pi_2$$
$$c_1(1 + c_1[(1 - x_1^2 + 2x_1(1 - x_1)q + x_1^2q^2]) = c_2(1 + c_2[(1 - x_2)^2\rho_{ss} + 2x_2(1 - x_2)q\rho_{s\ell} + x_2^2q^2\rho_{\ell\ell}]),$$

an equation matching the chemical potential of short rods, $\mu(s)$, in each phase,

$$\mu_1(s) = \mu_2(s)$$
$$\ln c_1 + \ln(1 - x_1) + 2c_1[(1 - x_1) + x_1q] = \ln c_2 + \ln(1 - x_2) + \sigma_1 + 2c_2[(1 - x_2)\rho_{ss} + x_2q\rho_{s\ell}],$$

an equation matching the chemical potential of the long rods, $\mu(\ell)$, in each phase,

$$\mu_1(\ell) = \mu_2(\ell)$$
$$\ln c_1 + \ln x_1 + 2c_1q[(1 - x_1) + x_1q] = \ln c_2 + \ln x_2 + \sigma_2 + 2c_2[(1 - x_2)q\rho_{s\ell} + x_aq^2\rho_{\ell\ell}],$$

as well as one more equation from the mass balance equations

$$cV = c_1V_1 + c_2V_2$$
$$xN = x_1c_1V_1 + x_2c_2V_2.$$

However,these equations, particularly Eq. (4) involving the orientation functions, cannot be solved analytically and researchers have used different numerical methods to obtain solutions. A trial function can be used for Ψ[1,26] or one can expand $\sin\gamma$[27] and solve the system numerically.[28,29] Here we employ Lekkerkerker's method, as briefly detailed in the Appendix, and approximate the integrals $\rho_{i,j}$ using a 32-point Gaussian integration. The liquid crystalline phase diagram of mixtures of fixed length is obtained numerically, using a Newton-Raphson method, for $0 \le x \le 1$ in increments of $\Delta x = 0.01$ with fixed q, as well as for fixed x with the length ratio varying between $q = 1$ (homogeneous rod length) and $q = 2$.

Figure 2 traces the critical concentrations, c_i^* and c_a^*, as a function of the fraction of longer rods in solution for a length ratio of $q = 1.2$ and 2.0. Note that $x = 0$ corresponds to a monodisperse solution of short rods, recovering the critical concentrations $c_i^* = 3.290$ and $c_a^* = 4.191$. This phase behavior of mixtures of fixed length rods has been predicted in earlier publications,[23,24] i.e., an isotropic phase (**i**) at small concentrations followed by isotropic-nematic coexistence (**ni**) at intermediate concentrations and a pure nematic phase (**n**) at large concentrations. The phase is determined by three variables: the overall concentration of the solution, c^*, the overall fraction of long rods in the solution, x, and the length ratio, q. The characteristic concentration where the major phase change occurs is near $c^* \approx 3$. Naturally, as the fraction of longer rods increases the concentration boundaries decrease, as it is much easier to form a nematic phase.

A. Switching diagrams

The goal here is to construct a solution of two-state rotaxane switches which will allow us to affect an isotropic to nematic phase transition without changing the concentration of rotaxanes in the solution. That is, our goal is to estimate the concentration range and extension length q, where molecular switching results in a macroscopic change in the orientational phase in solution. As we will show, even for the case of very modest efficiencies in switching on the molecular scale, we still achieve transitions from isotropic to nematic (**i** → **n**) and from isotropic to nematic-isotropic coexistence (**i** → **ni**). This is important because the presence of a nematic phase, even if the system is not purely nematic, will have an optical effect, and thus the length switching on the molecular scale will induce a macroscopically detectable change in the solution. A weaker optical effect due to molecular alignment occurs for the other transitions between nematic (**n**) and nematic-isotropic coexistence (**ni**) or nematic to nematic (**n** → **n**, **ni** → **ni**, and **ni** → **n**). While these phase transitions can be observed optically, a direct switch from a single isotropic phase to a single nematic phase is of most interest.

As the orientational phase of a solution is determined by 3 parameters, then the switching diagram is determined by four variables: (1) the fixed concentration c^* of the solution, (2) the length ratio, q, of the molecule, (3) the initial fraction of long rods in solution, x_i, and (4) the final fraction of long rods in solution, x_f, after molecular switching. He *et al.*[21] provided the switching diagram for the case of $x_i = 0.0$ and $x_f = 1.0$, or where switching is quantitative. Here we demonstrate four different switching inefficiencies: where the fraction of long rods changes as $x_i \to x_f$

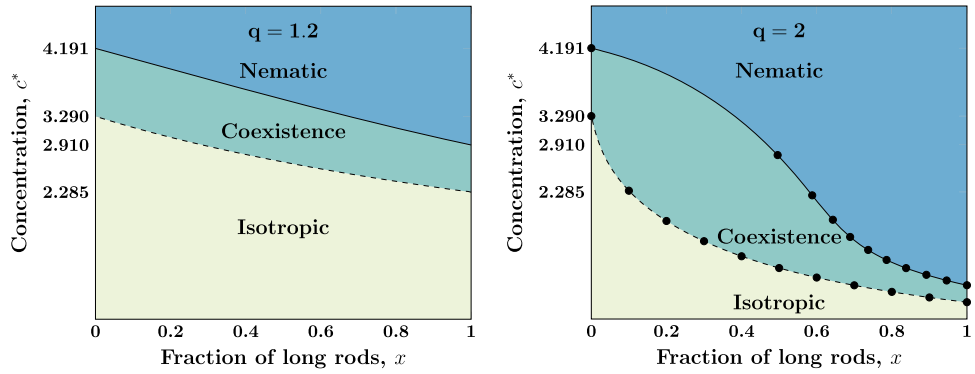

FIG. 2. Scaled concentration, $c^* = cv_0$, versus fraction of long rods for a solution of rods of bidisperse length with a length ratio of long to short of $q = 1.2$ (left) and $q = 2$ (right). The scaled concentration c_i^* (dashed line) separates the isotropic phase region from the region where isotropic and nematic phases coexist: it is the minimum concentration at which a nematic phase is present. The scaled concentration c_a^* (solid line) separates the coexistence region from the single phase nematic region: it is the maximum concentration at which an isotropic phase is present. The data points represent the results of Lekkerkerker.[23] At $x = 0$, corresponding to a solution of short rods of homogeneous length L, $c_i^* = 3.290$, and $c_a^* = 4.191$. The addition of longer rods reduces the concentration range over which an isotropic phase is present and increases the range over which a nematic appears. A large extension ratio q steepens the boundary curves, enhancing the nematic phase with an increase in population of the longer rod of length qL.

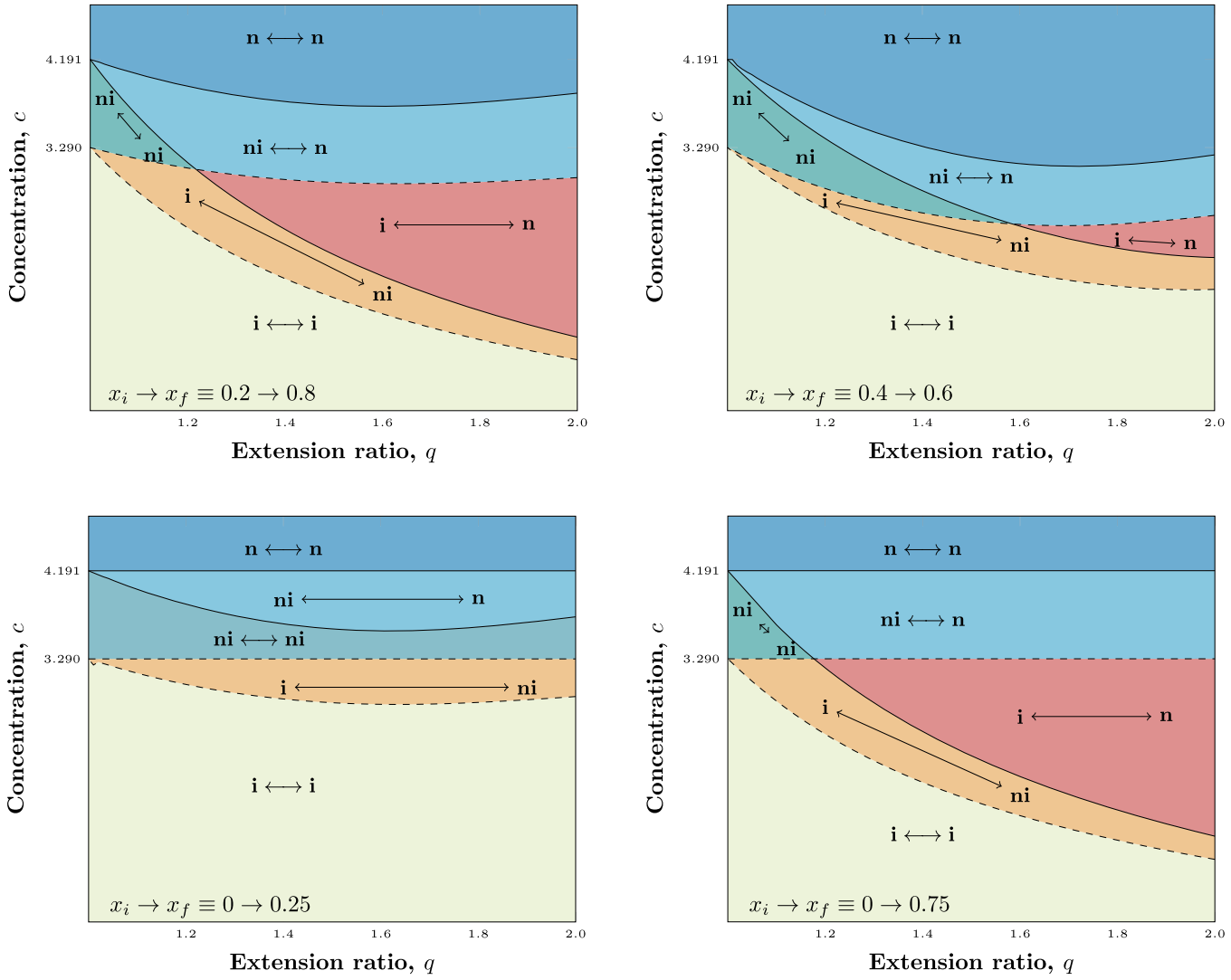

FIG. 3. The switching diagram, scaled concentration, c^*, versus extension ratio q with switching efficiency of $x_i = 0.2 \to x_f = 0.8$ (top left), $x_i = 0.4 \to x_f = 0.6$ (top right), $x_i = 0 \to x_f = 0.25$ (bottom left), and $x_i = 0 \to x_f = 0.75$ (bottom right). Isotropic(**i**), coexisting isotropic-nematic(**ni**), and nematic(**n**) phases are labeled. Dashed lines separate isotropic and coexistence regions and solid lines separate coexistence and nematic regions, for both initial solution of x_i and final solution x_f. In this way, (**i** → **ni**) indicates an isotropic phase at x_i switches to an isotropic-nematic coexistence phase at x_f. While a transition from isotropic to coexistence (**i** → **ni**) or coexistence to nematic(**ni** → **n**) can show change in optical properties, the transition from pure isotropic directly to a nematic phase is of most interest.

1. $x_i \to x_f \equiv 0.2 \to 0.8$
2. $0.4 \to 0.6$
3. $0 \to 0.25$
4. $0 \to 0.75$.

These cases are chosen because they all represent considerably less than 100% switching efficiency, and in two of the cases, the change in x is small, $\Delta x = 0.2$ or 0.25, corresponding to poor switching efficiency. Figure 3 shows these cases over a limited range of length ratio, $1.0 \le q \le 2.0$. These are constructed by overlapping phase diagrams of the initial solution of x_i and final switched solution of x_f.

For three of these cases, the transition from isotropic to pure nematic can be induced in this system by switching the length of the molecules, even for the case of a very modest change in x roughly at $c^* \approx 3$. A high switching efficiency ($\Delta x = x_f - x_i$ is large) creates a significant difference in the critical concentrations, facilitating $\mathbf{i} \leftrightarrow \mathbf{n}$ transitions of a greater range of q (as demonstrated by cases $0.2 \to 0.8$ and $0 \to 0.75$). When the switching efficiency is relatively low, for example, $x_i = 0 \to x_f = 0.25$, switching in molecular length is not enough to trigger a direct transition from isotropic to nematic phase with a reasonable extension ratio q. Importantly this is not the least efficient switch case: the case of $0.4 \to 0.6$ has a lower switching efficiency ($\Delta x = 0.2$) but still demonstrates a significant $\mathbf{i} \to \mathbf{n}$ phase switch because of the initial presence of long rods. This suggests that not all molecules incorporated need to be designed as switchable in order to achieve a macroscopic phase transition. For example, the same phase switching predicted for the inefficient switching case of $0.4 \to 0.6$ also holds for a solution mixture containing 40% *fixed-length* long (qL), 40% *fixed-length* short (L) molecules, and only 20% molecules that quantitatively switch from $L \to qL$. What the switching diagram does show is that even for this case of very modest changes in switching on the molecular scale (either inefficient switching or a small fraction of quantitative switches), we still get transitions from isotropic (**i**) to nematic-isotropic coexistence (**ni**).

IV. CONCLUSIONS

We have constructed the macroscopic isotropic-nematic phase switching diagram for a rod-like molecule that can switch between two different lengths via a mechanical bond. We have previously studied this system in the case where the microscopic switching in length was 100% efficient, i.e., all the molecules switch quantitatively between short and long states. Here we have examined the more realistic case of an inefficient system where molecular switching is not quantitative. We have shown that the macroscopic, switchable phase transition from isotropic to nematic is in fact fairly robust and can be found even for cases of very inefficient molecular switching. This also suggests that not all molecules in the solution need to be switchable in order to achieve a switchable phase change.

While our predictions have not yet been demonstrated in experiment, it is worth noting that a different kind of molecular switch, based upon photo-induced isomerisation of a fully covalent molecule (with no mechanical bond),[30] is used as a dopant to induce chirality in nematic liquid crystals. These photoswitchable molecules have been shown to provide thermally stable, reversible control[31] of the structure of cholesteric liquid crystals.

APPENDIX: NUMERICAL APPROACH TO SOLVE EQUATION (4)

Equation (4) cannot be solved analytically and researchers have used different numerical methods to obtain solutions. Here we follow Lekkerkerker's method[23] and expand $\sin\gamma$ in a Legendre series up to order 7, which is sufficiently accurate for our predictions. As explained in Lekkerkerker, symmetry allows us to recast the distribution functions in terms of θ or $\Psi_i(\Omega) \to \Psi_i(\theta)$ and the Legendre series must be of even order

$$\sin\gamma = \frac{\pi}{4} - \sum_{n=1}^{7} d_{2n} P_{2n}(\cos\gamma), \tag{A1}$$

where $d_{2n} = \frac{\pi(4n+1)(2n-3)!!(2n-1)!!}{2^{2n+2}n!(n+1)!}$. Using the addition theorem for spherical harmonics or

$$P_l(\cos\gamma) = P_l(\cos\theta)P_l(\cos\theta') + 2\sum_{m=1}^{l}\frac{(l-m)!}{(l+m)!}P_l^m(\cos\theta) \times P_l^m(\cos\theta')\cos[m(\phi-\phi')].$$

Lekkerkerker finds that the orientation distribution functions for the short and long rods are then

$$\Psi_s(\theta) = \frac{\exp\left[\sum_{n=1}^{7}\alpha_{2n}P_{2n}(\cos\theta)\right]}{N_s}, \qquad \Psi_\ell(\theta) = \frac{\exp\left[q\sum_{n=1}^{7}\alpha_{2n}P_{2n}(\cos\theta)\right]}{N_\ell}, \tag{A2}$$

where N_i is a normalisation constant so that $1 = \int d\theta\, \Psi_i(\theta)$ and α_{2n} is a set of 7 unknown Legendre coefficients. Equation (4) then reduces to a set of 7 equations,

$$\int d\theta\,[(1-x)\Psi_s(\theta) + xq\Psi_\ell(\theta)]P_{2n}(\cos\theta) = \frac{\pi\alpha_{2n}}{8cd_{2n}} \qquad 1 \le n \le 7. \tag{A3}$$

Equations (A2) and (A3) provide us with nine equations, which, for a specified concentration, c, and fraction of long rods, x, provide the set of Legendre coefficients or distribution functions Ψ_s and Ψ_ℓ for a solution of rods in a nematic phase. [Recall, in the isotropic phase, $\Psi_s = \Psi_\ell = (4\pi)^{-1}$.]

[1] L. Onsager, "The effects of shape on the interaction of colloidal particles," Ann. N. Y. Acad. Sci. **51**, 627–659 (1949).
[2] A. Khokhlov and A. Semenov, "Liquid-crystalline ordering in the solution of long persistent chains," Phys. A **108**, 546–556 (1981).
[3] J. F. Stoddart, "The chemistry of the mechanical bond," Chem. Soc. Rev. **38**, 1802–1820 (2009).
[4] G. Gil-Ramírez, D. A. Leigh, and A. J. Stephens, "Catenanes: Fifty years of molecular links," Angew. Chem., Int. Ed. **54**, 6110–6150 (2015).
[5] E. Wasserman, "The preparation of interlocking rings: A catenane1," J. Am. Chem. Soc. **82**, 4433–4434 (1960).
[6] C. Dietrich-Buchecker, J. Sauvage, and J. Kintzinger, "Une nouvelle famille de molecules: Les metallo-catenanes," Tetrahedron Lett. **24**, 5095–5098 (1983).
[7] C. O. Dietrich-Buchecker, J. P. Sauvage, and J. M. Kern, "Templated synthesis of interlocked macrocyclic ligands: The catenands," J. Am. Chem. Soc. **106**, 3043–3045 (1984).

[8]M. C. Jiménez, C. Dietrich-Buchecker, and J.-P. Sauvage, "Towards synthetic molecular muscles: Contraction and stretching of a linear rotaxane dimer," Angew. Chem., Int. Ed. **112**, 3422–3425 (2000).
[9]B. Champin, P. Mobian, and J.-P. Sauvage, "Transition metal complexes as molecular machine prototypes," Chem. Soc. Rev. **36**, 358–366 (2007).
[10]V. Balzani, A. Credi, G. Mattersteig, O. A. Matthews, F. M. Raymo, J. F. Stoddart, M. Venturi, A. J. P. White, and D. J. Williams, "Switching of pseudorotaxanes and catenanes incorporating a tetrathiafulvalene unit by redox and chemical inputs," J. Org. Chem. **65**, 1924–1936 (2000).
[11]S. Tsukagoshi, A. Miyawaki, Y. Takashima, H. Yamaguchi, and A. Harada, "Contraction of supramolecular double-threaded dimer formed by α-cyclodextrin with a long alkyl chain," Org. Lett. **9**, 1053–1055 (2007).
[12]F. Coutrot, C. Romuald, and E. Busseron, "A new ph-switchable dimannosyl[c2]daisy chain molecular machine," Org. Lett. **10**, 3741–3744 (2008).
[13]J. Wu, K. C.-F. Leung, D. Benitez, J.-Y. Han, S. J. Cantrill, L. Fang, and J. F. Stoddart, "An acid-base-controllable [c2]daisy chain," Angew. Chem., Int. Ed. **47**, 7470–7474 (2008).
[14]L. Fang, M. Hmadeh, J. Wu, M. A. Olson, J. M. Spruell, A. Trabolsi, Y.-W. Yang, M. Elhabiri, A.-M. Albrecht-Gary, and J. F. Stoddart, "Acid-base actuation of [c2]daisy chains," J. Am. Chem. Soc. **131**, 7126–7134 (2009).
[15]G. Du, E. Moulin, N. Jouault, E. Buhler, and N. Giuseppone, "Muscle-like supramolecular polymers: Integrated motion from thousands of molecular machines," Angew. Chem., Int. Ed. **51**, 12504–12508 (2012).
[16]M. Hmadeh, L. Fang, A. Trabolsi, M. Elhabiri, A.-M. Albrecht-Gary, and J. F. Stoddart, "On the thermodynamic and kinetic investigations of a [c2]daisy chain polymer," J. Mater. Chem. **20**, 3422–3430 (2010).
[17]S. Tsuda, Y. Aso, and T. Kaneda, "Linear oligomers composed of a photochromically contractible and extendable Janus [2] rotaxane," Chem. Commun. **29**, 3072–3074 (2006).
[18]R. E. Dawson, S. F. Lincoln, and C. J. Easton, "The foundation of a light driven molecular muscle based on stilbene and alpha-cyclodextrin," Chem. Commun. **34**, 3980–3982 (2008).
[19]S. Li, D. Taura, A. Hashidzume, and A. Harada, "Light-switchable Janus [2]rotaxanes based on alpha-cyclodextrin derivatives bearing two recognition sites linked with oligo(ethylene glycol)," Chem. - Asian J. **5**, 2281–2289 (2010).
[20]C. J. Bruns and J. F. Stoddart, "Rotaxane-based molecular muscles," Acc. Chem. Res. **47**, 2186–2199 (2014).
[21]H. He, E. M. Sevick, and D. R. M. Williams, "Fast switching from isotropic liquids to nematic liquid crystals: Rotaxanes as smart fluids," Chem. Commun. **51**, 16541–16544 (2015).
[22]H. He, E. M. Sevick, and D. R. M. Williams, "Isotropic and nematic liquid crystalline phases of adaptive rotaxanes," J. Chem. Phys. **144**, 124901 (2016).
[23]H. N. W. Lekkerkerker, P. Coulon, R. Van Der Haegen, and R. Deblieck, "On the isotropic liquid crystal phase separation in a solution of rod-like particles of different lengths," J. Chem. Phys. **80**, 3427–3433 (1984).
[24]T. Birshtein, B. Kolegov, and V. Pryamitsyn, "Theory of athermal lyotropic liquid crystal systems," Polym. Sci. U.S.S.R. **30**, 316–324 (1988).
[25]R. van Roij and B. Mulder, "Demixing versus ordering in hard-rod mixtures," Phys. Rev. E **54**, 6430–6440 (1996).
[26]J. P. Straley, "The gas of long rods as a model for lyotropic liquid crystals," Mol. Cryst. Liq. Cryst. **22**, 333–357 (1973).
[27]A. Isihara, "Theory of anisotropic colloidal solutions," J. Chem. Phys. **19**, 1142–1147 (1951).
[28]K. Lakatos, "On the statistics of a three-dimensional gas of long thin rods," J. Stat. Phys. **2**, 121–136 (1970).
[29]R. F. Kayser and H. J. Raveché, "Bifurcation in Onsager's model of the isotropic-nematic transition," Phys. Rev. A **17**, 2067–2072 (1978).
[30]R. A. van Delden, N. Koumura, N. Harada, and B. L. Feringa, "Unidirectional rotary motion in a liquid crystalline environment: Color tuning by a molecular motor," Proc. Natl. Acad. Sci. U. S. A. **99**, 4945–4949 (2002).
[31]T. van Leeuwen, T. C. Pijper, J. Areephong, B. L. Feringa, W. R. Browne, and N. Katsonis, "Reversible photochemical control of cholesteric liquid crystals with a diamine-based diarylethene chiroptical switch," J. Mater. Chem. **21**, 3142–3146 (2011).

Chapter 3

Isotropic and Nematic Liquid Crystaline Phase of Adaptive Rotaxane

The research presented in this publication was solely completed by the author of this thesis. The author was the main contributor to the statistical mechanical model and numerical calculations in this publication.

Isotropic and nematic liquid crystalline phases of adaptive rotaxanes

Hao He, Edith M. Sevick, and David R. M. Williams

Citation: The Journal of Chemical Physics **144**, 124901 (2016); doi: 10.1063/1.4943098
View online: https://doi.org/10.1063/1.4943098
View Table of Contents: http://aip.scitation.org/toc/jcp/144/12
Published by the American Institute of Physics

THE JOURNAL OF CHEMICAL PHYSICS **144**, 124901 (2016)

Isotropic and nematic liquid crystalline phases of adaptive rotaxanes

Hao He,[1] Edith M. Sevick,[1,a)] and David R. M. Williams[2,b)]
[1]*Research School of Chemistry, The Australian National University, Canberra ACT 0200, Australia*
[2]*Department of Applied Mathematics, Research School of Physical Sciences and Engineering, The Australian National University, Canberra ACT 0200, Australia*

(Received 11 December 2015; accepted 19 February 2016; published online 22 March 2016)

We describe the thermodynamics of a solution of rotaxanes which can change their length from a short state of length L to a long state of length qL in response to their surrounding environment. We call these rotaxanes "adaptive." We show that such a system can exhibit both isotropic and nematic liquid crystalline phases. The system shows several interesting kinds of behaviour. First we predict that the fraction of short-length rotaxanes increases linearly with concentration and is a maximum at the critical concentration that marks the isotropic to nematic transition. Second, the critical concentration shows a minimum at a certain value of q. Our model suggests that the effect of adaptive length changes is most dramatic at small q and where the long state is slightly favoured. © *2016 AIP Publishing LLC*. [http://dx.doi.org/10.1063/1.4943098]

I. INTRODUCTION

A rotaxane is a wheel and axle molecule, where a molecular ring or rings are threaded onto an axle. This is then stoppered at both ends so the rings cannot escape. Their synthesis is an active area of research[1–15] and the production of these mechanically linked molecules opens up many new possibilities for phenomena on the molecular scale. Some rotaxanes act as two-state switches. They can do this because they have 2 stations along the axle, and the rings attach preferentially to these stations. The switching between stations can be controlled by external influences such as solvent pH, ion interaction, redox reaction, solvent quality, or light. Another way of moving the ring is to attach a rigid rod to it and then compressing it with an AFM tip. This was done by Brough *et al.*[2] Later Sevick and Williams[16] showed how such a system, with many rings, could behave as a molecular shock absorber.[17] Switching changes the length of this piston-rotaxane molecule. In Figure 1 we depict such a switchable rotaxane where there is a short state and a long state, the ratio of the lengths of these states being q. This suggests that switching rotaxane molecules between states might create interesting, controllable liquid crystalline phases.

Liquid crystals[18] are solutions of anisotropic molecules which have no long-range positional order, like a liquid, but can have phases which possess different degrees of molecular orientation similar to crystalline ordering. The phases in lyotropic liquid crystals are determined by the concentration of the molecules, $c = N/V$ (N the number of solute particles in a volume V) which can be altered by addition of solvent, Figure 2. In dilute solutions, the fixed-sized anisotropic molecules have no long-range translational or orientation order—the solution is isotropic. However, with an increased concentration, a nematic phase appears where the molecules still have no translational order, but self-align to have directional order along their long axis. This orientationally ordered nematic phase is birefringent, optically detectable using cross polarised filters, and is the principle concept behind liquid crystalline displays. The fundamental theory for these systems was produced by Onsager in 1949.[19–21] Recently this work was extended to a two-state rotaxane system, where an *external* influence,[22] controlled by the experimenter, could switch the rod length from short to long. This enables a sudden transition from isotropic to nematic, without changing the concentration of rods.

In this paper, we describe a somewhat different rotaxane system. The rotaxane can exist in two different states, one of length L and the other of length qL, but the molecule itself decides which state to be in on the basis of the what minimises the total free energy of the system. We call such rotaxanes "adaptive." This is in marked contrast to the recent work of He *et al.*,[22] where the rotaxanes are forced to be in one state or the other by external control of the system, as for example, by changing the pH.

As a simple example, consider a dilute solution of adaptive rotaxanes between two plates a distance H apart. The rotaxanes can choose to have lengths L or qL, with $q > 1$. If the distance between plates is larger than the largest molecular dimension $H > qL$, we would find 1/2 of the molecules of length L and the other half of length qL. However, as H gets smaller, there will be a gradual bias towards shorter rods because the longer rods can only fit by re-orientating parallel to the plates. The rotaxanes "adapt" to their external environment.

In the case considered in this paper, the rotaxanes adapt, not because of an imposed confinement by plates, but because of hard-body interactions with surrounding rods. The remainder of the paper is organised in the following way. In Sec. II, we review Onsager's classical treatment of lyotropic liquid crystals formed from homogeneous, fixed-length rods. In Sec. III, we extend this theory to an adaptive 2-state rotaxane and present results in the following section. In particular, we show how the critical concentrations for the transitions, the order parameters, and the fraction of rotaxanes in the short

a)Electronic mail: Edie.Sevick@anu.edu.au
b)Electronic mail: D.Williams@anu.edu.au

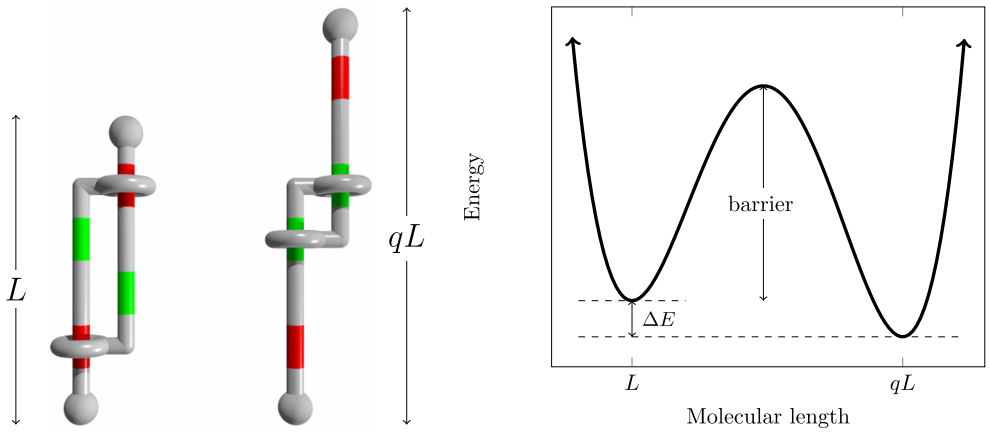

FIG. 1. Illustration of a 2-state rotaxane in short and long states and the energy of an isolated rotaxane switch as a function of molecular length, showing the short and long states as minimal energy states. Attractive stations along the axles are depicted as green and red regions. When the rings reside within the attractive red stations (left), the rotaxane is in its short state, characterised by the molecular length, L. When the rings reside within the attractive green stations (middle), the rotaxane is in its long state, characterised by the molecular length qL. The ratio of long to short state lengths, q, is set by the synthetic design of the molecule. In adaptive rotaxanes, the energy difference between states, ΔE, is small, on the order of k_BT. If the long state has lower energy, it is favoured at vanishingly small concentrations; but because ΔE is small, the short state may be favoured at high solution concentrations so as to lower the free energy of the solution. If $|\Delta E| \gg k_BT$, the rotaxane will not be adaptive and solutions of rotaxanes will behave like solutions of fixed-length rods. For the adaptive rotaxanes considered here, the energy barrier between the states is assumed to be large so that the individual rotaxane states (short or long) are the only allowed states. Here we consider the equilibrium liquid crystalline phases of a solution of this adaptive two-state rotaxane.

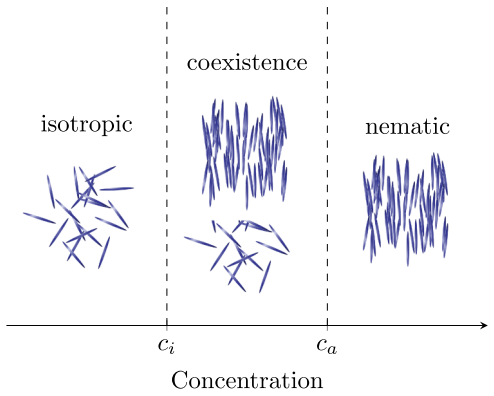

FIG. 2. Illustration of lyotropic liquid crystalline phases for a solution of fixed-length rods of one size and with simple hard-body interactions. The volume-excluding rods are isotropic for concentrations up to c_i, above which appears a coexisting nematic phase. As concentration increases from c_i to c_a, the volume of nematic phase increases at the expense of the isotropic phase, until at c_a, the solution is entirely in the nematic phase. Onsager predicted the critical concentrations of rods of length, L and diameter d to be $c_i = 3.34(\frac{\pi}{4}L^2d)$ and $c_a = 4.49(\frac{\pi}{4}L^2d)$.

state, depend on the synthetic design parameter q and energy bias between the two adaptive states. The behaviour we encounter is sometimes unexpected, and although we can give *post-hoc* explanations of all of it, it would be very difficult to predict it without the model and its numerical predictions.

This work should be seen in the context of other works on adaptive systems. In particular, wormlike micelles,[23] radially compressible rods,[24] and crowding of proteins.[25]

II. FIXED-LENGTH RODS

We start with a brief review of the classical Onsager theory[19] for monodisperse rods of length L, diameter d, and concentration $c = N/V$, where N is the number of rods in a volume V. The physics is essentially as follows. Onsager assumes that the only forces between the rods are those of hard bodies, i.e., the interaction is zero except in cases of attempted overlap, and all overlaps are forbidden. In such a system, the free energy is entirely entropic, and the system minimises the free energy by maximising the entropy. The entropy is k_B multiplied by the logarithm of the number of configurations, so that all we need to do is count the configurations. The entropy is of two kinds, translational and rotational. First there is the translational entropy of the centres of each molecule. This is maximised by having the rods placed randomly within the container. The second kind is the orientational entropy, which is maximised by the rods pointing in every direction with equal probability. At infinitely small concentrations, $c \to 0$, the rods do not interact and both the translational and orientational entropy are maximised by having the rods uniformly distributed in space and in direction. However, as c is increased towards the characteristic concentration $\sim 1/(L^2d)$, the rods begin to interact and we find overlap. At these low concentrations, the orientation is still totally random, but certain positions of the centre of mass of two rods are forbidden. These forbidden positions lead to a decrease in the translational entropy. The system can avoid some of these forbidden positions by aligning the rods so that they preferentially point along a particular direction. This decreases the orientational entropy, but increases the translational entropy.

The free energy per rod (see Appendices A and B) of a homogeneous solution of N rods of length L and diameter d in a volume V is

$$\frac{F[\Psi]}{Nk_BT} = \ln\frac{N}{V} - 1 + \int d\mathbf{u}\Psi(\mathbf{u})\ln[\Psi(\mathbf{u})] + \frac{1}{2}\frac{N}{V}\int\int d\mathbf{u}\,d\mathbf{u}'\Psi(\mathbf{u})\Psi(\mathbf{u}')2L^2d\,|\mathbf{u}\times\mathbf{u}'|\,. \quad (1)$$

Here $\Psi(\mathbf{u})$ is the orientational distribution function for the rods and $\mathbf{u}$ is a unit vector specifying the rod direction. The term $\ln(N/V) - 1$ is the translational entropy, assuming

a homogenous distribution. The term in $\ln(\Psi)$ is the orientational entropy, and the final term accounts for the rod-rod interactions. In essence, this final term is the reduction in translational entropy caused by rod-rod interactions.

The equilibrium orientation distribution is determined by the condition that the free energy is minimal for all variations of $\Psi(\mathbf{u})$, subject to the mathematical condition that the distribution is normalised. This results in a non-linear equation for $\Psi(\mathbf{u})$ which cannot be solved analytically. There is then a choice of solution methods. One approach is brute-force numerical minimisation. Onsager[19] chose a more elegant trial function approach, using the function (Figure 3),

$$\Psi(\mathbf{u}) = \frac{\alpha}{4\pi \sinh \alpha} \cosh[\alpha \mathbf{u} \cdot \mathbf{n}], \tag{2}$$

where $\mathbf{n}$ is an arbitrary unit vector (the director) and α is a parameter representing the degree of alignment, to be determined analytically from minimisation of the free energy. $\alpha = 0$ corresponds to an isotropic state where rods adopt all angles with equal likelihood or equivalently, $\Psi(\mathbf{u}) = (4\pi)^{-1}$, and $\alpha = \infty$ corresponds to a perfectly aligned collection of rods, Figure 3. This trial function method replaces a function with an infinite number of variables $\Psi(\mathbf{u})$ with a single variable α to be minimised over. It thus introduces some approximation, but is in keeping with the other approximations in the theory.

The parameter α is closely related to the order parameter, S, which also measures the degree of alignment. S is defined by $S \equiv \langle \frac{3}{2}\cos^2\theta - \frac{1}{2} \rangle$, where θ is the angle between the rod and the nematic director, $\mathbf{n}$. For the isotropic state, $S = 0$ and any non-zero S implies a nematic phase. In the limit of perfect alignment, $S \to 1$. We can easily express S in terms of α via

$$S = 1 + 3\alpha^{-2} - 3\alpha^{-1} \coth \alpha \tag{3}$$

so that for small α, $S \approx \alpha^2/15$, while for large α, $S \approx 1 - 3\alpha^{-1}$.

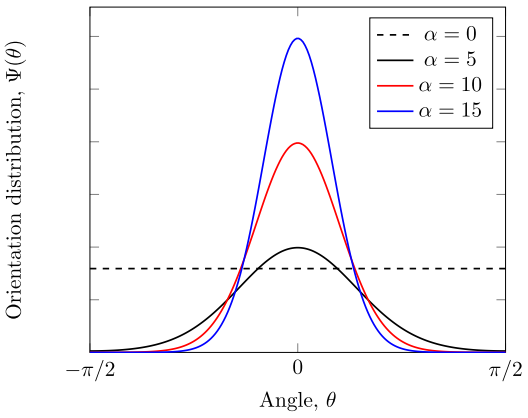

FIG. 3. Onsager's trial function, $\Psi(\theta)$, versus angle, θ for several different parameters, $\alpha \cdot \theta = \cos^{-1}(\mathbf{u} \cdot \mathbf{n})$ is the angle that the rod makes with an arbitrary vector, $\mathbf{n}$, the director. The parameter α characterises the degree of alignment, with $\alpha = 0$ describing the isotropic state with no orientational order, where $\Psi(\theta) = (4\pi)^{-1}$. In our extension to adaptive rotaxanes, we use this same trial function to describe the orientational ordering of rotaxanes in nematic phases. As rotaxanes in the short and long state will be orientationally ordered to different degrees, we introduce the orientation distribution Ψ_S, with parameter α_S to describe the orientational ordering of rotaxanes in the short state, and Ψ_L and α_L for rotaxanes in the long state.

At low concentration, the free energy is minimised when $\alpha = 0$; this corresponds to a single isotropic phase. At high concentration, the free energy is minimised when α takes on a larger value corresponding to a single nematic phase. However between two critical concentrations c_i and c_a, there are two coexisting phases, one isotropic at concentration $c = c_i$ and the other nematic at concentration $c = c_a$. In each of these phases, the value of α is different. The first phase corresponds to an isotropic phase of N_i rods and volume V_i. The free energy per rod in this isotropic phase is $F_i = F(N_i, V_i, \alpha_i = 0)$, where F is of the form given by Eq. (1). The second phase corresponds to a nematic phase of N_a rods in volume V_a with orientation α_a. The free energy per rod of the nematic phase is $F_a = F(N_a, V_a, \alpha_a)$. The number of rods in each phase and the relative volume of the phases vary within the concentration range $c_i \le c < c_a$, where c is the concentration of the entire solution i.e., $c = (N_i + N_a)/(V_i + V_a)$. These are determined by writing the free energy as a sum of the free energy of the isotropic and nematic phases,

$$F = F_i(N_i, V_i, \alpha_i = 0) + F_a(N_a, V_a, \alpha_a) \tag{4}$$

and minimising F with respect to N_i, V_i subject to the constraints of constant total volume and number of molecules, $V = V_i + V_a$ and $N = N_i + N_a$. Equivalently, we can determine the phase compositions and volumes by equating the chemical potential of the molecules in each coexisting phase

$$\frac{\partial F_i}{\partial N_i} = \frac{\partial F_a}{\partial N_a}, \tag{5}$$

and by equating the osmotic pressure in each phase, or

$$\frac{\partial F_i}{\partial V_i} = \frac{\partial F_a}{\partial V_a}. \tag{6}$$

These two thermodynamic relations coupled with the constraints of constant total number of molecules and constant total volume fully specify the concentrations and the relative fraction of coexisting isotropic and nematic phases. In practice, if we know c_i and c_a and we put N rods in a solution of volume V, we can calculate the number of rods in each coexisting phase and the volume of these phases using the fact that $V_i c_i + V_a c_a = N$ and $V_i + V_a = V$. To summarise the results for a solution of homogenous hard rods, we have the following:

1. $0 < c < c_i$ the solution is isotropic,
2. $c_i < c < c_a$ an isotropic phase of density c_i coexists with a nematic phase of density c_a,
3. $c_a < c$ the solution is nematic.

In Onsager's solution for homogeneous rods of fixed length L and diameter d, the critical concentrations are $c_i = 3.34(\frac{\pi}{4}L^2 d)^{-1}$ and $c_a = 4.49(\frac{\pi}{4}L^2 d)^{-1}$. Both these concentrations contain the characteristic concentration $\sim L^2 d$, which is essentially the inverse excluded volume of one rod.

III. 2-STATE ADAPTIVE ROTAXANES

Before we consider the free energy of the adaptive system, we first need to determine how many coexisting phases there can be in this system. In the case of rods of fixed length, the Gibbs phase rule gives that the number of coexisting phases

can be at most 2. In the system where we have rods of two possible lengths, this is also true, for the reason that we only have one species of rod, which can take two possible lengths, i.e., the rod lengths are always in equilibrium with each other. This in fact makes it less complicated than a system consisting of rods of two different fixed lengths.[26,27] We thus expect coexistence of only two phases, one isotropic and one nematic, just as in Onsager's fixed length rod problem. However, the critical concentrations for the transitions c_i and c_a will of course be different.

To describe the liquid crystalline phase diagram of 2-state adaptive rotaxanes, we extend Onsager's treatment to a solution of N molecules of fixed diameter d, a fraction x in the short state, having length L and a fraction $(1-x)$ in the long state with length qL. Molecules of different length may orient differently: in a dilute solution, the molecules will be randomly oriented irrespective of their length; however at higher concentrations molecules in the long state will be oriented more strongly than those in the short state. Consequently, we introduce two orientation distribution functions, $\Psi_S(\mathbf{u})$ representing molecules in the short state and $\Psi_L(\mathbf{u})$ in the long state. Moreover, there can be an intrinsic energy difference between short and long states (Figure 1) which will provide a bias or preference for one of the states: we let ΔE represent the energy of a rotaxane in the long state relative to the short state, $\Delta E = E_L - E_S$. We emphasise that this intrinsic bias is independent of the local environment of the molecule, so that in any case where $\Delta E \neq 0$, there will be differing populations of short and long states for an isolated rotaxane.

The free energy derivation is similar to that for the fixed-length system (see Appendices A and B), with the exception that, because of two possible states of each molecule, we have two orientational distribution functions and the partition function is augmented by a factor $Z_2[x]$,

$$Z[\Psi_S,\Psi_L,x] = Z_0[\Psi_S,\Psi_L,x]\, Z_1[\Psi_S,\Psi_L,x]\, Z_2[x].$$

$Z_2[x]$ corresponds to the number of ways that N non-interacting rotaxanes partition between the short and long states

$$Z_2[x] = \frac{N!}{(xN)!\,((1-x)N)!}\exp\left[\frac{xN\Delta E}{k_BT}\right],$$

where x is the fraction of short states. The contribution to the free energy associated with molecular switching is $F_2[x] = -k_BT \ln Z_2[x]$, or

$$\frac{F_2[x]}{Nk_BT} = x\ln x + (1-x)\ln(1-x) - x\frac{\Delta E}{k_BT}. \tag{7}$$

The first two terms of the RHS are recognisable as the entropy of mixing. Here they represent a configurational entropy. Any deviation from equal numbers of long and short is penalised. In the absence of any interactions between the rods, and assuming that there is no bias ($\Delta E = 0$), the minimum lies at $x = 1/2$. With an inbuilt bias but no interactions, we find the minimum is at $x = \frac{1}{2}\exp[-\frac{\Delta E}{k_BT}]$. The contribution to the free energy by distributing these non-interacting rotaxanes with orientational distribution functions Ψ_S and Ψ_L is $F_0[\Psi_S,\Psi_L,x] = -k_BT\ln[Z_0[\Psi_S,\Psi_L,x]]$, and is, following Sec. II,

$$\frac{F_0[\Psi_S,\Psi_L,x]}{Nk_BT} = \ln[N/V] - 1 + x\int d\mathbf{u}\Psi_S[\mathbf{u}]\ln[\Psi_S(\mathbf{u})] + (1-x)\int d\mathbf{u}\Psi_L(\mathbf{u})\ln[\Psi_L(\mathbf{u})]. \tag{8}$$

Finally, the contribution to the free energy from the interactions between rotaxanes requires the excluded volume between the 3 possible pairs (short-short, short-long, long-long). The excluded volume of a pair of molecules, β, depends upon the molecular length, which can take on values of L, in the short state, or qL in the long state. The 3 possible values of β are

$$\begin{aligned}\beta_{L,L}(\mathbf{u},\mathbf{u}') &= 2L^2d\,|\mathbf{u}\times\mathbf{u}'|,\\ \beta_{S,L}(\mathbf{u},\mathbf{u}') &= 2qL^2d\,|\mathbf{u}\times\mathbf{u}'|,\\ \beta_{S,S}(\mathbf{u},\mathbf{u}') &= 2q^2L^2d\,|\mathbf{u}\times\mathbf{u}'|.\end{aligned} \tag{9}$$

Amongst the $N^2/2$ pairwise interactions, x^2 is the mean fraction of the pairwise interaction that is between molecules in the short state, $(1-x)^2$ is the mean fraction of pairs in the long state, and $2x(1-x)$ is the mean fraction of pairwise interactions involving molecules in different length states. Thus, the contribution to the free energy due to pairwise interactions is

$$\begin{aligned}\frac{F_1[\Psi_S,\Psi_L,x]}{Nk_BT} &= \frac{N}{2V}\Big[(1-x)^2\int\int d\mathbf{u}\,d\mathbf{u}'\beta_{L,L}\Psi_L(\mathbf{u})\,\Psi_L(\mathbf{u}')\\ &\quad + 2x(1-x)\int\int d\mathbf{u}\,d\mathbf{u}'\beta_{S,L}\Psi_S(\mathbf{u})\,\Psi_L(\mathbf{u}')\\ &\quad + x^2\int\int d\mathbf{u}\,d\mathbf{u}'\beta_{S,S}\Psi_S(\mathbf{u})\,\Psi_S(\mathbf{u}')\Big].\end{aligned} \tag{10}$$

Then, the total free energy of a solution of N rotaxanes, a fraction x of length L and $(1-x)$ of length qL, all with diameter d, is

$$\begin{aligned}\frac{F[\Psi_S,\Psi_L,x]}{Nk_BT} &= \frac{F_0[\Psi_S,\Psi_L,x]}{Nk_BT} + \frac{F_1[\Psi_S,\Psi_L,x]}{Nk_BT} + \frac{F_2[x]}{Nk_BT}\\ &= \ln[N/V] - 1 + x\int d\mathbf{u}\Psi_S(\mathbf{u})\ln[4\pi\Psi_S(\mathbf{u})] + (1-x)\int d\mathbf{u}\Psi_L(\mathbf{u})\ln[4\pi\Psi_L(\mathbf{u})]\\ &\quad + \frac{1}{2}\frac{N}{V}\Big[(1-x)^2\int\int d\mathbf{u}\,d\mathbf{u}'\beta_{L,L}\Psi_L(\mathbf{u})\,\Psi_L(\mathbf{u}') + 2x(1-x)\int\int d\mathbf{u}\,d\mathbf{u}'\beta_{S,L}\Psi_S(\mathbf{u})\,\Psi_L(\mathbf{u}')\\ &\quad + x^2\int\int d\mathbf{u}\,d\mathbf{u}'\beta_{S,S}\Psi_S(\mathbf{u})\,\Psi_S(\mathbf{u}')\Big] + x\ln x + (1-x)\ln(1-x) - x\frac{\Delta E}{k_BT}.\end{aligned} \tag{11}$$

In complete analogy with Onsager's treatment, we replace the orientation distribution functions $\Psi_S(\mathbf{u})$ and $\Psi_L(\mathbf{u})$ with parameters α_S and α_L (Figure 3) that characterise the orientation of rotaxanes in the short (S) and long (L) states,

$$\begin{aligned}\Psi_S &= \frac{\alpha_S}{4\pi \sinh \alpha_S} \cosh\left[\alpha_S \mathbf{u}\cdot\mathbf{n}\right],\\ \Psi_L &= \frac{\alpha_L}{4\pi \sinh \alpha_L} \cosh\left[\alpha_L \mathbf{u}\cdot\mathbf{n}\right].\end{aligned} \tag{12}$$

This allows us to express the free energy of a solution of N rotaxanes at any concentration c as a function of the fraction x and orientational parameters α_S and α_L. This expression for the free energy is derived and given in Appendices A and B, and is referred to using the notation $F(x,\alpha_S,\alpha_L,c)$. At any given concentration, the orientation of the rotaxanes in their short and long states, as well as the fraction that adjust to the short state will adopt values that minimise the free energy. At the lowest concentration, $c < c_i$, where the solution is in a single isotropic phase, rotaxanes in the short and long states will orient randomly or $\alpha_S = \alpha_L = 0$. The fraction of rotaxanes in the short state in the isotropic solution of concentration c is determined by that value of $x(c)$ that satisfies $\partial F(x,\alpha_s = 0,\alpha_L = 0,c)/\partial x = 0$. At high concentration $c > c_a$, where a single nematic phase exists, all rotaxanes are oriented, although rotaxanes in the long state will be more highly oriented than those in the short state. The orientation of the short and long switch states, $\alpha_S(c)$ and $\alpha_L(c)$, as well as the fraction of short switch states $x(c)$, will adopt values that minimise the free energy and are determined by the solution of the 3 equations

$$\frac{\partial F(x,\alpha_S,\alpha_L,c)}{\partial x} = \frac{\partial F(x,\alpha_S,\alpha_L,c)}{\partial \alpha_S} = \frac{\partial F(x,\alpha_S,\alpha_L,c)}{\partial \alpha_L} = 0.$$

Between two critical concentrations, c_i and c_a, the free energy is minimised simultaneously by two sets of $\{\alpha_S,\alpha_L,x\}$: this corresponds to the coexistence of two phases, an isotropic phase and an (anisotropic) nematic phase. The isotropic phase with N_i rotaxanes and volume V_i, with fraction x rotaxanes in the short state and parameters $\alpha_S = \alpha_L = 0$, has a free energy per molecule of $F_i = F(N_i,V_i,x(c_i),\alpha_S = 0,\alpha_L = 0)$. In the nematic phase, the free energy per rotaxane is $F_a = (N_a,V_a,x(c_a),\alpha_S(c_a),\alpha_L(c_a))$. The relative amounts of the phases vary within the concentration range and this is determined by equating the chemical potential of the rotaxanes (irrespective of their state) in each of the phases, as well as the osmotic pressure in each phase.

IV. RESULTS AND DISCUSSION

The free energy expression (Eq. (11)) provides numerical results which yield the phase diagram of these liquid crystalline rotaxanes as a function of the length ratio, q, that is associated with the molecular design of the rotaxane. As stated previously, the phase diagram is similar to that of a system of fixed-length rods, in that there are three different regimes: isotropic; coexisting isotropic and nematic and pure nematic. The concentrations at which each of these regimes occur, are different to the fixed-length case, as we detail later. The system seems rather complicated, since we can vary two different parameters externally. These are the scaled concentration $\frac{\pi}{4}cL^2d$ and the ratio of the long to short states, q. Moreover, we have three different regimes (isotropic, nematic, and coexisting), and in each of these regimes, we can measure the order parameter, S for each of the different lengths, and the fraction of short rotaxanes x. Against this apparent complexity is the fact that the free energy is a simple sum of 4 terms. These are: the orientational entropy; the interaction term; the configurational entropy; and the energetic bias. The behaviour of the system can be understood as a competition between all of these terms. We present the results under a number of subheadings: the fraction of short states, the critical concentrations, and the order parameters.

A. Fraction of short states

First we consider a solution of unbiased ($\Delta E = 0$) rotaxanes with $q = 1.1$, and consider the fraction of short states, x, as we increase the total concentration, c, Figure 4. In the limit of infinite dilution, when the rotaxanes orient freely and randomly, the proportion of rotaxanes in the short state, x, is determined by the energy bias in between the states and the configurational entropy, Eq. (7), and is $x = 0.50$ for $\Delta E = 0$, independent of q. As the total concentration increases towards c_i, the molecules begin to interact and in order to maximise translational and orientational entropy, the rotaxanes increasingly adopt a short state at the expense of the configurational entropy. As we will see, this growth in the population of short states is more dramatic, as the ratio of long to short lengths, q increases—this is because switching a randomly oriented long rod to a randomly oriented short rod, increases the translational entropy of the solution. At a critical concentration, c_i, partial orientational ordering occurs and a nematic phase appears which coexists with the isotropic phase. The fraction of short rods in the coexisting phase is x_i for the isotropic phase and x_a for the nematic phase. This nematic or orientationally ordered phase has a larger fraction of rotaxanes in the long state than the coexisting isotropic phase ($x_a < x_i$)—this is because the translational entropy penalty in the nematic phase is reduced by alignment. In an isotropic phase, the randomly oriented long rod would greatly reduce translational entropy (due to collisions) at $c < c_i$, whereas collisions within a nematic phase are significantly less because the molecules are already well-aligned. As in the case of monodisperse rods, these coexisting phases persist over a range of concentrations $c_i < c < c_a$. As the total concentration, c, changes within this range, the concentrations of each phase and the fraction of rotaxanes in the short state within each phase do not change—only the relative amounts of isotropic and nematic phases change. At a total concentration of c_a, the isotropic phase disappears entirely leaving a single nematic phase which grows more ordered with concentration. Because of this, the length of the rods becomes less and less relevant (collisions become rarer for well-aligned systems), and there is not much translational entropy to be gained by being short. The configurational entropy again comes to the fore, and at large enough concentrations, we expect x to approach its "natural" value of 1/2.

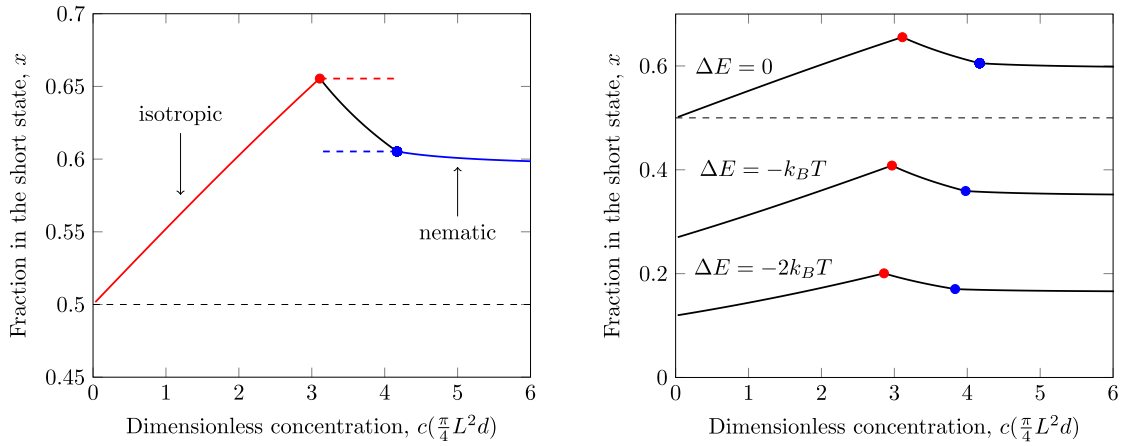

FIG. 4. Left: The fraction of rotaxanes in the short state, x, as a function of dimensionless concentration, $\frac{\pi}{4}cL^2d$, for unbiased rotaxanes ($\Delta E = 0$) and $q = 1.1$. The solid line gives the fraction of short rods in the solution where we use red to denote the isotropic phase and blue for the orientationally ordered or nematic phase. At and above a critical concentration c_i (red circle), the rotaxanes are in coexisting isotropic and nematic phases, with the fraction of short states differing in the coexisting isotropic (dashed red line) and nematic (dashed blue line) phases. As the total concentration increases within the coexistence region, the nematic phase grows at the expense of the coexisting isotropic phase and the overall fraction of short states decreases. At a critical concentration c_a (blue circle), the coexisting isotopic phase vanishes leaving a single nematic phase. The fraction of short states in the nematic phase decreases slightly with increased concentration and in the limit of very large concentrations, the fraction of short states is determined by the bias in the switch states, which for $\Delta E = 0$ is $x = 0.50$ (dashed black line). Right: The fraction of rotaxanes in the short state, x versus $\frac{\pi}{4}cL^2d$ for $q = 1.1$ in the presence of an intrinsic energy bias towards long states. From top to bottom, these are $\Delta E = 0$ (unbiased), $\Delta E = -1k_BT$, and $\Delta E = -2k_BT$ (chemical bias towards long states). When the energy bias $|\Delta E|$ becomes much greater than k_BT, the variation in x with concentration disappears, that is there is a lack of adaptivity, and the rotaxanes are effectively of fixed length.

We now introduce an energetic bias between the short and long states by having $\Delta E \neq 0$. In Figure 4, we compare the fraction of rotaxanes in the short state versus the concentration for the unbiased case $\Delta E = 0$ with two cases where there is chemical bias towards the long state, $\Delta E = -1k_BT$ and $\Delta E = -2k_BT$. The phase behaviour is similar to that in the unbiased case except that the fraction of short rods at infinite dilution, $x(c \to 0) = \exp[-\frac{\Delta E}{k_BT}](1 + \exp[-\frac{\Delta E}{k_BT}])$ is significantly reduced and switching between states is significantly reduced with an increased bias towards long states. Likewise if the short state is energetically preferred, $0 < \Delta E$, there will also be minimal switching. Indeed, without adaptive switching $|\Delta E| \gg k_BT$, the molecules become fixed-length rods with liquid crystalline phase diagram approaching that of Onsager's. If an external switch is applied to these non-adaptive rotaxanes, the rotaxanes can be forced into an Onsager-like liquid crystalline phase behaviour predicted by He *et al.*[22]

We now look at the effect of the length ratio q upon the fraction of rods in the short state. This is shown in Figure 5 where we plot x, as a function of concentration, $c(L^2d)^{-1}$, for unbiased rotaxanes for q ranging between 1.1 and 2.0. As noted before, as q increases, the variation in the fraction of short states becomes more dramatic for $c < c_i$. Except in the limits of $c \to 0$ and $c \to \infty$ where $x = 0.50$ for all values of q, the fraction of rotaxanes in the short state increases with q at a fixed c. In essence, this system has a choice between a short state and a long state. Short states always have less translational entropy penalty and thus are always favoured whenever there is the possibility of rotaxane overlap. Rotaxane overlap is not possible at infinite dilution, $c = 0$. In the case of highly concentrated solutions, within the Onsager approximation, there is perfect order, and the approximation for the excluded volume interaction gives no overlap. Hence, in both of these cases, $c \to 0$ and $c \to \infty$, q becomes irrelevant.

Apart from these numerical results, for the isotropic state, it is possible to produce some analytic results, valid for low concentrations. These will tell us how the fraction of short rods depends on concentration, energy bias, and length ratio. We start from the free energy per rod in the isotropic phase (ignoring irrelevant terms)

$$\frac{F}{Nk_BT} = x\ln x + (1-x)\ln(1-x) + \frac{\pi cL^2d}{4}\left[x^2 + 2qx(1-x) + q^2(1-x)^2\right] - x\frac{\Delta E}{k_BT}. \tag{13}$$

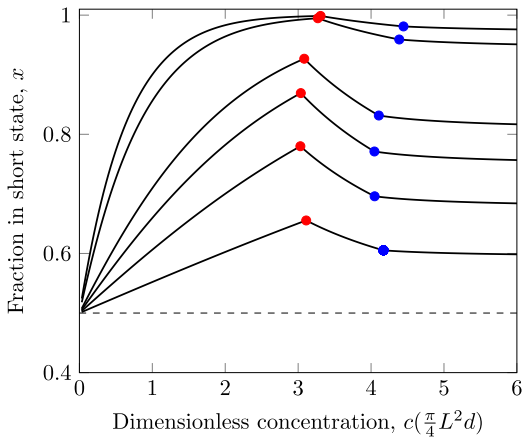

FIG. 5. The fraction of rotaxanes in the short state, x, as a function of the scaled concentration, $\frac{\pi}{4}cL^2d$ for unbiased rotaxanes ($\Delta E = 0$) and (bottom to top) $q = 1.1, 1.2, 1.3, 1.4, 1.8$, and 2.0. As the ratio of the lengths of the long to short states increases, we see a strong tendency to favour short rotaxanes. In the limit of $c \to 0$ and $c \to \infty$, the fraction of rotaxanes in the short state goes to $x = 0.50$ in the unbiased $\Delta E = 0$ case. At intermediate concentrations, the fraction in the short state increases with q, irrespective of phase or coexistence.

In the case of no bias $\Delta E = 0$ and zero concentration, this free energy is minimised when the fraction of short rotaxanes is $\frac{1}{2}$. At non-zero concentrations, we expand the free energy with respect to x about $x = \frac{1}{2}$ and to lowest order in c, minimising gives

$$x = \frac{1}{2} + \frac{\pi L^2 d}{16} c(q^2 - 1). \tag{14}$$

We are thus able to conclude that in the isotropic phase, the fraction of short rods grows linearly with the concentration. Moreover we also have the dependence on q from this equation. A similar procedure allows the dependence on ΔE to be included, but the results are more lengthy.

B. The effect of length ratio

The critical concentrations c_i and c_a, as well as the fraction of short states in the coexisting phases, x_i and x_a, depend critically upon the length ratio, q. First, it is important to recognise that the case of $q = 1$ corresponds to rotaxane states whose lengths are indistinguishable; that is, $q = 1$ is the same as the case of monodisperse rods where $c_i = 3.34(\frac{\pi}{4}L^2 d)^{-1}$ and $c_a = 4.49(\frac{\pi}{4}L^2 d)^{-1}$.

Figure 6 shows the critical concentrations c_i and c_a versus q for unbiased rotaxane states and the corresponding fraction of short states, x, in each of the coexisting phases versus q, again for the unbiased switch states. Taken together, these

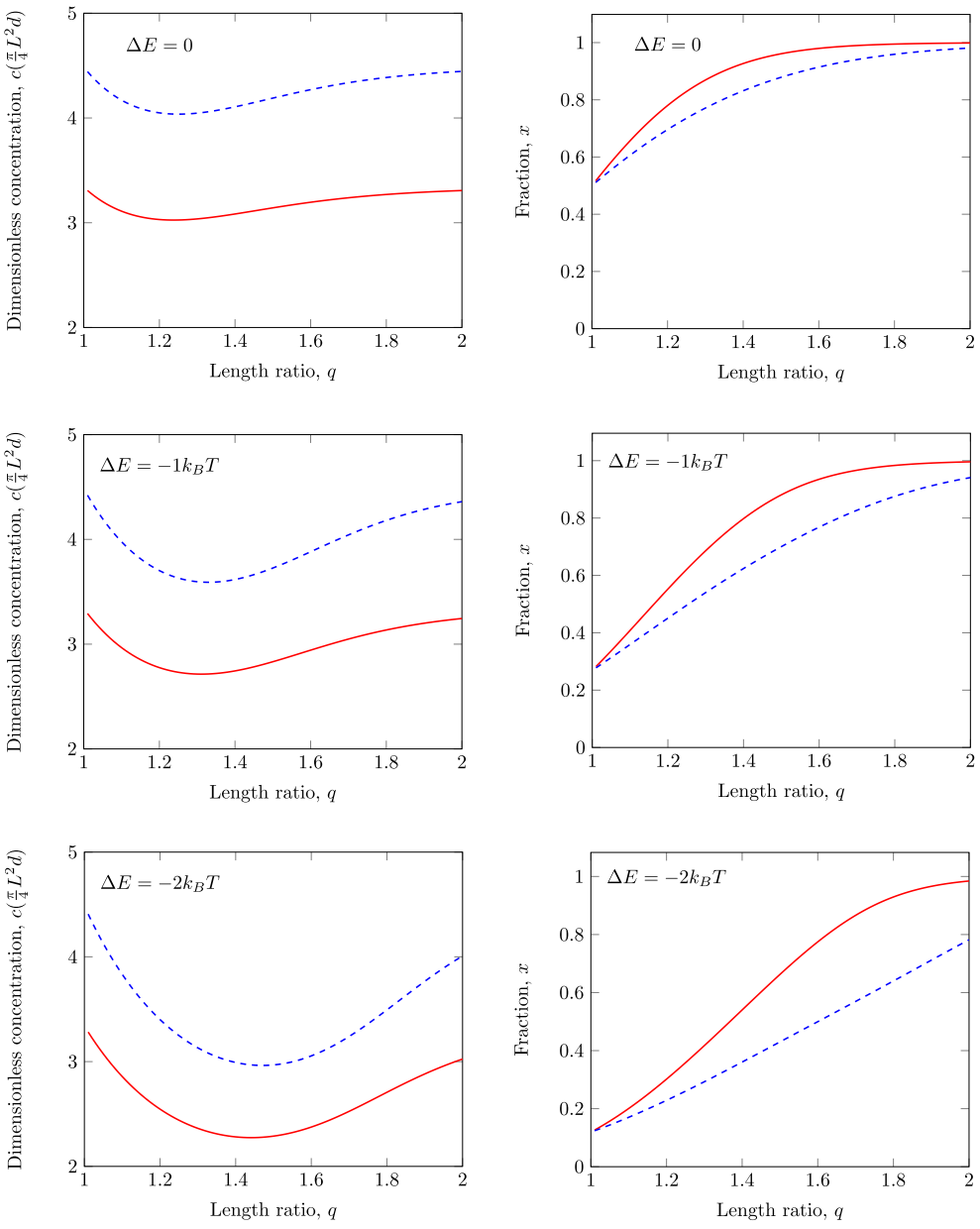

FIG. 6. Left: The critical concentrations as a function of the length ratio of long to short states for different values of the energy bias. The full line is for the isotropic to nematic-isotropic coexistence transition. The dotted line is for the transition from coexistence to pure nematic. At the top is the case $\Delta E = 0$ (no intrinsic bias towards long or short). At middle $\Delta E = -1k_BT$ (a slight bias towards long rods). At the bottom, $\Delta E = -2k_BT$ (stronger bias towards long rods). Right: The fraction of rods in the short state (right) at coexistence, as a function of the length ratio of long to short states for different values of the energy bias. The solid line is the fraction in the isotropic phase, and the dotted line is the fraction in the nematic phase. The values of ΔE are the same as for the left graphs. Two things are notable on these graphs. First the critical concentrations exhibit a minimum as the length ratio increases. Second, for any finite length ratio there is a substantial jump in x between the two different phases.

figures show that the coexistence of isotropic/nematic phases (for $\Delta E = 0$) in the case of large q, ($q > 2$) approaches that of the monodisperse or $q = 1$ case; that is, $c_i(q > 2) \to c_i(q = 1)$, $c_a(q > 2) \to c_a(q = 1)$ and $x_i(q > 2) \to 1, x_a(q > 2) \to 1$. That is, the coexisting phases become monodisperse in the short state as q increases in the unbiased case. This is because there is no energy bias between long and short states, and (outside of infinite dilution) switching to short states affords more translational entropy than the long state in both the isotropic phase and in the nematic phase. Indeed, even if there is a small chemical bias against short states, Figure 6, the isotropic and nematic phases are dominated by short states when q is significantly large. That is, as we make rotaxanes where q is large, the liquid crystalline phase behaviour is reduced to that of monodisperse short rods, outside of infinite dilution. Rotaxanes designed with too large a value of q do not utilise adaptability in all but the most dilute of concentrations. This contrasts with the case of a mixture of short and long fixed-length rods:[26,27] the smallest fraction of long rods results in a decrease in the critical concentrations c_i and c_a, and the larger the ratio of the long to short length or q, the more dramatic is this decrease in the critical concentrations.

Figure 6 also shows that rotaxanes which switch between states with $1 < q < 2$ have lower critical concentrations c_i and c_a, and that the critical concentrations are minimal at an intermediate q, q^*. This quantitative result from the free energy model is understood by considering the entropy compromises made when a molecule in a long state switches to a short state. When this happens, there is an increase in translational entropy. This is true if the long rotaxane is randomly oriented in the isotropic phase or oriented in a nematic phase, and this gain in entropy is larger if the difference in lengths of the states is greater. However, when a long state switches to a short state, there is also a penalty paid in configurational entropy, and this penalty is independent of the length of the states. Consequently, for rotaxane states that are nearly of the same length, (q is a little larger than unity), the increase in translational entropy for switching from a long to short state can be small compared to the penalty paid in configurational entropy—and consequently switching from long to short state is not favourable. We already mentioned that adding long fixed-length rods to short rod[26,27] lowers the critical concentrations c_i and c_a and the larger the length difference between the rods, the lower the critical concentrations. So consequently, for moderate values of q where switching is not entropically favourable, we see a decrease in c_i and c_a with an increase in q towards q^*. Next, as q increases beyond q^*, the length of the long state increases to such an extent that the gain in translational entropy overcomes the penalty in configurational entropy. At these larger values of q, switching is entropically favourable and the rotaxanes readily adopt a short state and the solution trends towards a monodisperse collection of short rotaxane states. The numerical results of the model confirm this: Figure 6 shows that the fraction of short states grows roughly linearly from $q = 1$, but that at large q, the fraction of short states is nearly constant at $x = 1$. Again, from the bidisperse fixed-length molecules, we know that when you decrease the fraction of long fixed-length molecules, the critical concentrations increase: In analogy, when $q > q^*$, the fraction of short states in both isotropic and anisotropic phases approaches unity and the critical concentrations c_i and c_a increase back to the $q = 1$ limit.

As a final note, it is clear from the graphs in Figure 6 that, provided the inbuilt bias, $|\Delta E|$ is not too large, for large q that almost all the molecules at coexistence are in the short state in the isotropic phase.

C. The order parameter, *S*

One other quantity of interest is the order parameter, S which quantifies how well-aligned the molecules are. The isotropic state has $S = 0$, and a perfectly aligned nematic phase has $S = 1$. We plot S against the length ratio q in the coexisting phase, for both the long and the short states in Figure 7. For the long states, these graphs show little that is surprising. The long molecules are better-ordered than the short ones, because a lack of order for the long molecules automatically gives more collisions and a reduction in translational entropy. Moreover, the longer the rod the higher the order.

The order parameter of the short molecules in the coexisting nematic phase exhibits a somewhat more complex behaviour in that it is non-monotonic in q. Again, this is due to a balance between translational and orientation entropy as detailed in the free energy model; however we can understand this in terms of the volume available to a short rotaxane in the nematic phase and Figure 6. When the volume available to an anisotropic rod decreases, it will orient, i.e., S will increase. From Figure 6, the concentration of the coexisting nematic phase, c_a, decreases from $q = 1$ to some q^*, that is, there is *more* volume per molecule in the nematic phase. Rotaxanes in the long state, whose excluded volume grows with q align, and the short rotaxanes, with fewer collisions in a larger molecular volume, are more free to rotate. Consequently, the order parameter for the short state decreases with q for $q < q^*$. However, for $q > q^*$, the concentration of the nematic phase increases with q, and there is *less* volume available to the rotaxanes: rotaxanes in both the short and long state become more aligned and S increases with q for both. This produces the minimum in $S(q)$ for the short state. As we increase q further, the order parameter of the long state increases; however the proportion of long states also vanishes at high q. Again, the disappearance of the long state which has an excluded volume that varies with q^2, provides additional volume for the growing population of short rotaxanes. With *more* volume per molecule, the rotaxanes in the short state again gain some orientational freedom and their order parameter diminishes. This produces a maximum in $S(q)$ for the short state. However, in the limit of high q, the coexisting nematic phase contains rotaxanes that are entirely in the short state and consequently, it is indistinguishable from the coexisting nematic phase for $q = 1$. That is, for the short state, $S(q \to \infty) = S(q = 1)$. When the rotaxane has a small intrinsic bias towards the long state, these changes in the order parameter with q become more dramatic, primarily because the variation in the proportion of short rods in coexistence varies more dramatically with q when there is intrinsic bias towards the long state: from Figure 6, we

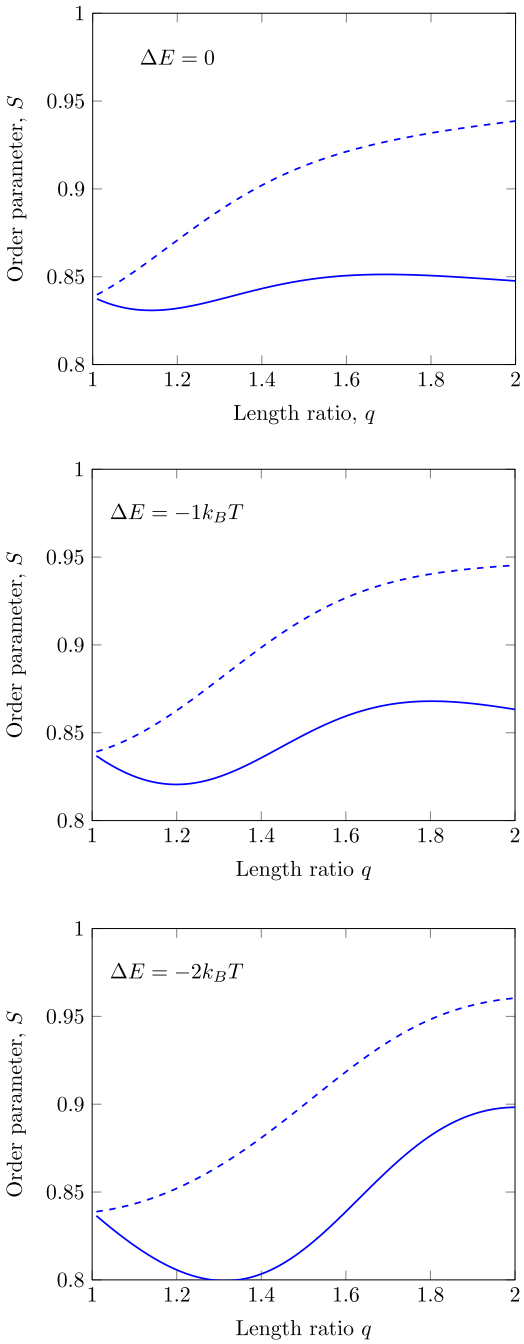

FIG. 7. The nematic order parameter, S for molecules in the short state (full line) and long state (dashed line) in the nematic phase at coexistence, as a function of the length ratio for different values of the energy bias, ΔE. At the top is the case $\Delta E = 0$ (no intrinsic bias towards long or short). At middle $\Delta E = -1k_BT$ (a slight bias towards long rods). At the bottom, $\Delta E = -2k_BT$ (stronger bias towards long rods). Note that the order parameter for long rods always increases, but that for short rods shows a minimum followed by a maximum.

see that $0.5(q = 1) \leq x \leq 1(q \to \text{large})$ for $\Delta E = 0$, but that $0.15(q = 1) \leq x \leq 1(q \to \text{large})$ for $\Delta E = -2k_BT$.

V. CONCLUSIONS

Here we examined the phase behaviour of 2-state adaptive rotaxanes. These rotaxanes should be contrasted with those studied earlier by the present authors,[22] where the length was externally controlled. Here the length is chosen by the rotaxane molecule itself in response to the local concentration environment. One major conclusion of this study is that the 2-state adaptive rotaxane forms isotropic and nematic phases, just as the fixed-length rod system does. However, the critical concentrations are different from the fixed-length system, and moreover they show a minimum as the length ratio is increased. In particular, for an unbiased rotaxane ($\Delta E = 0$), it is best to use a length ratio which is small $q \approx 1.2$. Large length ratios, $q > 2$, are counter-productive. The rotaxane has a choice of being of length L or length qL, and if q is made too large, the loss of translational entropy due to collisions becomes prohibitive. In the limit of large q, the system effectively ignores the possibility of having rods of length qL and behaves as if it had rods of fixed short length L.

There is a good reason why we cannot have $q > 2$ with only two axles. This means that such an extension would be geometrically impossible. Of course, we could have larger q values by using more axles per rotaxane, but in such a case, the flexibility of the extended molecule would need to be accounted for.

In the isotropic state, the fraction of short states increases with increasing concentration, because short states undergo fewer collisions. However, once the coexistence regime is entered, the alignment implies fewer collisions and the advantage short states have is reduced. Thus in the coexistence regime, the fraction of short states decreases (because the nematic phase increases in volume), and keeps decreasing when a pure nematic phase comes into being. The initial increase in the fraction of short states (Eq. (14)) is perhaps the simplest experimental test of the theory, because this occurs in the isotropic phase, and does not require the existence of a nematic phase. In particular, the linear increase in x with c should be relatively simple to detect.

One referee has raised the question of our energy biases, ΔE, in particular why they seem to have limited effect on the transition concentrations, and why we do not push them to higher negative values. The reason for their limited effect is that even $\Delta E = -2k_BT$ is not particularly large. For $\Delta E = -20k_BT$, we would expect a large effect. However, if we push $|\Delta E|$ to be large, we encounter a simple problem. The system no longer behaves as adaptive, and becomes one of the rods with a single length. It then reverts to the ordinary Onsager system, and all novelty is lost.

The most unexpected conclusion is that the order parameter for the short state in the nematic shows a minimum and a maximum as the rod length ratio is increased. This might be difficult to detect experimentally, because it requires a measurement of the order of only one species, but it should be easily measured in computer simulation.

An important question to ask is which experimental systems should be used to detect these effects. In the review by Bruns and Stoddart,[1] there are many systems which undergo extensions in the range we are interested in. What is required is one for which the Onsager theory should be approximately true. Such systems tend to have large ratios of length to

diameter. The first test that needs to be made in such cases is to take to axles individually, prior to rotaxane formation, and ensure that at high enough concentration a nematic state is formed.

ACKNOWLEDGMENTS

Hao He acknowledges Zhe Li for helping with the numerical work.

APPENDIX A: THE ONSAGER THEORY FOR RODS OF FIXED LENGTH

Here we review Onsager's theory[19,28] for rods of fixed length L and diameter d. The equilibrium partition function for a solution of N rods with orientational distribution Ψ is

$$Z[\Psi] = \frac{1}{N!}\int_{\Psi}\prod d\mathbf{u}_i \prod d\mathbf{R}_i \exp\left[-\frac{\sum_{i>j} U_{i,j}}{k_BT}\right],$$

where $\mathbf{u}_i$ is the unit vector, directed along the long axis of the ith rod, $\mathbf{R}_i$ is the rod's centre of mass position, and $U_{i,j}$ is the interaction energy between the ith and jth rods. We can rewrite this partition function as a product of functions,

$$Z[\Psi] = Z_0[\Psi]Z_1[\Psi].$$

Z_0 is the partition function associated with distributing non-interacting rods with an orientational distribution $\Psi(\mathbf{u})$, and Z_1 is the contribution from the interactions between the rods, or

$$Z_0 = \frac{1}{N!}\int_{\Psi}\prod d\mathbf{u}_i \prod d\mathbf{R}_i$$

and

$$Z_1 = \frac{\int_{\Psi}\prod d\mathbf{u}_i \prod d\mathbf{R}_i \exp\left[-\frac{\sum_{i>j} U_{i,j}}{k_BT}\right]}{\int_{\Psi}\prod d\mathbf{u}_i \prod d\mathbf{R}_i} = \langle \exp[-\frac{\sum_{i>j} U_{i,j}}{k_BT}]\rangle_{\Psi}.$$

Z_0 is determined in the following way: the position of each rod can be any location within the volume, so $\int d\mathbf{R_i} = V$ or $\int \prod_i^N d\mathbf{R_i} = V^N$. However, the orientation vectors of the rods are constrained by the distribution $\Psi(\mathbf{u})$. The set of all possible unit-vectors, $\mathbf{u}$, sweeps out the surface of a sphere, which we divide into small regions of area (or solid angle) Ω. As the rods are oriented according to $\Psi(\mathbf{u})$, then the number of rods oriented within $\mathbf{u}_a \pm d\mathbf{u_a}$, or solid angle of size Ω, is $n_a = N\Psi(\mathbf{u}_a)\Omega$. Thus $\int_{\Psi}\prod_i^N d\mathbf{u_i}$ is evaluated discretely as the number of ways of assigning N rods to a set of differential solid angles, each of size Ω with population n_a or

$$\int_{\Psi}\prod_i^N d\mathbf{u_i} = \frac{N!}{\prod n_a!}\Omega^N.$$

Taken together, this yields

$$Z_0 = \frac{(\Omega V)^N}{\prod_i^N n_a!}.$$

As $\sum_a n_a = N$ and $\sum_a \Omega\Psi(\mathbf{u}_a) = 1$, then the free energy (entropy) associated with distributing non-interacting rods with an orientational distribution $\Psi(\mathbf{u})$ is

$$F_0[\Psi] = -k_BT\ln[Z_0[\Psi]] = Nk_BT\left[\ln[N/V] - 1 + \int d\mathbf{u}\Psi(\mathbf{u})\ln[\Psi(\mathbf{u})]\right]. \quad \text{(A1)}$$

The contribution to the free energy from the interactions between rods can also be found from the corresponding partition function, $F_1[\Psi] = -k_BT\ln[Z_1[\Psi]]$, or alternatively, we can make simple use of a simple virial expansion of the free energy written in terms of particle number,

$$F_1[\Psi] = -k_BT\ln\left\langle\exp\left[-\frac{\sum_{i>j} U_{i,j}}{k_BT}\right]\right\rangle = B_2N + B_3N^2 + \cdots,$$

where B_j is the jth virial coefficient. In dilute solutions of rods, we only need to consider B_2N, first term in the virial expansion which accounts for the pairwise interaction between two rods of orientation $\mathbf{u}$ and $\mathbf{u}'$,

$$B_2N = \frac{N^2k_BT}{2V}\int d\mathbf{u}d\mathbf{u}'\Psi(\mathbf{u})\Psi(\mathbf{u}')\beta(\mathbf{u},\mathbf{u}'),$$

where $\beta(\mathbf{u},\mathbf{u}')$ is

$$\beta(\mathbf{u},\mathbf{u}') = \int dR\left[1 - \exp\left[-\frac{U(\mathbf{u},\mathbf{u}',R)}{k_BT}\right]\right].$$

For a pair of rigid rods which interact as hard bodies (or where the interaction energy is $U = \infty$ when overlapping and $U = 0$ otherwise), $\beta(\mathbf{u},\mathbf{u}')$ corresponds to the volume that one rod excludes to another rod. For rods of diameter d, but of two different, fixed lengths, L and L^*, the excluded volume for two rods that make an angle $|\gamma| \equiv |\mathbf{u}\times\mathbf{u}'|$ is

$$\beta(\mathbf{u},\mathbf{u}') = 2LL^*d\ |\mathbf{u}\times\mathbf{u}'|. \quad \text{(A2)}$$

The contribution of pairwise interactions of rods of the same length L to the free energy is

$$\frac{F_1[\Psi]}{Nk_BT} = \frac{1}{2}\frac{N}{V}\int\int d\mathbf{u}\,d\mathbf{u}'\Psi(\mathbf{u})\,\Psi(\mathbf{u}')2L^2d\ |\mathbf{u}\times\mathbf{u}'|. \quad \text{(A3)}$$

APPENDIX B: CALCULATION OF THE ADAPTIVE FREE ENERGY

(i) **Free energy of the isotropic phase**. In the isotropic phase,[28] all molecules are randomly oriented, irrespective of whether they are in the short or long state, so that the orientational distribution function is a constant, $\Psi_S[\mathbf{u}] = \Psi_L[\mathbf{u}] = \frac{1}{4\pi}$. Consequently, there is no orientational entropy of non-interacting rods in the isotropic phase and $\int d\mathbf{u}\Psi[\mathbf{u}]\ln[4\pi\Psi[\mathbf{u}]] = 0$. To simplify the three terms for the free energy associated with pairwise interactions between rods, we need to specify the excluded volume of pairs of molecules. Let γ be the angle made by two molecules so that we have

$$\beta_{S,S}(\gamma) = 2L^2d|\mathbf{u}\times\mathbf{u}'| = 2L^2d|\sin\gamma|, \quad \text{(B1)}$$

$$\beta_{S,L}(\gamma) = 2qL^2d|\mathbf{u}\times\mathbf{u}'| = 2qL^2d|\sin\gamma|, \quad \text{(B2)}$$

$$\beta_{L,L}(\gamma) = 2q^2L^2d|\mathbf{u}\times\mathbf{u}'| = 2q^2L^2d|\sin\gamma|. \quad \text{(B3)}$$

$d\mathbf{u}$ is a differential solid angle, expressible in terms of polar and azimuthal angle or $d\mathbf{u} = \mathbf{d}\phi\sin\theta\mathbf{d}\theta$. The integrals are of the form

$$\int\int d\mathbf{u}\, d\mathbf{u}' \beta_{S,S} \Psi(\mathbf{u})\, \Psi(\mathbf{u}') = \frac{1}{16\pi^2} \int_0^{2\pi} d\phi \int_0^{2\pi} d\phi' \int_0^{\pi} \sin\theta d\theta \int_0^{\pi} 2L^2 d|\sin\gamma| \sin\theta' d\theta' = \frac{\pi L^2 d}{2},$$

$$\int\int d\mathbf{u}\, d\mathbf{u}' \beta_{S,L} \Psi_s(\mathbf{u})\, \Psi_s(\mathbf{u}') = \frac{\pi L^2 dq}{2},$$

$$\int\int d\mathbf{u}\, d\mathbf{u}' \beta_{L,L} \Psi(\mathbf{u})\, \Psi(\mathbf{u}') = \frac{\pi L^2 dq^2}{2}.$$

These are readily performed by rotating the coordinate system so that one rod always lies along the z axis. The free energy of the isotropic phase of concentration c with fraction of short rotaxane states x is

$$\begin{aligned}\frac{F_{\text{isotropic}}}{Nk_BT} &= \frac{F_{0,\text{isotropic}}}{Nk_BT} + \frac{F_{1,\text{isotropic}}}{Nk_BT} + \frac{F_{2,\text{isotropic}}}{Nk_BT} \\ &= \ln\left[\frac{N}{V}\right] - 1 + x\ln x + (1-x)\ln(1-x) + \frac{N}{2V}\left[x^2\frac{\pi L^2 d}{2} + 2x(1-x)\frac{\pi L^2 dq}{2} + (1-x)^2\frac{\pi L^2 dq^2}{2}\right] - x\frac{\Delta E}{k_BT} \\ &= \ln c - 1 + x\ln x + (1-x)\ln(1-x) + \frac{\pi c L^2 d}{4}\left[x^2 + 2qx(1-x) + q^2(1-x)^2\right] - x\frac{\Delta E}{k_BT}.\end{aligned}$$

(ii) **Free energy of the nematic phase**. In the nematic phase, molecules are oriented and those in the long state will be oriented more strongly than those in the short state. We use the angle, θ, that the molecule makes with a director as a measure of the orientation and define two orientational distribution functions, one for the short state, $\Psi_S(\theta)$ and another for the long state, $\Psi_L(\theta)$, using Onsager's trial function, Eq. (2) with $\mathbf{u}\cdot\mathbf{n} = \cos\theta$,

$$\Psi_S(\theta) = \frac{\alpha_S \cosh(\alpha_S \cos\theta)}{4\pi \sinh(\alpha_S)}, \tag{B4}$$

$$\Psi_L(\theta) = \frac{\alpha_L \cosh(\alpha_L \cos\theta)}{4\pi \sinh(\alpha_L)}. \tag{B5}$$

The orientational entropy contribution associated with distributing non-interacting rods in the nematic phase, $F_0[\Psi, x]$, is then

$$\int d\mathbf{u}\Psi_S(\theta) \ln 4\pi[\Psi_S(\theta)] = \log(\alpha_S \coth\alpha_S) - 1 + \frac{\arctan(\sinh\alpha_S)}{\sinh\alpha_S}, \tag{B6}$$

$$\int d\mathbf{u}\Psi_L(\theta) \ln 4\pi[\Psi_L(\theta)] = \log(\alpha_L \coth\alpha_L) - 1 + \frac{\arctan(\sinh\alpha_L)}{\sinh\alpha_L}. \tag{B7}$$

As in the isotropic case, the three terms for the free energy associated with pairwise interactions between rods can be readily calculated by rotating coordinates. However, unlike the isotropic case, the orientation distribution function, Ψ, is no longer a constant but depends upon θ as well as the state of the rotaxane, long or short.

$$\int\int d\mathbf{u}\, d\mathbf{u}' \beta_{S,S} \Psi_S[\mathbf{u}]\, \Psi_S[\mathbf{u}'] = \int_0^{2\pi} d\phi \int_0^{2\pi} d\phi' \int_0^{\pi} \sin\theta \Psi_S[\theta] d\theta \int_0^{\pi} 2L^2 d|\sin(\gamma)|\sin\theta \Psi_S[\theta'] d\theta' = \frac{2L^2 d I_2(2\alpha_S)}{(\sinh\alpha_S)^2}, \tag{B8}$$

$$\int\int d\mathbf{u}\, d\mathbf{u}' \beta_{L,L} \Psi(\mathbf{u})\, \Psi(\mathbf{u}') = \frac{2q^2 L^2 d I_2(2\alpha_L)}{(\sinh\alpha_L)^2}, \tag{B9}$$

where I_2 is second order Bessel function.[19] The contribution due to pairwise interaction of molecules of different size is rather involved. Here we simply write down Onsager's result; in his original work, he describes the derivation in great detail, referring to this as the covolume,

$$\begin{aligned}&\int\int d\mathbf{u}\, d\mathbf{u}' \beta_{S,L} \Psi_S(\mathbf{u})\, \Psi_L(\mathbf{u}') \\ &= qL^2 d\sqrt{\frac{\alpha_S + \alpha_L}{2\pi\alpha_S\alpha_L}}\left\{1 - \frac{3}{8}\left(\frac{1}{\alpha_S} + \frac{1}{\alpha_L} + \frac{1}{\alpha_S + \alpha_L}\right) + \frac{15}{128}\left[\frac{8}{\alpha_S\alpha_L} - \left(\frac{1}{\alpha_S} + \frac{1}{\alpha_L} + \frac{1}{\alpha_S + \alpha_L}\right)^2\right] + \cdots\right\}.\end{aligned} \tag{B10}$$

Like Onsager, we ignore the higher order terms in the last expression, so that the free energy per molecule in the nematic phase, F_2, reduces to

$$\frac{F_2[\alpha_S,\alpha_L,x,c]}{Nk_BT} = \ln[N/V] - 1 + x\left[\ln(\alpha_S\coth\alpha_S) - 1 + \frac{\arctan(\sinh\alpha_S)}{\sinh\alpha_S}\right] + (1-x)\left[\ln(\alpha_L\coth\alpha_L) - 1 + \frac{\arctan(\sinh\alpha_L)}{\sinh\alpha_L}\right] + \frac{1}{2}\frac{N}{V}\left[(1-x)^2\left[2q^2L^2d\,\frac{I_2(2\alpha_L)}{\sinh^2\alpha_L}\right] + x^2\left[2L^2d\,\frac{I_2(2\alpha_S)}{\sinh^2\alpha_S}\right] + 2x(1-x)\,qL^2d\sqrt{\frac{\alpha_S+\alpha_L}{2\pi\alpha_S\alpha_L}}\left[1 - \frac{3}{8}\left(\frac{1}{\alpha_S}+\frac{1}{\alpha_L}+\frac{1}{\alpha_S+\alpha_L}\right) + \frac{15}{128}\left[\frac{8}{\alpha_S\alpha_L} - \left(\frac{1}{\alpha_S}+\frac{1}{\alpha_L}+\frac{1}{\alpha_S+\alpha_L}\right)^2\right] + \cdots\right]\right] + x\ln x + (1-x)\ln(1-x) - x\frac{\Delta E}{k_BT}. \quad \text{(B11)}$$

[1]C. J. Bruns and J. F. Stoddart, "Rotaxane-based molecular muscles," Acc. Chem. Res. **47**, 2186–2199 (2014).
[2]B. Brough, B. Northrop, J. Schmidt, H. Tseng, K. Houk, J. Stoddart, and C. Ho, "Evaluation of synthetic linear motor-molecule actuation energetics," Proc. Nat. Acad. Sci. U. S. A. **103**, 8583–8588 (2006).
[3]L. Kobr, K. Zhao, Y. Shen, A. Comotti, S. Bracco, R. K. Shoemaker, P. Sozzani, N. A. Clark, J. C. Price, C. T. Rogers, and J. Michl, "Inclusion compound based approach to arrays of artificial dipolar molecular rotors. A surface inclusion," J. Am. Chem. Soc. **134**, 10122–10131 (2012).
[4]G. Barin, R. S. Forgan, and J. F. Stoddart, "Mechanostereochemistry and the mechanical bond," Proc. R. Soc. A **468**, 2849–2880 (2012).
[5]R. S. Forgan, J.-P. Sauvage, and J. F. Stoddart, "Chemical topology: Complex molecular knots, links, and entanglements," Chem. Rev. **111**, 5434–5464 (2011).
[6]L. Fang, M. A. Olson, D. Benitez, E. Tkatchouk, W. A. Goddard III, and J. F. Stoddart, "Mechanically bonded macromolecules," Chem. Soc. Rev. **39**, 17–29 (2010).
[7]C. Cheng, P. R. McGonigal, W.-G. Liu, H. Li, N. A. Vermeulen, C. Ke, M. Frasconi, C. L. Stern, W. A. Goddard III, and J. F. Stoddart, "Energetically demanding transport in a supramolecular assembly," J. Am. Chem. Soc. **136**, 14702–14705 (2014).
[8]M. M. Boyle, R. A. Smaldone, A. C. Whalley, M. W. Ambrogio, Y. Y. Botros, and J. F. Stoddart, "Mechanised materials," Chem. Sci. **2**, 204–210 (2011).
[9]J. Berna, D. Leigh, M. Lubomska, S. Mendoza, E. Perez, P. Rudolf, G. Teobaldi, and F. Zerbetto, "Macroscopic transport by synthetic molecular machines," Nat. Mater. **4**, 704–710 (2005).
[10]C. J. Bruns and J. F. Stoddart, "Molecular Machines Muscle Up," Nat. Nanotech. **8**, 9–10 (2013).
[11]P. Gavina and S. Tatay, "Synthetic strategies for the construction of threaded and interlocked molecules," Curr. Org. Synth. **7**, 24–43 (2010).
[12]K. D. Haenni and D. A. Leigh, "The application of cuaac 'click' chemistry to catenane and rotaxane synthesis," Chem. Soc. Rev. **39**, 1240–1251 (2010).
[13]W. R. Dichtel, O. S. Miljanic, W. Zhang, J. M. Spruell, K. Patel, I. Aprahamian, J. R. Heath, and J. F. Stoddartt, "Kinetic and thermodynamic approaches for the efficient formation of mechanical bonds," Acc. Chem. Res. **41**, 1750–1761 (2008).
[14]O. S. Miljanic, W. R. Dichtel, I. Aprahamian, R. D. Rohde, H. D. Agnew, J. R. Heath, and J. F. Stoddart, "Rotaxanes and catenanes by click chemistry," QSAR Comb. Sci. **26**, 1165–1174 (2007).
[15]H. Li, C. Cheng, P. R. McGonigal, A. C. Fahrenbach, M. Frasconi, W.-G. Liu, Z. Zhu, Y. Zhao, C. Ke, J. Lei, R. M. Young, S. M. Dyar, D. T. Co, Y.-W. Yang, Y. Y. Botros, W. A. Goddard III, M. R. Wasielewski, R. D. Astumian, and J. F. Stoddart, "Relative unidirectional translation in an artificial molecular assembly fueled by light," J. Am. Chem. Soc. **135**, 18609–18620 (2013).
[16]E. M. Sevick and D. R. M. Williams, "Piston-rotaxanes as molecular shock absorbers," Langmuir **26**, 5864–5868 (2010).
[17]E. M. Sevick and D. M. Williams, "A piston-rotaxane with two potential stripes: Force transitions and yield stresses," Molecules **18**, 13398–13409 (2013).
[18]J. Prost and P. G. de Gennes, *The Physics of Liquid Crystals* (Oxford University Press, 1994).
[19]L. Onsager, "The effects of shape on the interaction of colloidal particles," Ann. N. Y. Acad. Sci. **51**, 627–659 (1949).
[20]G. Vroege and H. Lekkerkerker, "Phase-transitions in lyotropic colloidal and polymer liquid-crystals," Rep. Prog. Phys. **55**, 1241–1309 (1992).
[21]T. Odijk, "Theory of lyotropic polymer liquid-crystals," Macromolecules **19**, 2313–2329 (1986).
[22]H. He, E. M. Sevick, and D. R. Williams, "Fast switching from isotropic liquids to nematic liquid crystals: Rotaxanes as smart fluids," Chem. Commun. **51**, 16541–16544 (2015).
[23]N. A. Spenley, M. E. Cates, and T. McLeish, "Nonlinear rheology of wormlike micelles," Phys. Rev. Lett. **71**, 939–942 (1993).
[24]K. Shundyak, R. van Roij, and P. van der Schoot, "Theory of the isotropic-nematic transition in dispersions of compressible rods," Phys. Rev. E **74**, 021710 (2006).
[25]J. Stegen and P. van der Schoot, "Self-crowding induced phase separation in protein dispersions," J. Chem. Phys. **142**, 244901 (2015).
[26]H. N. W. Lekkerkerker, P. Coulon, R. Van Der Haegen, and R. Deblieck, "On the isotropic liquid crystal phase separation in a solution of rodlike particles of different lengths," J. Chem. Phys. **80**, 3427 (1984).
[27]T. M. Birshtein, B. I. Kolegov, and V. Pryamitsyn, "Theory of athermal lyotropic liquid crystal systems," Polym. Sci. U.S.S.R. **30**(2), 316–324 (1988).
[28]M. Doi and S. Edwards, *The Theory of Polymer Dynamics* (Clarendon Press, Oxford, 1986).

Chapter 4

Can Switchable Molecules be Used as Depletants to Affect Colloid Stability?

The research presented in this manuscript was solely completed by the author of this thesis. The author was the main contributor to the statistical mechanical model and numerical calculations in this manuscript.

Can Switchable Molecules be Used as Depletants to Affect Colloid Stability?

Hao He,[1, a)] Edith M. Sevick,[1, b)] and David R.M. Williams[2, c)]

[1)] *Research School of Chemistry, The Australian National University, Canberra ACT 2601 AUSTRALIA*

[2)] *Department of Applied Mathematics, Research School of Physical Sciences & Engineering, The Australian National University, Canberra ACT 2601 AUSTRALIA*

(Dated: 18 June 2019)

We examine a colloidal solution of non-adaptive two-state rotaxane molecules as depletants, using statistical thermodynamics. The rotaxane molecules are externally driven to switch between a short state of length qL ($q < 1$) to a long state of length L. We demonstrated the first numerical calculation of concentration profile and deletion interaction at a surface. We show that the molecular length upon switching can affect the range and magnitude of depletion interaction in colloid solution. This suggests the potential application of rotaxane switch of controlling colloid stability.

[a)] Electronic mail: u4785782@anu.edu.au

[b)] Electronic mail: Edie.Sevick@anu.edu.au

[c)] Electronic mail: D.Williams@anu.edu.au

I. INTRODUCTION

A depletant force is an attractive force that arises between large colloidal particles due the presence of dilute, smaller solutes, called depletants. This attractive force was first explained as an entropic force in the 1954 Asakura-Oosawa model[1]; this entropic force is based upon the concept of excluded volume, or the volume inaccessible to smaller solutes by larger colloids. When two large colloids are sufficiently close, the exclusion volume of each colloid overlaps and the total volume excluded to the depletants is reduced or the volume accessible to the solute depletants increases. This increases the depletants' translational entropy and minimises the solution free energy, resulting in an effective or entropic attractive force between the colloids. The use of depletants has long been used to tune the stability of colloidal dispersions. An early example is the creaming process of rubber where polysaccharides are added as depletants to induce attractive interactions which lead to separation into a dense latex phase which can be more cheaply transported, and later restored by dilution[2].

Since Asakura-Oosawa's 1954 model, depletion forces have been characterized for polymeric and biological depletants using theory as well as experimental measurement. When the depletant is anisotropic or rod-like , the increase in translational entropy is accompanied by an increase in the orientational entropy of the rod-like depletant, and as a result, the entropic attraction is increased in both range and magnitude[3–5]. This entropic force can be significant as it leads to phase separation of hard-core spheres and rods in simulation[6]. In this paper, we consider a possible rod-like depletant comprised of interlocked components, called a rotaxane-switch. A rotaxane-switch corresponds to a molecular axle upon which attractive stations are built; the ring switches between different station, driven by a number of difference external factors[7–9], most notably by light[10–12]. A significant class of length-extending rotaxane-switches, generically illustrated in Figure 1, have already been synthesized[13] to switch between short and long rods with a length variation in excess of a factor of 3. Can we use this molecular switching to alter the stability of colloidal dispersions through depletion forces? The potential advantage of photo-switchable switchable depletants is that colloidal stability can be controlled by light rather than the addition/dilution of the solvent.

In this chapter, we calculate the attractive interaction imparted by a fixed depletant con-

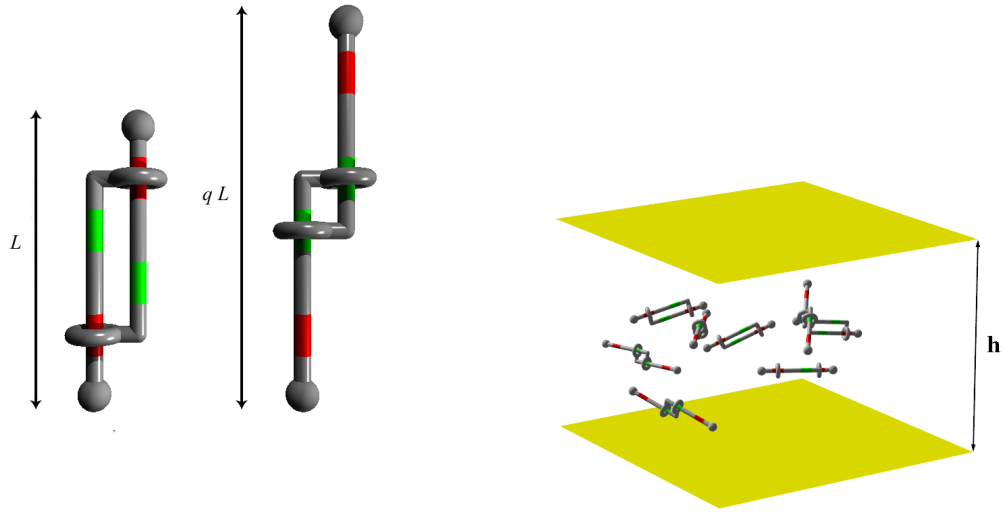

FIG. 1. Left: A two state 2-rotaxane consisting of two axles or rods interlocked to each other. When the rings are engaged at the red stations, the molecule is in a short state of length L. When the rings are engaged to the green station, the molecule is in long state of length qL. Switching between long and short state is by external influences such as light or a change in pH which alters the state is of minimal energy. We assume that the energy difference in the long and short states is always much greater than k_BT, irrespective which state is minimal. This means that the switch is unaffected by the local alignment or density of molecules. Right: rotaxane switches as depletants sandwiched between parallel plates of separation h. This length switching process provides a possible mechanism to accomplish a significant change in the range and magnitude of depletion force.

centration of 2-state rotaxanes which switch length from a long state, of length L, to a short state of length qL with $0 < q \leq 1$.. We use the simplest of models, where depletants of switchable length L or qL and fixed diameter D, and colloids, or radius R, interact only through their mutual excluded volume. We also consider the rod-like depletants in the Onsager limit of high aspect ratio, or where $qL/D \to \infty$. The depletion attraction of a solution of *monodisperse* fixed-length rod-like depletants in the Onsager limit as been characterised by Mao, Lekkekerker and Cates[3,4], and our approach closely follows this work. However, here we generalise their approach to calculate depletion interaction due to any mixture of rod-like depletant in Onsager Limit. I particular we focus on case where rod-like depletants are bidisperse in length, *i.e.,* a mixture of rods of length L and qL. This is necessary as

switching of a solution of 2-state rotaxanes in not quantitative. The Onsager limit not only simplifies the model considerably, but it also excludes any possibility of de-mixing by molecular length[14]. Furthermore, we consider the switching process to be externally driven and not adaptive; that is the energy barrier to switching states is much larger than kT so that a molecule does not change its length state in response to its surrounding. In this way, we consider the switching process as process which alters the composition of mixture.

The original Asakura and Oosawa model considered the depletion attraction between two parallel plates, a distance h apart, immersed in a solution of depletants. When the plates are separated by a distance small enough to exclude depletant molecules, the concentration of depletants between the plates is smaller than that of the bulk. This gradient in depletant concentration across each of the plates gives rise to an osmotic pressure, or force per unit area, f_p, pushing the plates towards one another. For rod-like depletants in the Onsager limit, this force is proportional to the difference in the density of rods ends which are sandwiched between the plates and in contact with the plate, $n(h)$, and the density of rod ends touching the opposite side of the plate, $n(h = \infty)$

$$f_p = k_B T(n(h) - n(h = \infty)). \tag{1}$$

This force per unit area can be related to the force that would exist between two spheres of radius R, whose centres are separated by $2R + h$, by the Derjaguin approximation,

$$f_s(h) = -\pi \int_{\infty}^{h} f_p(h')dh'. \tag{2}$$

Here the subscript s denotes that it is sphere between which the depletion force acts. The depletion interaction between two spheres is then

$$W_s(h) = \int_{h}^{\infty} f_s(h')dh' \tag{3}$$

In order to find the depletion interaction, we need to solve for the number density of rod-ends in contact with a plate. Both Poniewierski[15] and Mao et al.[4] have determined the number density of needle-like rods and their alignment near a plate, where the bulk density is low and corresponds to an isotropic solution. Based on Mao's method, we purpose generalise theory of polydisperse rods in solution and provide results for bidisperse case. These results demonstrate the first numerical calculation of alignment of bidisperse rods at a surface, as well as depletion interactions.

II. THEORY OF DEPLETION FORCE DUE TO POLYDISPERSE ROD-LIKE DEPLETANTS

Consider a polydisperse rods solution with k types of rods of length $L_1, L_2, ..., L_k$ and constant diameter D in Onsager limit, $L_i >> D$, $i = 1, ..., k$. The geometry associated with this problem is illustrated in figure 2, where ends of rod i locate at z and z_1 from the plate, ends of rod j locate at z_2 and z_3. s_i and s_j are the distance between the end of rod i & j to the point at which the rods intersect. The orientation of rod 2, $\Omega_j = \{\theta_j, \phi_j\}$, is defined with rod i as normal axis. These geometric parameters are related as follows:

$$z_1 = z + L_i t$$
$$z_2 = z + s_i t - (L_j - s_j)(t\cos\theta_j + \sqrt{1-t^2}\sin\theta_j\cos\phi_j) \quad (4)$$
$$z_3 = z + s_i t + s_j(t\cos\theta_j + \sqrt{1-t^2}\sin\theta_j\cos\phi_j), \quad (5)$$

where $t = \cos\theta = \frac{z_1 - z}{L_i}$ and $t' = \frac{z_3 - z_2}{L_j}$. Without loss of generality, we choose z to be the lower end of rod i,$z < z_1$.

Depletion interaction is entropically-driven, the free energy per unit area of plate in plates separated by h in solution of mixed depletant, is written as sum of translational, rotational entropy and and mixing entropy, S_{trans}, S_{ori} & S_{mix}.

Translational entropy and mixing entropy of rod i is function of the end density $n_i(h, z, \Omega)$:

$$S_{trans,i}(h) = \int dz\, d\Omega\, n_i(h, z, \Omega)(\ln \Lambda^3 n_i(h, z, \Omega) - 1), \quad (6)$$

$$S_{mix,i}(h) = \int dz\, d\Omega\, n_i(h, z, \Omega) \ln\left(\frac{n_i(h, z, \Omega)}{n_0(h, z, \Omega)}\right), \quad (7)$$

where $n_0(h, z, \Omega)$ is the concentration of all rods, $n_0(h, z, \Omega) = \sum_{i=1}^{k} n_i(h, z, \Omega)$.
Rotational entropy are given by the pairwise excluded-voulme interaction between two rods:

$$S_{rot,ij}(h) = \frac{1}{2}\int dz_i\, d\Omega_i\, n_i(h, z_i, \Omega_i) G_{ij}(h, z_i, \Omega_i) \quad (8)$$

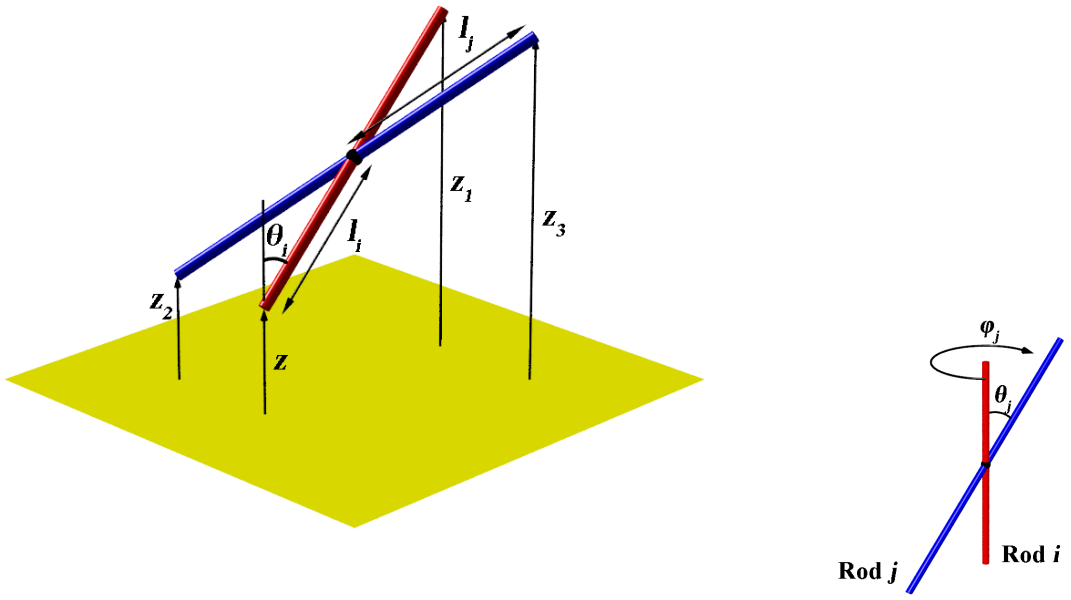

FIG. 2. Parameter setup for two intersecting rods near a flat solid wall. Without loss of generality, z is always the lower end of rod 1, $z < z_1$. But for rod 2 this is not the case, $-L_j < z_3 - z_2 < L_j$. Orientation of rod j is defined with rod i as normal axis.

where

$$G_{ij}(h, z_i, \Omega_i) = 2D \int d\Omega_j \int_0^{L_i} ds_i \int_0^{L_j} ds_j \, n_j(h, z_j, \Omega_j) |\sin\theta_j|, \tag{9}$$

Direct integration of G_{ij} is difficult[4]. One can rewrite G_{ij} as follows

$$G_{ij}(h, z, \Omega) = 2DL_iL_j \int_{-1}^{1} dt' \int_A^B dz_2 \, \Xi(z_2, z_2 + L_jt') f(t, t') g_{ij}(z, z_2, t, t') n_j(h, z_2, t'), \tag{10}$$

where integration bounds A and B are

$$\begin{cases} A = \max(z, -L_jt') \quad , B = z + L_it - L_jt, \text{ when } -1 < t' < 0 \\ A = \max(z - L_jt', 0), \; B = z + L_it \qquad , \text{when } 0 \le t' < 1. \end{cases} \tag{11}$$

$f(t, t')$ is

$$f(t, t') = \int_0^1 d\cos\theta_j \int_0^{2\pi} d\phi \delta(t' - t\cos\theta_j - \sin\theta_j\sqrt{1 - t^2}\cos\phi_j) |\sin\theta_j|, \tag{12}$$

and g_{ij} is

$$g_{ij}(z, z_2, t, t') = \int_0^{L_i} dS_i \int_0^{L_j} dS_j \, \delta(z_2 - z + t' - tS_i - t'S_j). \tag{13}$$

Functions $f(t, t')$ and g_{ij} effectively integrate all possible contacting rods that satisfy equations 4 and 5. Computation time can be greatly reduced by calculating $f(t, t')$ as 2-dimensional array beforehand. g_{ij} are simple integrals that specify a linear segment in S_i, S_j plane. In bulk solution with monodisperse length, equation 9 can be integrated directly to give

$$G_{ij,bulk} = \int d\Omega \, G(h = \infty, z = \infty, \Omega) = 2DL_iL_jn_j. \tag{14}$$

thus the free energy for a polydisperse rods solution with k types of rods of length $L_1, L_2, ..., L_k$ is

$$\frac{F(h)}{k_BT} = \sum_{i=1}^{k} S_{trans,i} + \sum_{i=1}^{k}\sum_{j=1}^{k} S_{rot,ij} + \sum_{i=1}^{k} S_{mix,i}, \tag{15}$$

The chemical potential at all points in the solution is equal, $\partial F_{bulk}/\partial n_{i,bulk} = \partial F/\partial n(h, z, \Omega)$. $\partial F_{bulk}/\partial n_{i,bulk}$ can be calculated by equation 14 and 15 given bulk rod concentrations $n_{1,bulk}, ..., n_{k,bulk}$. Uniform chemical potential allows self-consistent relations for each end density of rod n_i,

$$n_i(h, z_i, \Omega_i) = \frac{n_{i,bulk}}{2\pi}\Xi(z, z_1)\frac{\exp\left[(\sum_{j=1}^{k} G_{ij,bulk}) + \ln\left(\frac{n_{i,bulk}}{n_{0,bulk}}\right)\right]}{\exp\left[(\sum_{j=1}^{k} G_{ij}(h, z_i, \Omega_i)) + \ln\left(\frac{n_i(h,z,\Omega)}{n_0(h,z,\Omega)}\right)\right]}, \tag{16}$$

The total rod center density, $n_c(h, z_c)$, can be caculated by summing up that of rods of lengths,

$$n_c(h, z_c) = 2\pi \sum_{i=1}^{k}\left[\int_0^{min(1,2z_c/L_i)} n_i(h, z_c - \frac{L_it}{2}, t)dt\right]. \tag{17}$$

The depletion force per unit area between the two parallel plates is proportional to the end density difference between the 2 sides of plate:

$$\frac{f_p(h)}{k_BT} = \sum_{i=1}^{k} \int d\Omega \left[n_i(h, 0, \Omega) - n_i(\infty, 0, \Omega)\right] \tag{18}$$

and the depletion force and interaction between spherical colloid particles can be found from equations 2 and 3 using Derijaguin Approximation. Given any length profile $L_1, L_2, ..., L_k$ and the corresponding bulk density $n_{1,bulk}, n_{2,bulk}, ..., n_{k,bulk}$, depletion force and concentration profile near plates can be calculated.

Case $k = 1$ corresponds to depletion theory of monodisperse rod. This case is thoroughly discussed by Mao et al.[4], and will not be discussed further. In this paper, we focus on the depletion due to bidisperse rod, $k = 2$. The longer rod is of length $L_1 = L$ and the shorter one of length $L_2 = qL$ $(0 < q < 1)$, and in the Onsager limit, $L > qL >> D$. The corresponding bulk concentrations are $n_{1,bulk} = n_{bulk}x$ and $n_{2,bulk} = n_{bulk}(1 - x)$, with x the fraction of short rod in bulk solution. In our calculations, the total bulk rods density is fixed at $c_{bulk} = n_{bulk}DL^2 = 1$, which is well below the minimum critical concentration $\frac{\pi nDL^2}{4} = 4$ for a nematic phase formation[16]. Plug in these parameters to equation 16, the end density for long and short rods, n_1 and n_2 are solved by numerical iteration using equations 6-16. To help quick convergence, the input for next iteration is a linear combination of the output n_{out} and input n_{in} of current step, $n = \alpha n_{in} + (1 - \alpha)n_{out}$, where alpha is a randomly generated number between 0.1 and 0.5. With n_1, n_2 and plate separation h, rod center density n_c and depletion profile f_p is then calculated with equation 17 and 18.

III. RESULT AND DISCUSSION

We first construct density profiles of rods near an isolated plate or where plate separations are sufficiently large that the bulk densities are achieved midway between two plates, *i.e.,* the plate separation is larger than the longest rod length, $h > L$. Figure 3 (left) shows the end-density, normalized by the bulk end density as a function of distance from the plate; and Figure 3 (right) shows the center density, again normalized by bulk center density as a function of distance from the plate. The dashed line in each plot corresponds to a reconstruction of the predictions of Mao[17] & Poniewierski[15] for monodisperse rods or $x = 1$. The density of rod end increase relative to the bulk near a surface while the rod centre density shows a discontinuous maximum or "kink" at $z = L/2$: rods whose centers are located $z \geq L/2$ are orientationally unrestricted; but at $z < L/2$ rods, the rods become orientational restricted. A rod whose center is located close to the plate, $z \sim 0$, will

contribute both ends to the end density as the rod will be aligned with the plate. At the total rod density investigated, the solution of monodisperse long rods seems to have have a slightly larger center density near the plate than solution of the same number density but where smaller rods are incorporated.

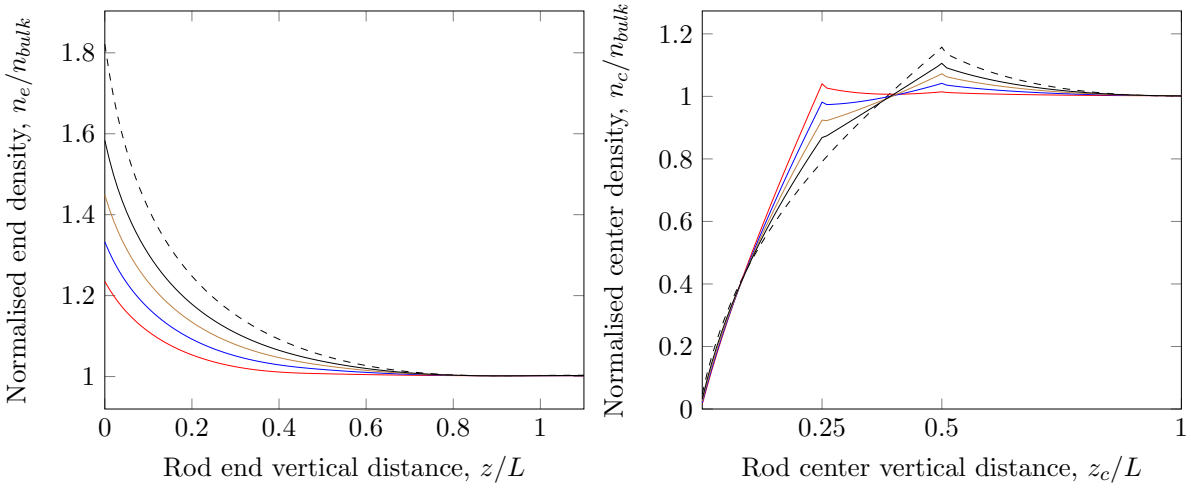

FIG. 3. Normalised rod end density $n/(n_{1,bulk} + n_{2,bulk})$ (left) and center density $n_c/(n_{1,bulk} + n_{2,bulk})$(right) versus vertical distance z with $q = 0.5$ and bulk fraction of long rods, $x = 0.1$ (red), $x = 0.3$ (blue), $x = 0.5$ (black), $x = 0.7$ (brown). The dashed line is the end and center density for mondisperse rods of the same bulk concentration. The monodisperse concentration profile agrees well with the results of Mao et al.[17] and Poniewierski[15]. Higher presence of short state rod (lower x) result in smaller end density at the wall. For center density profile, an extra kink contributed to the presence of short rod appears.

Also included in these plots are results for mixtures where the shorter rod has length qL with $q = 0.5$, with fraction of long rods in the solution being $x = 0.7, 0.5, 0.3$, and 0.1. Increasing the fraction of short rods at this fixed overall rod density results in a decrease in the end density at the plate and a "kink" in the center density at $z = qL/2$ grows with the fraction of short rods. As expected, increasing the fraction of short rods leads to a means that the bulk density, both center and end, is achieved at distances closer to the plates.

Depletion force between parallel plates f_p is calculated by equation 1 from the end densities at the plate. Again, the dotted line in figure 4 corresponds to a monodisperse solution of

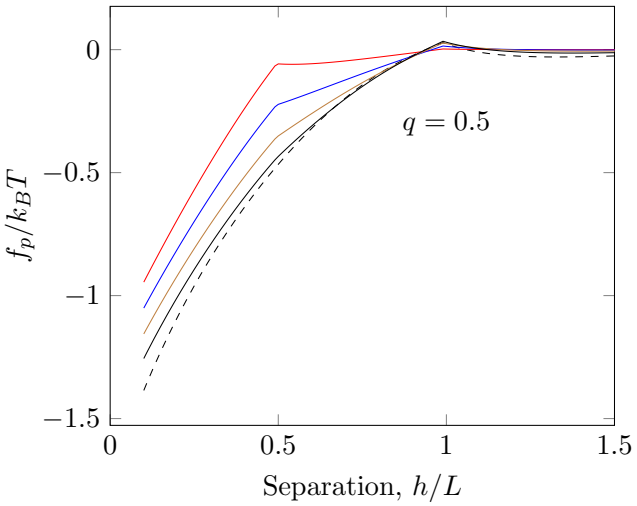

FIG. 4. Depletion force between plates, f_p/k_BT due to mixed long and short rod with length ratio $q = 0.5$ versus separation h/L. Bulk fraction of long rods fixed at $x = 0.1$ (red), $x = 0.3$ (blue), $x = 0.5$ (black), $x = 0.7$ (brown) and $x = 1$ (dashed). On top of showing depletion profile for binary rod mixture, this is essentially the switching diagam of depletion interaction of 2-state length switchabble molecules as depletant. and can provide information on how the attractive depletion interaction changes when exteranlly driven length switching alters the relative composition of long and short rods.

long rods or $x = 1.0$. where an attractive force first appears between plates separated by $h = L$ and is more attractive as h is decreased towards $h = 0$. The conversion of long rods of length L to short rods of length qL, forming binary mixtures of $x = 0.7, 0.5, 0.3$ and 0.1, weakens the attractive depletion interaction, especially at separation qL. Finally, we can reinterpret this force between plates in terms of the depletion interaction between large spherical colloid with Derjaguin Approximation in equations 2 and 3: Figure 5, shows the dimensionless depletion interaction of a pair of spherical colloid of radius $R = 10L$ due to binary mixture of rod-like depletants with dimension $L = 20D$ and $q = 0.5$, as calculated in our Onsager limit with a bulk depletant concentration $c_{bulk} = 1$, which corresponds to approximately 4% by volume of depletant. Here the attractive interaction is strongest for depletants which are 100% in the long state (dashed line), but as a large fraction ($x = 0.1$) of these molecules is switched to the short qL state, the attractive interaction is diminished by 10s of k_BT at a surface-to-surface equal to qL. More importantly, the range of the attractive interaction is reduced by nearly 1/2 or twofold. Thus switching from long to short depletants

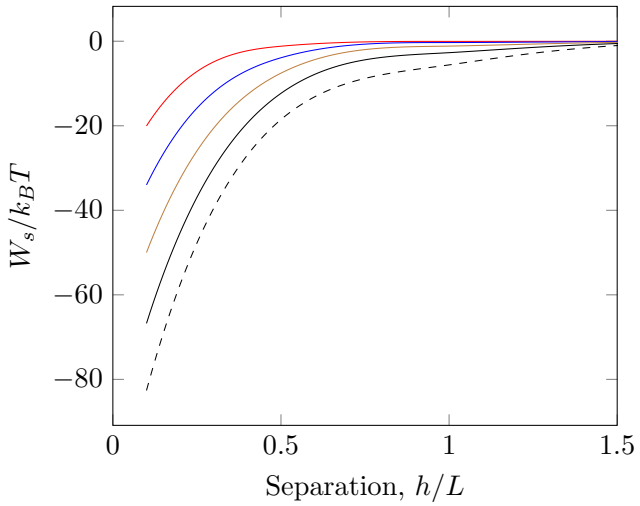

FIG. 5. Depletion potential W_s between 2 spherical colloid of radius $R = 10L$, due to mixed long and short rod with $q = 0.5$, $L = 20D$ versus separation h. Bulk fraction of long rods fixed at $x = 0.1$ (red), $x = 0.3$ (blue), $x = 0.5$ (black), $x = 0.7$ (brown) and $x = 1$ (dashed).

reduces the short range, attractive depletion interaction between purely hard sphere colloids.

The depletion potential of monodisperse rod of volume fraction v_r in Onsager limit is[4,18]

$$W(h) = \frac{2}{3} k_B T v_r \frac{L}{D} \frac{R}{D} (1 - \frac{h}{L})^3 \tag{19}$$

Koenderink et al. has confirmed by experiment that rod-like depletants are highly effective and even low rod concentration, which induce near theoretical minimum of attractive depletion interaction predicted by equation 19, is sufficient to induce flocculation in rod-sphere mixture[19]. Our calculation at monodisperse limit $x = 1$ (dashed line) agrees well with equation 19 at low h. When $h = 0.1$, depletion potential due to pure long rod is $\approx -83 k_B T$, 4 times greater than that due to pure short rods. The attractive depletion potential for binary mixture of rods at $h = 0$ lies between these two limits. As depletants switch towards a short rods majority (say from $x = 1$ to $x = 0.1$), attractive depletion interaction is greatly weakened and diminished by 10s of $k_B T$ at a surface-to-surface equal to qL. More importantly, the range of the attractive interaction is reduced by nearly 1/2 or twofold. Of course, this change in the depletion interaction will affect colloidal stability most dominantly if it can mask and overcompensate short-range repulsion between colloidal particles when $x \sim 1.0$

resulting in colloidal aggregation, but upon switching can unmask this repulsion at small values of x to disperse the colloidal particle. For instance, if the spherical colloids in this case has DLVO repulsive potential of $\approx 50k_bT$ at contact $h \approx 0.1$, switching the rod-like depletant between $x = 1$ and $x = 0.3$ will induce reversible colloid flocculation.

IV. CONCLUSION

We have numerically calculated depletion interaction between two parallel plates due to binary rod-like molecules mixture. Then we examined the idea of using 2-state length-switchable molecules as depletant. We have shown that range and magnitude of depletion interaction can be effectively controlled by externally driven depletant molecule length switching. This is suggesting an alternative way of colloid suspension stability control other than addition or removal of depletant.

REFERENCES

[1]S. Asakura and F. Oosawa, "On Interaction between Two Bodies Immersed in a Solution of Macromolecules," J. Chem. Phys. **22**, 1255–1256 (1954).

[2]H. C. Baker, "The Concentration of Latex by Creaming," Trans. Inst. Rubb. Ind. **13**, 70–82 (1937).

[3]Y. Mao, M. E. Cates, and H. N. W. Lekkerkerker, "Depletion Stabilization by Semidilute Rods," Phys. Rev. Lett. **75**, 4548–4551 (1995).

[4]Y. Mao, M. E. Cates, and H. N. W. Lekkerkerker, "Theory of the Depletion Force due to Rodlike Polymers," J. Chem. Phys. **106**, 3721–3729 (1997).

[5]K. Yaman, C. Jeppesen, and C. M. Marques, "Depletion Forces between Two Spheres in a Rod Solution," Europhys. Lett. **42**, 221 (1998).

[6]P. Bolhuis and D. Frenkel, "Numerical Study of the Phase Diagram of a Mixture of Spherical and Rodlike Colloids," J. Chem. Phys. **101**, 9869–9875 (1994).

[7]F. Coutrot, C. Romuald, and E. Busseron, "A New pH-Switchable Dimannosyl[c2]Daisy Chain Molecular Machine," Org. Lett. **10**, 3741–3744 (2008).

[8]J. Wu, K. C.-F. Leung, D. Benitez, J.-Y. Han, S. J. Cantrill, L. Fang, and J. F. Stoddart, "An Acid-Base-Controllable [c2]Daisy Chain," Angew. Chem. Int. Ed. **47**, 7470–7474

(2008).

[9]L. Fang, M. Hmadeh, J. Wu, M. A. Olson, J. M. Spruell, A. Trabolsi, Y.-W. Yang, M. Elhabiri, A.-M. Albrecht-Gary, and J. F. Stoddart, "Acid-Base Actuation of [c2]Daisy Chains," J. Am. Chem. Soc. **131**, 7126–7134 (2009).

[10]S. Tsuda, Y. Aso, and T. Kaneda, "Linear Oligomers Composed of a Photochromically Contractible and Extendable Janus [2] Rotaxane," Chem. Commun. , 3072–3074 (2006).

[11]R. E. Dawson, S. F. Lincoln, and C. J. Easton, "The Foundation of a Light Driven Molecular Muscle based on Stilbene and Alpha-Cyclodextrin," Chem. Commun. , 3980–3982 (2008).

[12]S. Li, D. Taura, A. Hashidzume, and A. Harada, "Light-Switchable Janus [2]Rotaxanes Based on alpha-Cyclodextrin Derivatives Bearing Two Recognition Sites Linked with Oligo(ethylene glycol)," Chem. Asian. J. **5**, 2281–2289 (2010).

[13]C. J. Bruns and J. F. Stoddart, "Rotaxane-Based Molecular Muscles," Acc. Chem. Res. **47**, 2186–2199 (2014).

[14]R. van Roij and B. Mulder, "Demixing Versus Ordering in Hard-Rod Mixtures," Phys. Rev. E **54**, 6430–6440 (1996).

[15]A. Poniewierski, "Ordering of Hard Needles at a Hard Wall," Phys. Rev. E **47**, 3396–3403 (1993).

[16]R. F. Kayser and H. J. Raveché, "Bifurcation in Onsager's Model of the Isotropic-Nematic Transition," Phys. Rev. A **17**, 2067–2072 (1978).

[17]Y. Mao, P. Bladon, H. N. W. Lekkerkerker, and M. E. Cates, "Density Profiles and Thermodynamics of Rod-Like Particles between Parallel Walls," Mol. Phys. **92**, 151–159 (1997).

[18]S. Asakura and F. Oosawa, "Interaction between particles suspended in solutions of macromolecules," Journal of Polymer Science **33**, 183–192 (1958).

[19]G. H. Koenderink, G. A. Vliegenthart, S. G. J. M. Kluijtmans, A. van Blaaderen, A. P. Philipse, and H. N. W. Lekkerkerker, "Depletion-induced crystallization in colloidal rod-sphere mixtures," Langmuir **15**, 4693–4696 (1999).

Chapter 5

Conclusion

In this thesis, a solution of 2-state rotaxane has been described with statistical thermodynamics. It is found that molecular motion upon external driven switching can be harvested to affect physical behavior in solution.

A simple model shows that switching between isotropic and nematic liquid crystalline phases us possible in 2-state rotaxane switch system without changing concentration and temperature. While it is first demonstrated assuming quantitative switching between elongated and contracted states of rotaxane, it is subsequently shown that "real world" rotaxane switches, which switches incompletely between states or are in mixture with mesogens, can achieve externally-driven isotropic-nematic phase switching.

Using similar theoretical model, rotaxane switches are found to shown interesting behavior as depletants. Molecular motion upon switching can significantly alter the range and magnitude of depletion interaction, giving rotaxane switches the potential to exert control over colloidal stability in solution.

And finally, an interesting case of "adaptive" rotaxane that change length in response to surrounding environment is investigated. Theoretical prediction on isotropic-nematic critical concentrations and order parameters are made.